PHYSICOCHEMICAL APPROACHES FOR THE REMEDIATION OF MANUFACTURED GAS PLANT TAR IN POROUS MEDIA

Scott C. Hauswirth

A dissertation submitted to the faculty of the University of North Carolina at Chapel Hill in partial fulfillment of the requirements for the degree of Doctor of Philosophy in the Department of Environmental Sciences and Engineering.

Chapel Hill
2014

Approved by:

Cass T. Miller

Gaylen Brubaker

William G. Gray

Jingfang Huang

Richard Kamens

Lee Pedersen

ABSTRACT

SCOTT C. HAUSWIRTH: PHYSICOCHEMICAL APPROACHES FOR THE REMEDIATION OF MANUFACTURED GAS PLANT TAR IN POROUS MEDIA
(Under the direction of Cass T. Miller)

Tars produced as a by-product of coal and oil gasification at former manufactured gas plants (FMGPs) during the 19th and early 20th centuries were often released into the environment through poor disposal practices or leaks in holding tanks and piping. These tars are persistent contaminants, leaching polycyclic aromatic hydrocarbons (PAHs) into groundwater and posing a significant risk to human and ecological health. FMGP tars also have several properties that make them notoriously difficult to remediate. They are dense non-aqueous phase liquids (DNAPLs), so they can migrate to depths which make removal by excavation difficult or impossible, and their relatively high viscosities and ability to alter the wetting characteristics of porous media result in inefficient removal by traditional pump-and-treat methods. This work investigates the relationship between tar composition and properties, and explores several remediation approaches. The interfacial tension (IFT) of a set of FMGP tars was measured as a function of pH and correlated with compositional features. It was observed that IFT is a strongly decreasing function of pH, suggesting the potential use of high pH (alkaline) solutions to mobilize FMGP tar in porous media systems. Laboratory column experiments were conducted to investigate the use of alkaline solutions, alone and in combination with natural polymers (xanthan gum) and surfactants,

to remediate tar-contaminated porous media. The results of these experiments indicated that alkaline-surfactant-polymer (ASP) solutions could efficiently remove 95% of residual tar. Surfactant-polymer (SP) solutions removed an even greater fraction of residual tar, over 99%, but required a larger flushing volume to do so. These experiments also illustrated that both ASP and SP flushing significantly reduced dissolved-phase PAH concentrations, which are often the primary concern at contaminated FMGP sites.

ACKNOWLEDGMENTS

I honestly would not have made it through this endeavor without the help and support of a number of individuals. I first want to thank my adviser, Dr. Casey Miller, for having faith in me over these years and for giving me the space to explore and learn on my own. I am also highly appreciative of Gaylen Brubaker, Bill Gray, Jingfang Huang, Richard Kamens, and Lee Pedersen for serving on my committee.

I am honored to have had the opportunity to work with my collaborators and coauthors, including Pam Schultz, Joe Pedit, Seth Rylander, Stephen Richardson, and Michael Aitken. Additionally, I am indebted to the Masters and undergraduate students in Dr. Miller's research group who have assisted me through the years; they are Zineb Bouzoubaa, Caroline Tapscott, Dominion Rognstad, Emily Chapin, and Dana Williams. The camaraderie of my lab- and classmates, especially Ben Scandella, Ben Lebron, Arne Newman, Collin Ward, Harshal Parikh, and, of course, Amanda Dye, is also greatly appreciated and made the hardest times bearable.

Finally, I would like to thank my parents, Bill and Wendy, without whom I would not be here. They along with my sister, Heather, have loved and supported me throughout this stage of my life and all that have preceded it.

TABLE OF CONTENTS

LIST OF TABLES

LIST OF FIGURES

LIST OF ABBREVIATIONS

1MN	1-methylnaphthalene
2EN	2-ethylnaphthalene
2MN	2-methylnaphthalene
ACE	acenaphthene
ACY	acenaphthylene
ANT	anthracene
AP	alkaline-polymer
ASP	alkaline-surfactant-polymer
ASPH	asphaltene
BaA	benzo[a]anthracene
BaP	benzo[a]pyrene
BbF	benzo[b]fluoranthene
BgP	benzo[ghi]perylene
BkF	benzo[k]fluoranthene
BEN	benzene
CHR	chrysene
CWG	carburetted water gas
DaA	dibenzo[ah]anthracene
DCM	dichloromethane
DDI	distilled, deionized water
DNAPL	dense non-aqueous phase liquid
ETH	ethylbenzene

FID	flame ionization detector (for GC)
FLU	fluoranthene
FLE	fluorene
FMGP	former manufactured gas plant
GC	gas chromatography
HPLC	high-performance liquid chromatography
IFT	interfacial tension
INA	indane
INE	indene
IND	indeno[123-cd]pyrene
IPA	isopropanol
ISCO	*in situ* chemical oxidation
LNAPL	light non-aqueous phase liquid
MAH	monocyclic aromatic hydrocarbon
MGP	manufactured gas plant
MS	mass spectrometer (for GC)
MSR	molar solubilization ratio
NAP	naphthalene
NAPL	non-aqueous phase liquid
PAH	polycyclic aromatic hydrocarbon
PCB	polycholorinated biphenyl
PCE	tetrachloroethylene
PHE	phenanthrene
PV	pore volume

PYR	pyrene
SP	surfactant-polymer
SPAH	sum of 15 PAHs measured by HPLC
TCE	trichloroethene
TOL	toluene
TPAH	total PAHs measured by GC-FID
TX100	Triton X-100
VPO	vapor pressure osmometry
XG	xanthan gum
XYL	xylenes

CHAPTER 1

INTRODUCTION

1.1 Non-aqueous Phase Liquids

Groundwater is the second largest source of freshwater for human use, accounting for approximately 26% of the United States' freshwater [218]. Contamination of groundwater is a major concern and may arise from a wide range of sources, including discharges from industrial operations and wastewater treatment plants, leaking underground storage tanks, septic systems, mining operations, improper disposal of chemical wastes, runoff from agricultural lands and roadways, or from natural sources (e.g., arsenic and radon). Hazardous waste sites, estimated to number 300,000 in the U.S., represent an important source of groundwater contamination [217].

One of the largest concerns at these sites is non-aqueous phase liquids (NAPLs), which are organic liquid contaminants that are immiscible with water [150]. NAPLs are commonly classified according to their density relative to water as either a light NAPL (LNAPL) or a dense NAPL (DNAPL). Common LNAPLs include gasoline, diesel, heating oil, most crude oils, and aromatic solvents (e.g., the BTEX compounds: benzene, toluene, ethylbenzene and xylenes). DNAPLs include trichloroethylene (TCE), an industrial solvent, tetrachloroethylene (PCE), a dry-cleaning solvent, wood preservatives (creosote, chlorophenols) and former manufactured gas plant (FMGP) tars.

Many NAPL components are toxic, carcinogenic, or otherwise harmful to humans and ecological systems. These components can dissolve into groundwater and potentially migrate to sensitive receptors in the vicinity of waste sites. The solubilities of many components is sufficiently low that NAPLs can persist in the environment as a source of groundwater contamination for years to centuries after their release [39, 150]. The following sections discuss the behavior of NAPL contaminants in the environment and remediation technologies used in the clean-up of NAPL contaminated sites.

1.1.1 Behavior of NAPLs in the Subsurface

The behavior of NAPLs is controlled by a complex set of factors that includes local and regional geology and groundwater flow patterns, the amount and rate of the release of the NAPL, the physiochemical properties of the NAPL and the interactions between the solid, aqueous, and NAPL phases [131]. NAPLs may be released into the environment through leaks from storage tanks and piping, spills, or improper disposal in waste ponds/lagoons, landfills, or wells. The NAPL will tend to migrate downward through the unsaturated zone under the force of gravity until reaching the capillary fringe or an impermeable geologic material [26].

DNAPLs, due to their higher density, can migrate downward through the water table to infiltrate deeper geological strata. The degree to which a DNAPL will sink is dependent on the density and interfacial properties of the phase as well as the heterogeneity and properties of the porous media, and the volume and spatial and temporal scale of the release [39, 150]. DNAPLs tend to follow preferential flow pathways through fractures and higher permeability (i.e., coarser-grained)

geologic units [150]. NAPL pools may form at the top of low permeability units and subsequently migrate laterally as a function of the topography of the unit [39, 45, 131]. Further vertical migration may occur once the NAPL reaches a height above the finer-grained material sufficient to overcome capillary forces. Layering of the porous media, even when the differences between the layers are small, can result in the formation of horizontal stringers or lenses of NAPL [150]. As NAPLs move through porous media, both above and below the water table, disconnected NAPL ganglia become trapped in pore spaces as a result of snap-off and bypassing processes [25, 157, 205]. Residual NAPL is generally immobile under natural conditions and may constitute a large portion of the total NAPL mass present at a site [45].

The presence of NAPLs in the subsurface results in groundwater contamination due to the continuous dissolution of the NAPL constituents. The maximum concentration of dissolved contaminants depends on the aqueous solubility of individual compounds, the mole fraction of those compounds in the NAPL, and mass transfer rates. The lateral and vertical extent of a dissolved plume is impacted by a number of additional factors, including the groundwater flow velocity, the distribution of NAPL in the source zone, degradation rates, dispersivity, the heterogeneity of the porous media, and the rates and equilibria associated with the sorption of compounds to the porous media. It has been shown that to significantly reduce dissolved phase concentrations, nearly complete removal of the NAPL is required [230]. Complete depletion of NAPL source zones may take up to thousands of years under natural conditions, and therefore human intervention is required if more immediate reductions in contaminant concentration in

groundwater are desired [150].

1.1.2 Remediation of NAPLs

The remediation of NAPL-contaminated sites has been the focus of a great deal of research over the last several decades. Remediation can be classified into four general categories: (1) removal, (2) separation, (3) destruction, and (4) containment. Each of these remediation classes is discussed below.

Removal generally refers to the excavation of contaminated soils and NAPL source zones, which are disposed of off-site (i.e., in landfills). This approach is relatively straight-forward and is commonly practiced. In many cases, however, it is impractical, including when the NAPL is deep or utilities, roads, or buildings overlie the source zone [65, 120, 128, 150].

Initial efforts to remediate NAPL-contaminated sites without excavation focused on pump-and-treat approaches, which extract groundwater from wells and remove contaminants (either NAPLs or dissolved phase contaminants) using ex situ treatment methods [128, 130]. Where mobile NAPL is present, such an approach can remove some portion of it, but residual NAPL will remain in place. Pumping groundwater containing dissolved phase contaminants is generally ineffective at removing significant quantities of NAPL due to low aqueous solubilities of most NAPL components, mass transfer rate limitations, and heterogeneities in the subsurface [58, 130, 152, 159].

To improve the effectiveness of in situ separation methods, researchers have employed several techniques to improve the mobilization and dissolution of NAPLs. The solubility of NAPLs can be increased with cosolvents, frequently alcohols (e.g.,

methanol, ethanol, isopropanol, and *tert*-butanol).

Surfactants have also been applied for the purpose of increasing NAPL solubility [52, 57, 121, 156, 158]. Above the critical micelle concentration (CMC) of a surfactant, the surfactant molecules will group together to form spherical micelles. Within the micelles, the surfactant molecules are oriented such that the hydrophobic (lipophilic) portions of the molecules are in the center of the sphere and the hydrophilic portions are directed outward. The micelle acts as an organic pseudophase into which NAPL components may partition, increasing the effective solubility [182, 225]. Enhanced-solubility approaches suffer from reduced efficiencies in heterogeneous media, where NAPL trapped in finer-grained material is less accessible to the flushing solution [197].

Mobilization-based approaches attempt to improve the removal of free-phase NAPL by altering the balance of forces acting on the NAPL.Three dimensionless numbers, the capillary number (N_C), the Bond number (N_B), and the trapping number (N_T), are frequently employed to indicate the relative impacts of the relevant forces. These non-dimensional numbers are derived from a balance of forces acting on a trapped NAPL droplet, and are defined as [160]:

$$N_C \equiv \frac{\mu_a q_a}{\sigma_{a,n} \cos\theta} \tag{1.1}$$

$$N_B \equiv \frac{(\rho_a - \rho_n) g k k_{ra}}{\sigma_{a,n} \cos\theta} \tag{1.2}$$

$$N_T \equiv \sqrt{N_C^2 + 2 N_C N_B \sin\alpha + N_B^2} \tag{1.3}$$

where μ_a is the aqueous phase dynamic viscosity, q_a is the magnitude aqueous phase Darcy velocity, k is the intrinsic permeability of the media, ρ_a and ρ_a are the NAPL and aqueous phase densities, k_{ra} is the aqueous phase relative permeability, and α is the angle between the flow direction and horizontal. N_C and N_B represent the ratio of viscous forces to capillary forces and gravitational forces to capillary forces, respectively. N_T takes viscous and gravitational forces into account simultaneously.

N_T, N_C, and N_B have been found to correlate with residual NAPL saturation, with higher values corresponding to lower saturations [32, 33, 160, 170]. The general approach in designing mobilization-based remediation techniques is to increase the value of these numbers by decreasing the capillary forces that trap NAPLs (i.e., decreasing IFT) or by increasing viscous forces (i.e., increasing flow rate or viscosity). Of these, IFT reduction has received the most attention from researchers, and is usually accomplished using surfactants (or in some cases alcohols) [55, 95, 108, 127, 151, 159, 160, 227, 230]. The use of polymer solutions to increase flushing fluid viscosity has been applied in the petroleum industry for enhanced oil recovery (EOR), and has received some attention from remediation researchers [63, 93, 108, 127]. Alteration of flow rate is less common for field implementation due to limitations to fluid injection and extraction rates [150, 171]. The major drawback of mobilization-based methods is that complete removal of the NAPL is not achieved, and the remaining NAPL will persist as a source of dissolved-phase contamination [230].

Destructive methods include in situ chemical oxidation (ISCO), enhanced biodegradation, and natural attenuation (i.e., biological degradation under nat-

ural conditions). ISCO involves injecting oxidants, including hydrogen peroxide (H_2O_2), potassium permanganate ($KMnO_4$), sodium persulfate (NaS_2O_8), and ozone, into the subsurface to destroy contaminants [89]. ISCO approaches may be applied to either NAPLs or dissolved phase contaminants, although high NAPL saturations are more difficult to remediate by this method due to mass transfer limitations and chemical delivery problems [92]. Additionally, sites with high natural oxidant demands are not well suited to ISCO remediation [92].

Enhanced bioremediation involves the injection of oxygen, nutrients, or electron donor compounds to increase the growth and activity of contaminant-degrading microorganisms present in the soil. Mass transfer limitations and toxicity of high concentrations of contaminants to microorganisms make this approach ineffective when significant quantities of NAPL are present [149].

Natural attenuation involves allowing natural processes to degrade contaminants. This approach is generally applicable as a primary remediation method only when the risks to humans and the environment are limited, other methods are impractical, or the contaminants present are readily biodegradable [150]. Natural attenuation has been used effectively after NAPL source zones are removed [120, 145].

Containment methods include in situ stabilization (ISS), installing slurry walls, and capping contaminated zones with impermeable materials. ISS involves mixing cement and other binders into the contaminated zone to immobilize NAPL and reduce groundwater flow, thereby preventing off-site transport of dissolved-phase contaminants [23]. Similarly, slurry walls are constructed of impermeable materials (clays, cements) in the subsurface in locations designed to prevent off-site

migration of NAPLs and dissolved phase contaminants [128]. Capping approaches use natural and synthetic materials to prevent vertical migration of contaminants or to prevent water from entering and mobilizing contaminants in a contaminated zone. This method is frequently used for preventing movement of contamination between groundwater and surface water, and for remediating contaminated sediments [81, 155].

1.2 Manufactured Gas Plants

FMGPs constitute an important category of DNAPL-contaminated sites, and are the focus of the work described in this dissertation. Manufactured gas plants (MGPs[1]) were common in the U.S. and Europe in the 19th and early 20th centuries, with an estimated 36,121 and 55,001 facilities in the U.S. [217]. These plants produced a flammable gas used for heating, cooking, and lighting from coal and petroleum products. As a by-product of this process, an estimated 11.5 billion gallons of tar DNAPL were produced between 1880 and 1950 [214]. This tar was frequently released into the subsurface through on-site disposal practices or leaks in plant infrastructure. FMGP tars possess several properties that make them among the most challenging of DNAPLs to manage, including high viscosities, compositional complexity, and the ability to alter the wetting characteristics of porous media. A summary of the history and processes of gas production and a description of wastes produced at these sites are provided in the following sections.

[1] A note on semantics: "MGP" is used to refer to the historic facility whereas "FMGP" references the site at which an MGP was formerly located.

1.2.1 History and MGP Processes

Manufactured gas, frequently referred to as town gas, is a flammable gas that was historically used for heating and lighting purposes. The first commercial MGP was operated by the Gas Light and Coke Company in London, England starting in 1812 [74]. The technology quickly spread to Europe and the United States, and the first U.S. commercial MGP was constructed in Baltimore, Maryland in 1816 [70]. Early processes involved the heating of bituminous coal or oil shale in iron or baked-clay "retorts" in the absence of oxygen. The hydrocarbons of the source material were cracked to form coal gas, which was composed of methane (CH_4), hydrogen (H_2), carbon monoxide (CO), ethylene (C_2H_4), and acetylene (C_2H_2) [70]. Where coal was unavailable or prohibitively expensive (i.e., the West coast of the U.S.), petroleum oil was used as the source material. The oil gas produced contained relatively higher concentrations of C_2H_4 and C_2H_2 than coal gas [18].

In the late 1800s and early 1900s, the two-stage carburetted water gas (CWG) process became widespread throughout the U.S. In the first step, water steam was passed through heated anthracite coal or coke to form water gas, which was composed primarily of CO and H_2. Petroleum oils, initially naphtha and later heavier oils, were then injected into the still-hot gas through a carburettor to increase the heating and lighting value of the gas [70, 140]. A number of alternative processes were employed, but these three major classes (coal, oil, and CWG gas) constitute the majority of gas manufacturing in the U.S.[203].

Once the gas was produced, it was passed through a condenser to cool the gas and remove vaporized oil and tar. Additional filtration units were employed to

remove hydrogen cyanide (HCN), ammonia (NH_3), and hydrogen sulfide (H_2S)[70]. The purified gas was then pumped into gas holders for storage prior to distribution. With the construction of a widespread natural gas distribution network in the 1940s–1950s, the manufactured gas industry rapidly declined, and the last U.S. MGP was decommissioned in 1968 [69].

1.2.2 Wastes at FMGP Sites

The vast majority of the 36,000–55,000 FMGPs are suspected to have had releases of solid and liquid waste products, which include tars, cyanide-bearing purifier waste, slag, and coke [70, 128, 217]. Many of these materials were valuable commodities and were sold or recycled for use in the MGP. Coal tar, a byproduct of coal gas production, contained numerous useful chemicals, including dyes, saccharin, quinoline, lubricating oils, and asphalt for road paving, and was frequently sold by MGPs. When coal and coke prices were high, it could also be burned as a fuel source at the plant. Oil gas and CWG tars, on the other hand, contained much lower concentrations of the valuable chemicals, and frequently had high water contents, making them unsuitable for burning. As a result, these tars were frequently disposed of on-site in ponds, pits, and tar wells [18, 128]. Even at coal gas MGPs, accidental releases through spills and leaks in piping were common. Although cyanide, heavy metal, and other contamination is a concern at some FMGPs, most remediations at these sites focus on tars due to their relatively high mobility and carcinogenicity [38].

1.2.2.1 Chemical Composition of FMGP Tars

FMGP tars are complex mixtures, estimated to contain up to 10,000 individual compounds [147]. Polycyclic aromatic hydrocarbons (PAHs), hydrocarbons composed of two or more fused aromatic rings, are the dominant class of compounds in tars. While hundreds of individual PAH species have been identified in tars [21, 66, 68, 228, 238, 239], the compounds which are most often monitored for the purposes of remediation, and which are frequently present at the highest concentrations, are the 16 EPA Priority Pollutant (PP) PAHs. These compounds, along with their molecular masses and aqueous solubilities, are shown in Table 1.1. Other compound classes present in tars include: mononuclear aromatic hydrocarbons (MAHs; e.g., benzene and alkylated benzenes), tar acids (phenolics) and bases (pyridines), neutral heterocyclic compounds (e.g., thiophenes, furans, pyrroles), aliphatics, cyanide compounds, oxygenated PAHs, and trace metals [18, 54, 56, 83, 126, 137, 148]. The exact composition of a tar is controlled by the process and source material that created it. One important example of this is that tars resulting from the carbonization of coal (coal tars) contain much higher concentrations of tar acids and bases than those resulting from the cracking of petroleum (oil and CWG tars) [70].

Fractionation methods provide another approach to characterizing complex mixtures. A common method in the petroleum field is a separation into saturate, aromatic, resin, and asphaltene (SARA) fractions based on solubility and polarity. Asphaltenes are the fraction which is insoluble in a given alkane, typically n-pentane or n-heptane. The alkane-soluble portion is further separated

Table 1.1: EPA Priority Pollutant PAHs

Compound	No. of rings	Molecular weight (g/mole)	Solubility (mg/L)
Naphthalene	2	128	31
Acenaphthene	3	154	3.8
Acenaphthylene	3	152	16.1
Anthracene	3	178	0.045
Phenanthrene	3	178	1.1
Fluorene	3	166	1.9
Fluoranthene	4	202	0.26
Benzo(a)anthracene	4	228	0.011
Chrysene	4	228	0.0015
Pyrene	4	202	0.132
Benzo(a)pyrene	5	252	0.0038
Benzo(b)fluoranthene	5	252	0.0015
Benzo(k)fluoranthene	5	252	0.0008
Dibenz(a,h)anthracene	5	278	0.0005
Benzo(g,h,i)perylene	6	276	0.00026
Indeno(1,2,3-cd)pyrene	6	276	0.062

into, in order of increasing polarity, saturate, aromatic, and resin fractions using column chromatography. Asphaltenes have received a great deal of attention in the petroleum industry due to their tendency to clog pipelines and pores in oil reservoirs, and are suspected to play a major role in the interfacial behavior of crude oils and FMGP tars [17, 29, 30, 88, 105, 115, 186, 240–243]. Resins have received less attention than asphaltenes, but may also be expected play a role in interfacial properties due to their polarity [198, 241]. The chemical compositions of resins and asphaltenes are uncertain, but are believed to be high molecular weight (>500 g/mole), aromatic compounds with aliphatic side-chains and multiple heteroatomic groups, with resins being somewhat smaller and less polar than asphaltenes [8, 64, 107, 132, 199]. In FMGP tars, asphaltene concentrations of up to 36% have been reported, considerably higher than most crude oils, which generally contain between 0.1 and 12.6% [80, 242]. Conversely, resins are present

at relatively lower concentrations in FMGP tars (0.4–7.2%) than in crude oils (9–37.3%) [18, 115].

1.2.2.2 Physical Properties of FMGP Tars

FMGP tars are DNAPLs, with reported specific gravities of between 1.005 and 1.424 [18]. Reported dynamic viscosities of MGP tars range from about 10 cP to more than 500,000 cP (35°C) [18]. As with composition, the density and viscosity of tars is impacted by the processes and source materials used at the MGP. The greatest factors impacting the tar characteristics are the temperature of the process and whether the tar derives from coal (coal gas) or petroleum oils (CWG and oil gas). Higher temperature processes, such as those used in oil gas production, result in higher concentrations of larger compounds and, consequently, denser and more viscous tars [70]. In general, these factors result in density and viscosity differences following the order: oil gas tars > coal tars > CWG tars [18].

Tar-water IFT, a critical factor in controlling the movement and entrapment of tars in the subsurface, has only been reported for tars from four sites, with a range of 20–25 mN/m at neutral pH [17, 221, 242]. This range is significantly lower than other common DNAPLs, such as TCE and PCE, which have IFTs of 34.5 and 47.5 mN/m, respectively [9]. Tar-water IFT has been found to be strongly dependent on pH, with values as low 0.6 mN/m reported at pH 12.4 [17]. This effect is believed to be the result of the formation of surfactants from acidic groups associated with asphaltenes, as further discussed in Chapters 2 and 3.

FMGP tars have been noted to alter wettability, defined as the relative tendency of one fluid to coat the solid phase in the presence of another fluid, from

water-wet to tar-wet [172, 241]. A greater tar-wet character results in higher tar residual saturations and reduced efficiencies during tar recovery efforts as compared to water-wet and intermediate-wet systems [88, 172]. Like IFT, wetting behavior has also been found to be pH dependent, with a low pH being associated with greater tar-wetting behavior. Organic bases in the tar are protonated to form positively-charged ions, resulting in an increased electrostatic attraction to the typically negatively-charged solid phase [46, 88, 125, 172, 241, 242]. As noted in Section 1.2.2.1, major differences in acid and base concentrations are observed between coal tars and CWG tars, and therefore differences may also be expected in the interfacial behavior of different tar types.

1.3 Research Objectives

The remainder of this dissertation is divided into four chapters, the first three of which represents a body of work that has been or will be published in a peer-reviewed journal. A summary of each the chapters is provided below.

1. **Relationship Between Interfacial Tension and Tar Composition** The objective of this chapter is to improve the understanding of the role of tar composition on IFT behavior. Published investigations of the IFT behavior of FMGP tars are limited to two studies, which provide measurements for only two tars and one creosote sample [17, 242]. This work adds to the existing published data by measuring IFT as a function of pH for several tars from two FMGPs, as well as a commercially-available coal tar. The tars were characterized in terms of acid, base, resin, and asphaltene content, and Fourier-transform infrared (FTIR) spectroscopy was performed to provide

additional information regarding the chemical groups present in the tars and resin and asphaltene fractions. IFTs of synthetic DNAPLs containing asphaltenes and resins extracted from the tar samples will be measured to isolate the impact of composition on IFT behavior. This chapter was published in the peer-reviewed journal *Environmental Science & Technology* in 2012 [76] .

2. **Mobilization of Manufactured Gas Plant Tar with Alkaline Flushing Solutions** The objective of this work is to assess the feasibility of the use of alkaline (NaOH) solutions to reduce tar IFT, alter wetting behavior, and mobilize residual tars from porous media. Tar IFT and contact angle is measured as a function of NaOH concentration (0–1 wt. %), and a series of one-dimensional column studies is conducted with 0.2, 0.35, and 0.5% NaOH flushing solutions both with and without the addition of xanthan gum (XG) as a viscosifying agent. This chapter was published in the peer-reviewed journal *Environmental Science & Technology* in 2012 [75].

3. **A Comparison of Physicochemical Methods for the Remediation of Porous Medium Systems Contaminated with Tar** This chapter has several objectives: (1) to compare the performance of alkaline flushing, surfactant flushing, and alkaline-surfactant flushing in terms of the removal of residual tar in one-dimensional column experiments, (2) to investigate the use of ISCO using base-activated persulfate for the remediation of remaining free-phase FMGP tar, and (3) to demonstrate the ability of a these approaches individually or in series to remediate FMGP tars using aqueous-

phase PAH concentrations as the criteria for success.

4. **Conclusions and Recommendations** This chapter provides overall conclusions for this work and recommends directions for future research.

CHAPTER 2

COMPOSITIONAL AND PH EFFECTS ON THE INTERFACIAL TENSION BETWEEN COMPLEX TAR MIXTURES AND AQUEOUS SOLUTIONS [1]

2.1 Introduction

Former manufactured gas plants (FMGPs) operated throughout the U.S. and Europe between the early-1800s and mid-1900s and produced a flammable gas for heating and lighting for commercial and residential purposes. The U.S. Environmental Protection Agency (EPA) indicated that there may be as many as 50,000 FMGPs and related sites in the U.S, with the majority of these sites expected to have some level of contamination [217]. The primary contaminant of concern at FMGPs is tar, which was produced as a by-product of the gasification of coal and petroleum, and was frequently released into the environment either intentionally or through leaks in plant infrastructure [128].

FMGP tars possess a number of characteristics that make them among the most challenging of nonaqueous phase liquids (NAPLs) to remediate. They are generally denser than water (i.e., dense NAPLs or DNAPLs) and are usually significantly more viscous than water or other NAPLS, with reported dynamic viscosities ranging from 10 to 500,000 cP [18]. FMGP tars have exhibited the ability to alter the wetting characteristics of porous media, further decreasing

[1] Reprinted (adapted) with permission from Hauswirth, S. C., et al. (2012) *Environmental Science and Technology* 46(18), 10214–10221. Copyright (2012) American Chemical Society.

recovery efficiencies [88, 172]. Additionally, the tars are chemically complex and can compositionally vary greatly from site to site, and within a given site, due to differences in the source materials and processes used in the plant operation, as well as due to environmental alteration after being released into the subsurface [27, 54]. These variations can have significant implications for the physiochemical properties and subsurface behavior of tars, and subsequently to risk assessment and remedial design at contaminated FMGP sites.

A major source of the variation in tar characteristics is a result of differences in the gas production process used at the FMGP. Coal tars were a by-product of coal carbonization. Carburetted water gas (CWG) tars were a by-product of a process that first used coal to produce water-gas and then sprayed oil in the gas stream. Oil-gas tars were a by-product of gas produced from cracking oils. Birak and Miller [18] provide a summary of historic tar data highlighting differences between tars produced by different processes. Briefly, coal tars were considered distinct in that they contained phenolic acids and nitrogenous bases, and lacked paraffinic compounds. Being petroleum based, oil-gas and CWG tars were almost entirely absent of the acids and bases, but contained a small amount of aliphatic compounds (<5%). Early CWG plants used mostly anthracite coal, and the resultant tars were also generally absent of the acids and bases. In later years, bituminous coal was sometimes used and the resulting CWG tars could more closely resemble coal tars. Though much of the recent literature does not distinguish between these tar types, referring to tars at FMGPs as "coal tars," CWG tars are more likely to be sources of contamination at FMGP sites because they had less commercial value than coal tars and were more likely to be disposed

of on-site [18, 70].

Interfacial tension (IFT) is a property of major importance in determining the behavior of NAPLs in porous media. Unlike most DNAPLs (e.g., chlorinated solvents), FMGP tars exhibit IFTs that are strongly pH dependent. This behavior was first reported by Barranco and Dawson [17], who observed a drop in IFT from an average of 23.5 mN/m for pH 3.4–9.1 to 0.6 mN/m at pH 12.4. Zheng and Powers [242] reported a similar finding and suggested that asphaltenes, the fraction of tar that is insoluble in a given short alkane (usually n-pentane or n-heptane), are responsible for the observed IFT behavior. They observed that the IFT of asphaltenes dissolved in toluene decreased with increasing asphaltene concentration. Asphaltenes are composed of a large number of individual species, but generally consist of relatively high-molecular weight polar compounds containing aromatic, aliphatic, and heteroatomic groups [8, 64, 107, 132, 199]. The reduction of IFT at high pH is believed to be due to the deprotonation of acidic groups within the asphaltenes, resulting in the formation of surface active ionic compounds [17, 242]. These two studies combined, however, measured IFT as a function of pH for only two FMGP tars and a creosote sample, and therefore provide an incomplete picture of the potential range of behavior for FMGP tars.

Hauswirth et al. [75] recently found that the pH dependence of IFT can be exploited for the remediation of tar-contaminated porous media. The use of basic aqueous solutions containing xanthan gum to increase viscosity were capable of removing over 90% of residual CWG tar (sample B1-07 in this study) in column studies [75]. To assess the widespread applicability of such a method to FMGP tars, a better understanding of tar IFT behavior is necessary.

The overall goal of this work is to advance our understanding of the factors that influence the IFT of FMGP tars. The specific objectives of this study are the following: (1) to characterize tars from eight wells at two FMGPs, as well as a commercially-available coal tar using a variety of analytical techniques, (2) to measure the IFT as a function of pH for the tars, as well as synthetic DNAPLs containing asphaltenes and resins extracted from the tars, and (3) to correlate the results of the tar characterization with the pH-dependent IFT behavior of the tars.

2.2 Methods and Materials

2.2.1 Materials

Reagents All reagents were obtained from Fisher Scientific and were ACS Reagent grade or better. Standards for the 16 Priority Pollutant PAHs, benzene, toluene, ethylbenzene, and trimethylbenzenes were obtained from Spex Certiprep. Additional compound standards were made from neat compounds obtained from Alfa Aesar, Acros Organics, and Ultra Scientific. Buffer solutions were produced for pH values of 3 (citrate), 5 (acetate), 7 (phosphate), 9 (borate), and 11 (carbonate) by dissolving appropriate quantities of each salt in distilled, deionized water (DDI) and titrating to the desired pH. Buffer strength was 1 mM with a normalized total ionic strength of 10 mM (with NaCl). Measurements of pH were conducted with an Orion Research EA 940 expandable ion meter.

Tar Samples Samples from FMGP sites in Portland, Maine, and Baltimore, Maryland, as well as a commercially available coal tar were analyzed. The Port-

land FMGP operated from the late 1800s until at least 1950, using a coal gas process exclusively until the early 1900s at which point simultaneous water gas production was begun. By 1950, the plant produced solely carburetted water gas [214]. Samples were collected from two monitoring wells near a presumed tar source (P1 and P2) and from three wells 400–500 ft downgradient (P3–P5). It is believed that the tar has migrated through the subsurface from source area to the downgradient wells. The Baltimore FMGP operated over a similar time span as the Portland FMGP, and, while complete historic information is not available, is believed to have used water gas and CWG processes for most of the plant's lifespan [214]. Five samples were collected from this site; two samples were collected from a well near a former gas holder during two sampling events (B1-07 and B1-09), one was collected from an adjacent well (B2), and one was collected from a well near a gas holder in a different area of the site (B3). A commercial coal tar (Fisher) was also included in this study (CT). This tar was produced from a byproduct coke oven operating at 1100°C.

Synthetic Tars Synthetic tars were produced using a PAH mixture composed of naphthalene (12.8 wt.%), 1-methylnaphthalene (56.5%), phenanthrene (18.8%), and pyrene (11.9%). Asphaltenes were dissolved in the PAH mix at a concentration of 15 wt.% by sonicating the mixture for 1 hour then allowing to sit for 24 hours. This procedure was repeated until there was no visible indication of undissolved asphaltenes. Resins were dissolved in the PAH mixture at a concentration of 5 wt.%. The asphaltene and resin concentrations chosen were approximately the average concentrations of these fractions in the tars.

2.2.2 Methods

Asphaltene and Resin Determination Two methods were used to extract asphaltenes from the tar. The first was the ASTM D2007 method, which has been used by a number of others investigating FMGP tars [17, 162, 242, 243]. With this method, n-pentane is added to the sample at a 10:1 ratio, the mixture is warmed, stirred, settled for 30 min, and filtered [10]. As noted in the petroleum literature, however, ASTM D2007 is an imperfect method for asphaltene determination, as it allows for the trapping of nonasphaltene compounds [4, 6, 199, 200]. Therefore, asphaltenes were extracted from all tars using an improved method which is described in detail elsewhere [75]. Briefly, this method uses an n-pentane to tar ratio of 40:1 ratio, sonication, and multiple reprecipitations from toluene.

Resins were extracted by reducing the n-pentane solutions from the asphaltene extraction to 50 mL under nitrogen. This solution was passed through an SPE column containing 2 g of Florisil. The Florisil (60-100 mesh) was purchased from Acros Organics, activated at 130°C overnight, and stored in a vacuum desiccator. The saturate and aromatic fractions were eluted with 75 mL of 4:1 n-pentane/dichloromethane (DCM). The resins were eluted from the column with a 1:1 toluene/acetone mixture, then dried under nitrogen and weighed.

Acid/Base Extraction Measurement of the acid/base content of the tars was attempted using acid and base number analyses, however, it was found that the tars were not sufficiently soluble in the solvents used for these methods (methyl isobutyl ketone, 1:1 isopropanol/toluene). Therefore, a gravimetric extraction method based on that of [85] was used to quantify extractable acid and base

fractions. Acids were extracted by shaking 2 g tar with 15 mL 1 M NaOH, centrifuging to separate layers, then pipetting off the aqueous phase. The organic phase was rinsed with three additional 10-mL portions of 1 M NaOH and the aqueous extracts collected. The basic aqueous phase was washed twice with DCM to remove neutral organic compounds, then acidified with HCl. The organic acids were extracted with three 5 mL portions of DCM. The DCM was dried with Na_2SO_4, then evaporated under a gentle stream of N_2. The bases were extracted in the same manner using 10% H_2SO_4 containing 20 g/L Na_2SO_4.

Gas Chromatography Compound identification was conducted with a Hewlett-Packard 5890 GC, coupled with an Hewlett-Packard 5971 quadrapole MS. NIST's AMDIS deconvolution software and 2003 mass spectral database was used to analyze the MS data. Peak identification was based on MS library matches, comparison with standard compounds, and Lee retention index values [21, 111, 117, 126, 220, 223, 229]. Quantification of 39 compounds was conducted on a Hewlett-Packard 5890 II GC equipped with a flame-ionization detector (GC-FID) using internal and external standards.

Fourier Transform Infrared Analysis Tar, asphaltene and resin samples were analyzed on a Nicolet Nexus 870 Fourier Transform Infrared (FTIR) Spectrophotometer from 400-4000 cm^{-1}. Asphaltenes (0.1 g) were analyzed in KBr pellets; the tars and resins (0.1 g) were analyzed as films on KBr windows.

Average Molecular Weight A Knauer K-7000 vapor pressure osmometer (VPO) was used to determine the number-average molecular mass (M_N) of the tar samples and the isolated asphaltenes. Measurements were made in toluene at 60°C using sucrose octaacetate ($\bar{M}$ = 678.59 g/mol) as the calibration standard.

Biphenyl ($\bar{M}$ = 154.21 g/mol) was used as a check standard and was analyzed every five runs or fewer. Measurements were made for solutions containing 5–50 g/kg of the standard compound, tar, or asphaltene. The data was analyzed using the limiting slopes method by fitting data to the truncated virial equation [24]:

$$\triangle E = aC + bC^2 \tag{2.1}$$

where $\triangle E$ is the voltage difference between the sample and reference thermistors, C is the concentration in g sample per kg solvent, and a and b are coefficients to be determined. The molar mass was then calculated from the following relationship:

$$M_N = \frac{K}{a} \tag{2.2}$$

where K is the calibration constant of the instrument for the given solvent and temperature.

Interfacial Tension IFT was measured using the pendant drop method. An optical glass cell (Krüss) was filled with buffer solution, and a drop of tar was suspended from a 1.6-mm outer diameter stainless steel needle. A digital video camera captured images of the drop, and Krüss's Drop Shape Analysis II (DSA2) software was used to determine the native IFT, for which $\triangle\rho$ = 1 g/cm^3. The density of each phase was measured with an Anton Paar DMA 48 density meter and used to determine the actual IFT. The IFT was measured every five minutes, with each measurement consisting of the average of three drop images. Measurements were continued until three consecutive measurements were within 2%, typically between 20–60 min. A minimum of three drops were measured for each

sample. All measurements were conducted at 22 ± 1 °C. IFT was measured for all tar samples, as well as synthetic mixtures containing resins and asphaltenes from samples P1, P3, B1-07, B3, and CT. The accuracy of the method was confirmed with DCM.

2.3 Results

2.3.1 Composition

Fractionation The results of the asphaltene, resin, acid, and base analyses are provided in 2.1. Asphaltenes are a major fraction of all the tars in this study, with concentrations ranging from 12.5 to 23%. The highest asphaltene concentration, 23%, was observed for sample B3. Sample B1-07, collected in 2007, has a concentration of 17.2%, while the samples collected from the same area of the site in 2009, B1-09 and B2, have somewhat lower concentrations (15.2 and 16.1%, respectively). At the Portland site, concentrations in the near-source samples (P1, P2) are 16.5 and 17.0%, while downgradient samples (P3–P5) contain lower concentrations, ranging from 12.5–13.6%. The coal tar sample has an asphaltene concentration of 17.4%. As expected, asphaltene concentrations determined by ASTM D2007 were higher than those determined with the modified method by as much as three times. The difference between the methods is likely due to the trapping of non-asphaltene compounds that are not liberated during a simple precipitate-and-rinse procedure [4, 6, 199, 200].

Resin concentrations were significantly lower than those of the asphaltenes, with a range of 2.6 to 6.7%. Although a clear pattern among samples was not

Table 2.1: Concentration of Asphaltene, Resin, Acid, and Base Fractions. ± 95% CI.

Sample	ASPH (%)	ASPH-ASTM (%)	Resin (%)	Acid (%)	Base (%)
Portland					
P1	16.5 ± 0.3	30 ± 5	4.1 ± 0.7	0.10 ± 0.01	0.05 ± 0.01
P2	17.0 ± 0.2	−−	−−	0.09 ± 0.04	0.07 ± 0.01
P3	13.6 ± 0.8	−−	6.7 ± 0.1	0.73 ± 0.05	0.32 ± 0.06
P4	12.8 ± 0.1	38 ± 8	5.2 ± 0.7	0.94 ± 0.03	0.54 ± 0.02
P5	12.5 ± 0.4	−−	−−	0.9 ± 0.2	0.49 ± 0.07
Baltimore					
B1-07	17.2 ± 0.5	−−	2.1 ± 0.3	0.21 ± 0.03	0.09 ± 0.02
B1-09	15.2 ± 0.5	−−	4.7 ± 0.2	0.24 ± 0.01	0.08 ± 0.02
B2	16.1 ± 0.3	−−	2.6 ± 0.3	0.18 ± 0.02	0.04 ± 0.01
B3	23 ± 1	−−	5.0 ± 0.3	0.22 ± 0.01	0.024 ± 0.004
CT	17.4 ± 0.7	60 ± 4	6.7 ± 0.2	1.8 ± 0.1	2.4 ± 0.2

evident, sample CT and the downgradient Portland samples (P3–P4) tended to have higher concentrations, while the Baltimore and Portland near-source samples tended to be lower. GC-MS analysis indicated that the composition of the resin fractions varied between samples. The resins from the near-source Portland and Baltimore samples were composed of oxygenated compounds, including 9,10-anthracenedione, indanone, fluorenone, and phenalenone. The resins from sample CT contained pyrridinic and phenolic compounds, but no oxygenated compounds were detected. The downgradient Portland samples contained a combination of oxygenated compounds, pyridines and phenols. It is likely that the resin fractions also contain high molecular weight compounds that cannot be observed by standard GC-MS approaches.

The extractable acid and base fractions were present at the greatest concentrations in the CT sample. The concentrations in the downgradient Portland samples are considerably lower than sample CT, but are an order of magnitude

higher than those in the near-source samples. The acid concentrations in the Baltimore samples are higher than the near-source Portland samples, while the base concentrations are similar or lower. GC-MS analysis indicated that for all tars the acid fraction is composed of phenols and hydroxy-PAHs, while the base fraction contains predominately pyridinnic compounds (e.g., quinolines, acridines, azabenzopyrenes). While a similar suite of compounds were present for all tars, the chromatograms indicated significantly different distributions of the compounds. For the field-collected tars, peaks corresponding to the low molecular weight compounds (i.e., phenols, quinolines) were significantly less pronounced relative to the higher molecular weight compounds. This trend was observed most strongly in the near-source Portland and Baltimore samples. The chromatograms for the coal tar acid and base fractions indicated a relative enrichment in the lower molecular weight compounds (i.e., phenol, cresols, and quinoline).

Gas Chromatography For all tars, naphthalene is the dominant compound, with concentrations ranging from 60–104.6 mg/g (6–10.46%). The methylnaphthalenes, acenaphthene, acenaphthylene, phenanthrene, fluoranthene, and pyrene are also major components of the tars. Concentrations of MAHs are considerably lower in sample CT than the field collected samples, while parent PAHs are present at generally higher concentrations. Phenol, cresols and quinoline were present above the quantification limit only in the CT sample, and dibenzofuran was detected at 5 times the highest concentration in FMGP tars. Differences in composition between the near-source and downgradient Portland samples are also observed, primarily manifested as a shift toward lower molecular weight compounds in the downgradient samples. Detailed results of the GC-FID analysis are

provided in the Supporting Information (Table S1).

Molar Mass The $\bar{M}$ of the tars are generally similar, and, with the exception of B3, range from 230 to 260 g/mol. Sample B3 has a somewhat higher $\bar{M}$ of 340 g/mol. The $\bar{M}$ of the asphaltenes extracted from the tars, however, exhibited a greater range. The Baltimore asphaltenes had the highest $\bar{M}$, with a range of 1210–1360 g/mol. The asphaltenes from the near-source Portland samples (P1 and P2) were 1200 and 1140 g/mol, while those of the downgradient Portland tars were between 800 and 870 g/mol. The $\bar{M}$ of the CT asphaltenes was 610 g/mol, significantly lower than the FMGP field samples. It is well established that coal asphaltenes are smaller than petroleum asphaltenes, and it is likely that the variation observed here is a reflection of the source material used to produce the tar [13, 22, 64, 87, 187, 235].

Table 2.2: Average molar mass of tars and asphaltenes

Sample	**Tar**	**Asphaltene**
P1	260 ± 30	1200 ± 100
P2	250 ± 20	1140 ± 30
P3	250 ± 20	830 ± 20
P4	240 ± 20	800 ± 20
P5	230 ± 20	870 ± 20
B1-07	260 ± 30	1240 ± 90
B1-09	260 ± 20	1210 ± 40
B2	270 ± 20	1360 ± 50
B3	340 ± 30	1300 ± 100
CT	240 ± 20	610 ± 50

FTIR The tar, asphaltenes, and resins have generally similar spectra, with predominantly aromatic, aliphatic, and oxygen-containing moieties (Figure S1). Differences between samples can be assessed semi-quantitatively using a variety of

peak absorbance ratios. The use of ratios, as opposed to absolute peak areas, has the advantage of minimizing errors associated with FTIR sample preparation (i.e., variations in KBr pellet concentration or mixing) [196]. The A-factor provides a measure of aromaticity (with lower values indicating greater aromaticity) and is defined as a ratio of peak intensities as follows [60]:

$$\text{A-factor} = \frac{I(2860\ \text{cm}^{-1}) + I(2930\ \text{cm}^{-1})}{I(2860\ \text{cm}^{-1}) + I(2930\ \text{cm}^{-1}) + I(1601\ \text{cm}^{-1})} \tag{2.3}$$

where the peak at 1601 cm^{-1} corresponds to aromatic C=C bonds, 2860 cm^{-1} to $-CH_2$ and $-CH_3$ stretching, and 2930 cm^{-1} to $-CH_2$ stretching. The aromaticity would not be expected to play a major role in controlling the IFT pH-dependence, but does provide useful information regarding the structure of the tars and fractions.

The carbonyl index ($I_{C=O}$) provides a measure of the carbonyl and carboxyl content and is calculated based on the following peak area ratio [100]:

$$I_{C=O} = \frac{A(1800 - 1640\ \text{cm}^{-1})}{A(1800 - 1640\ \text{cm}^{-1}) + A(1640 - 1533\ \text{cm}^{-1})} \tag{2.4}$$

where the range 1800–1640 cm^{-1} includes carbonyl peaks and 1640–1533 represents aromatic ring stretching and C=C bonds. The $I_{C=O}$ includes carboxylic acids, which are known to exhibit pH-dependent surface activity [28, 41, 42], and may therefore be expected to relate to the IFT behavior of the tars.

The A-factor and $I_{C=O}$ for tars, asphaltenes, and resins are presented in 2.3. The A-factors are highest for the Baltimore and near-source Portland samples, with the downgradient Portland tars being slightly more aromatic (lower

Table 2.3: A-factor and $I_{C=O}$ from FTIR analysis.

	A-Factor			$I_{C=O}$		
Sample	Tar	ASPH	Resin	Tar	ASPH	Resin
Portland						
P1	0.82	0.64	0.74	0.31	0.28	0.57
P2	0.80	0.66	–	0.32	0.33	–
P3	0.74	0.53	0.80	0.23	0.09	0.33
P4	0.78	0.53	0.62	0.22	0.09	0.39
P5	0.75	0.57	–	0.20	0.12	–
Baltimore						
B1-07	0.85	0.62	0.73	0.31	0.18	0.55
B1-09	0.87	0.62	0.81	0.30	0.20	0.56
B2	0.85	0.60	0.73	0.32	0.21	0.57
B3	0.80	0.68	0.82	0.32	0.27	0.69
CT	0.48	0.34	0.44	0.03	0.01	0.34

A-factor). The CT sample exhibits significantly greater aromaticity than the FMGP tars. Asphaltenes for all samples are more aromatic than the corresponding tar, with the aromaticity of the resins generally falling between the tars and asphaltenes.

The $I_{C=O}$ values follow a similar trend; they are highest for the Baltimore and near-source Portland tars, somewhat lower for the downgradient Portland samples and lowest for the coal tar sample. The values are lower for the asphaltenes, and significantly higher for the resins.

2.3.2 Interfacial Tension

IFT was measured as a function of pH for all samples; the results for a representative selection of tars is shown in Figure 2.1(a). At pH 7, IFTs ranged from 18.1 mN/m (P1) to 23.7 mN/m (CT). The Baltimore and near source Portland samples (P1 and P2) exhibited an increase in IFT as the pH was decreased to 5, then remained largely unchanged as pH was further reduced to pH 3. Conversely,

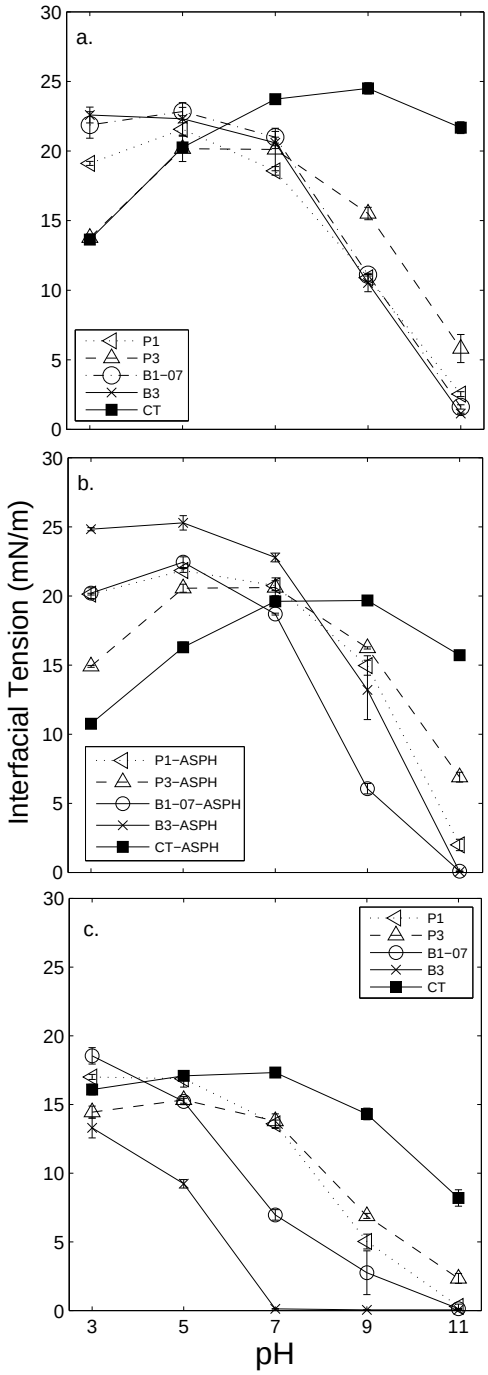

Figure 2.1: Interfacial tension of (a) tars and synthetic mixtures containing (b) asphaltenes and (c) resins as a function of pH. Error bars represent 95% CI. The IFTs of B3 at pH 9 and 11 were below the method quantification limit of 0.05 mN/m.

the IFT of the CT and the downgradient Portland samples (P3–P5) at pH 3 was about 30% lower than at pH 7.

At high pH, all field-collected FMGP tars exhibited a steep decrease in IFT. The greatest reductions between pH 7 and 11 were observed for the Baltimore (92–95%) and near source Portland samples (86–88%). Somewhat lower reductions were observed for the downgradient Portland samples (71–79%), and very little reduction was observed for the coal tar (9%).

To investigate the impact of asphaltene and resin groups on IFT behavior, the IFTs of synthetic DNAPLs containing asphaltenes and resins from a representative selection of samples were measured (Figure 2.1). The IFT behavior of the PAH mixtures containing asphaltenes was generally very similar to that of the corresponding tar, with a similar pattern of IFT decrease at low pH for the P3 and CT samples and high pH for all samples except CT.

The IFT measurements for the PAH mixtures containing 5% resin are shown in Figure 2.1(c). Similar to the tar and asphaltene mixtures, the resin mixtures exhibited an IFT decrease at high pH. For the Baltimore samples (B1-07 and B3), the IFTs decrease with increasing pH over the entire pH range. The low-pH IFT reduction observed for the P3 and CT tars and asphaltenes is not observed for the resins from these samples. The CT resins also exhibit a much greater IFT reduction at high pH than was observed for the tar. With the exception of sample CT at pH 3, the IFTs of the resin mixtures were lower than either the tar or asphaltene mixture at all pH values.

2.4 Discussion

As noted in previous studies, the IFT of field-collected FMGP tars was found to decrease as pH was increased above pH 7 [17, 75, 242]. However, the effect was observed to vary significantly between tars. Unlike the field-collected samples, the IFT of the coal tar sample exhibited only a minor decrease at high pH. Furthermore, the IFT of P3 at pH 11 was over two times greater than that of P1, despite having similar IFTs at pH 5 and 7 and being collected at the same site. Sample P3 also exhibited a decrease in IFT at pH 3, whereas P1 did not. The IFTs of synthetic PAH mixtures containing asphaltenes were very similar to those of the corresponding tar, indicating that, as noted elsewhere, asphaltenes are strong contributers to IFT behavior [242]. Resins, however, were observed to be more interfacially active, with mixtures containing 5% resins producing lower IFTs than mixtures containing 15% asphaltenes over the entire pH range. The tar IFT behavior, however, does not directly correlate with the concentration of resins or asphaltenes (Figure 2.4), indicating that additional factors must be at work.

The reduction of IFT at high pH is believed to be due to the presence of acidic compounds in the tars, which become deprotonated, and subsequently interfacially active, at high pH. While the extractable acid concentrations (2.1) do correlate with the high pH-IFT reduction, the relationship is an inverse one (Figure 2.5). This finding indicates that the extractable acids are not the primary contributers to the observed IFT reduction at high pH. Since the method uses an aqueous extraction technique, it may be that higher molecular weight compounds (i.e.

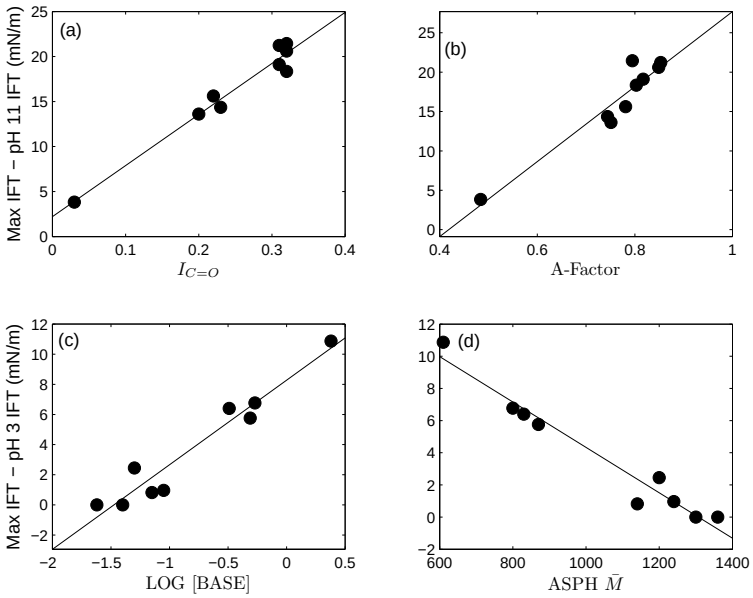

Figure 2.2: The reduction in IFT at high pH as a function of (a) $I_{C=O}$ and (b) A-factor, and the reduction of IFT at low pH as a function of (c) the log of the extractable base concentration and (d) asphaltene molar mass. The lines represent linear least squares fits.

resins and asphaltenes) are excluded. The relatively high water-solubility of the extractable acids may decrease their interfacial activity due to a tendency to diffuse away from the tar-water interface and into the bulk aqueous phase. It has also, however, been found that phenols present in crude oil are not interfacially active at high pH [190], suggesting the possibility that the same is true for the extractable acid fraction (which is composed of phenolic compounds).

The $I_{C=O}$ value, alternatively, provides an indication of the concentration of carbonyl groups. The very strong linear relationship ($R^2 = 0.96$, $p = 4 \times 10^{-6}$) observed between the reduction from the maximum IFT to the IFT at pH 11 versus $I_{C=O}$ is shown in Figure 2.2(a). This correlation strongly suggests that the reduction of IFT is caused by the deprotonation of carboxylic acids at high pH to form surface active compounds, which is consistent with studies of crude oils

[94, 116, 185, 190]. The fact that the reduction of IFT occurs at pH well above the pK_a of most carboxylic acids (generally < 5) is consistent with previous studies of the IFT reduction associated with pure carboxylic acids and petroleum products [28, 41, 42, 72, 77, 165]. These studies have found that the apparent interfacial pK_a of the acids is higher than the bulk pK_a due to the formation of a double layer, resulting in a lower H^+ concentration near the interface [28, 41, 116], or due to intermolecular forces between the acid molecules [101, 102].

It is also worth noting that the extractable acid and $I_{C=O}$ values are inversely proportional (2.6a). The differences are most apparent when comparing the coal tar with the Baltimore samples, which are strongly suspected to be CWG tars. The coal tar contains a large amount of extractable acids (composed of primarily phenolic compounds) but very low $I_{C=O}$ values, while the opposite is true of the CWG tars. This finding is consistent with investigations of coal and petroleum composition, which have found that oxygen is predominately present as phenolic and furanic groups in coals (and even more so in coal-derived liquids), as opposed to petroleum for which carbonyl/carboxyl groups are more pronounced [7, 22, 180, 226, 235].

The IFT reduction at low pH shows a strong positive correlation ($R^2 = 0.93$, $p = 2 \times 10^{-5}$) with the log extractable base concentration, as shown in Figure 2.2(c). The protonation of basic compounds at low pH results in the formation of charged, surface active compounds and the observed reduction in IFT.

While the $I_{C=O}$ values and base concentrations explain the varied response of IFT to pH, the asphaltene $\bar{M}$ and A-factor also correlate well with the IFT reduction at both low and high pH (2.2(b) and (d) and Figure 2.7 (a) and (b)). These

properties would not be expected to impact an IFT-pH relationship, as they do not correspond to acidic or basic compounds. Rather, these correlations are reflective of overall structural differences between tars from different sources. Tars derived from coal maintain certain characteristics from the source material, most notably a high aromaticity with few, short aliphatic chains, a relatively low asphaltene $\bar{M}$, and oxygen present primarily as hydroxyl groups [7, 22, 62, 180, 189, 235]. Each of these is observed for the coal tar used in this study. Similarly, the Baltimore CWG tars retain petroleum-like characteristics: lower aromaticity, longer aliphatic chains, higher asphaltene $\bar{M}$, and greater carbonyl/carboxylic content [22, 235]. The near-source Portland samples are very similar to the Baltimore samples, and are presumed to be CWG tars. The downgradient Portland samples fall between the Baltimore and CT samples in terms of $I_{C=O}$ and asphaltene $\bar{M}$ but have an A-factor similar to the CWG tars, perhaps representing a mixture of multiple tar types, a tar derived from both coal and petroleum sources (e.g., a CWG process using bituminous rather than anthracite or coke), or possibly loss of the larger and more polar asphaltenes by means of environmental alteration (e.g., sorption of these compounds to porous media during tar migration).

The results of this study improve understanding of the relationship between tar composition and IFT behavior. This is especially important in the application of alkaline flushing remediation approaches [75]. Such an approach would have limited effectiveness for tars like the coal tar used in this study. Furthermore, differences in the IFT behavior of tars at a given site would be important to recognize prior to designing an alkaline flushing remediation system.

2.5 Supporting Information

The information in this section was submitted to *Environmental Science and Technology* as Supporting Information to be made available online as a supplement to the paper.

Table 2.4: Results of GC-FID Analysis for Samples P1–P5. All values are mg/g ± 2 standard deviations

Compound	P1	P2	P3	P4	P5
MAHs					
Benzene	1.4 ± 0.1	2.4 ± 0.1	7.2 ± 0.1	7.3 ± 0.2	6.8 ± 0.3
Toluene	3.1 ± 0.4	7.2 ± 0.2	13.1 ± 0.1	12.8 ± 0.8	13.0 ± 0.7
Ethylbenzene	9.9 ± 0.9	12.0 ± 0.3	2.23 ± 0.02	1.4 ± 0.1	1.8 ± 0.1
m/p-Xylene	9.3 ± 0.9	11.3 ± 0.3	8.1 ± 0.1	7.8 ± 0.4	7.9 ± 0.5
Styrene	1.5 ± 0.3	2.42 ± 0.04	8.4 ± 0.1	8.3 ± 0.4	8.1 ± 0.5
o-Xylene	4.9 ± 0.5	5.8 ± 0.1	4.0 ± 0.1	3.8 ± 0.2	3.9 ± 0.2
1,3,5-Trimethylbenzene	2.4 ± 0.1	2.5 ± 0.2	1.6 ± 0.1	1.8 ± 0.1	1.9 ± 0.1
1,2,4-Trimethylbenzene	8.7 ± 0.5	10.6 ± 0.3	9.8 ± 0.8	9.9 ± 0.7	10.6 ± 0.2
1,2,3-Trimethylbenzene	3.5 ± 0.4	3.24 ± 0.03	2.0 ± 0.1	2.2 ± 0.1	2.3 ± 0.2
PAHs					
Indane	3.5 ± 0.2	4.2 ± 0.1	1.0 ± 0.1	1.1 ± 0.1	1.1 ± 0.1
Indene	22 ± 1	26.6 ± 0.9	29 ± 2	30 ± 1	30.2 ± 0.8
Naphthalene	70 ± 2	84 ± 2	103 ± 7	102 ± 7	104.6 ± 0.9
2-Methylnaphthalene	25.9 ± 0.5	26.6 ± 0.9	36 ± 2	39 ± 3	40.0 ± 0.2
1-Methylnaphthalene	17.3 ± 0.7	17.8 ± 0.3	24 ± 2	27 ± 2	28.0 ± 0.5
Biphenyl	2.5 ± 0.3	2.4 ± 0.1	2.6 ± 0.2	2.8 ± 0.3	2.9 ± 0.2
2-Ethylnaphthalene	4.4 ± 0.4	3.1 ± 0.1	1.5 ± 0.1	2.0 ± 0.1	2.1 ± 0.3
Acenaphthylene	10.9 ± 0.4	12.2 ± 0.4	13.9 ± 0.9	15.6 ± 0.7	16.3 ± 0.3
Acenaphthene	4.3 ± 0.1	3.8 ± 0.2	2.5 ± 0.2	2.6 ± 0.2	2.6 ± 0.1
Fluorene	6.3 ± 0.1	6.3 ± 0.3	8.3 ± 0.4	8.5 ± 0.5	8.84 ± 0.02
Phenanthrene	16.9 ± 0.6	17.0 ± 0.9	19 ± 1	18 ± 1	17.6 ± 0.4
Anthracene	5.4 ± 0.3	5.1 ± 0.3	5.4 ± 0.4	5.6 ± 0.4	5.5 ± 0.2
Fluoranthene	6.5 ± 0.2	6.5 ± 0.3	7.3 ± 0.4	6.9 ± 0.4	6.7 ± 0.1
Pyrene	9.4 ± 0.2	9.4 ± 0.4	9.1 ± 0.5	8.2 ± 0.1	8.3 ± 0.1
Benzo(a)anthracene	4.9 ± 0.4	4.8 ± 0.2	4.1 ± 0.4	4.0 ± 0.4	4.0 ± 0.3
Triphenylene/chrysene	3.7 ± 0.3	3.6 ± 0.1	3.1 ± 0.3	3.0 ± 0.3	3.0 ± 0.2
Benzo(b)fluoranthene	1.5 ± 0.2	1.3 ± 0.1	1.5 ± 0.1	1.4 ± 0.1	1.3 ± 0.1
Benzo(k)fluoranthene	2.1 ± 0.1	1.8 ± 0.1	1.8 ± 0.1	1.7 ± 0.1	1.5 ± 0.1
Benzo(a)pyrene	2.9 ± 0.3	2.4 ± 0.1	2.2 ± 0.1	1.9 ± 0.1	1.8 ± 0.2
Indeno(1,2,3-CD)pyrene	1.4 ± 0.1	1.3 ± 0.1	1.20 ± 0.03	1.1 ± 0.1	0.9 ± 0.1
Dibenz(a,h)anthracene	0.58 ± 0.04	0.52 ± 0.03	0.45 ± 0.01	0.43 ± 0.02	0.38 ± 0.03
Benzo(ghi)perylene	1.5 ± 0.1	1.4 ± 0.1	1.27 ± 0.01	1.08 ± 0.04	0.89 ± 0.02
Heterocylcic Compounds					
Benzo(b)thiophene	1.2 ± 0.1	1.3 ± 0.1	3.4 ± 0.2	3.7 ± 0.3	4.0 ± 0.1
Dibenzothiophene	1.16 ± 0.04	1.2 ± 0.1	2.7 ± 0.2	2.7 ± 0.2	2.64 ± 0.01
Dibenzofuran	1.4 ± 0.1	1.56 ± 0.04	2.3 ± 0.1	2.6 ± 0.2	2.52 ± 0.02
Carbazole	0.69 ± 0.03	0.7 ± 0.1	1.3 ± 0.1	1.3 ± 0.1	1.3 ± 0.3
Quinoline	*ND*	*ND*	*ND*	*ND*	*ND*
Phenolics					
Phenol	*ND*	*ND*	*ND*	*ND*	*ND*
o-Cresol	*ND*	*ND*	*ND*	*ND*	*ND*
m/p-Cresol	*ND*	*ND*	*ND*	*ND*	*ND*

Table 2.5: Results of GC-FID Analysis for Samples B1–B3 and CT. All values are mg/g ± 2 standard deviations

Compound	B1-07	B1-09	B2	B3	CT
MAHs					
Benzene	0.5 ± 0.0	0.5 ± 0.1	0.53 ± 0.05	1.4 ± 0.2	0.137 ± 0.001
Toluene	1.4 ± 0.2	2.3 ± 0.3	2.4 ± 0.3	2.0 ± 0.1	0.61 ± 0.01
Ethylbenzene	1.7 ± 0.3	2.1 ± 0.2	2.3 ± 0.2	1.3 ± 0.2	0.66 ± 0.04
m/p-Xylene	3.0 ± 0.4	3.8 ± 0.4	3.9 ± 0.4	7.0 ± 0.9	0.98 ± 0.05
Styrene	*ND*	0.1 ± 0.0	0.15 ± 0.02	0.9 ± 0.2	*ND*
o-Xylene	1.5 ± 0.2	1.9 ± 0.2	2.0 ± 0.2	3.2 ± 0.5	0.33 ± 0.01
1,3,5-Trimethylbenzene	1.0 ± 0.0	0.8 ± 0.1	0.91 ± 0.01	1.49 ± 0.05	0.17 ± 0.01
1,2,4-Trimethylbenzene	3.0 ± 0.1	2.5 ± 0.2	2.76 ± 0.04	6.0 ± 0.3	0.4 ± 0.1
1,2,3-Trimethylbenzene	1.4 ± 0.1	1.1 ± 0.1	1.21 ± 0.02	1.24 ± 0.05	0.15 ± 0.02
PAHs					
Indane	3.9 ± 0.1	3.3 ± 0.2	3.6 ± 0.1	1.1 ± 0.7	5.1 ± 0.2
Indene	3.0 ± 0.2	4 ± 1	4.5 ± 0.1	12.5 ± 0.4	0.64 ± 0.04
Naphthalene	93.0 ± 1.9	84 ± 4	90 ± 1	60 ± 4	88 ± 3
2-Methylnaphthalene	32.9 ± 0.7	30 ± 2	32.5 ± 0.7	33 ± 2	19.9 ± 0.9
1-Methylnaphthalene	23.7 ± 0.6	20 ± 1	21.7 ± 0.2	22 ± 2	9.0 ± 0.4
Biphenyl	4.6 ± 0.1	4.2 ± 0.2	4.54 ± 0.03	2.5 ± 0.3	3.8 ± 0.1
2-Ethylnaphthalene	4.4 ± 0.1	3.2 ± 0.2	3.57 ± 0.02	1.6 ± 0.1	2.1 ± 0.1
Acenaphthylene	1.8 ± 0.1	1.7 ± 0.2	1.9 ± 0.1	3.5 ± 0.1	0.8 ± 0.1
Acenaphthene	11.6 ± 0.4	10.8 ± 0.6	11.8 ± 0.1	4.2 ± 0.3	2.10 ± 0.04
Fluorene	9.0 ± 0.3	8.5 ± 0.5	9.1 ± 0.5	6.3 ± 0.4	21 ± 1
Phenanthrene	22.9 ± 0.8	22 ± 1	23 ± 1	13.3 ± 0.6	49 ± 4
Anthracene	6.1 ± 0.2	6.0 ± 0.3	6.3 ± 0.2	4.1 ± 0.1	8.9 ± 0.5
Fluoranthene	10.0 ± 0.3	9.1 ± 0.5	9.8 ± 0.2	3.4 ± 0.2	28 ± 3
Pyrene	12.0 ± 0.4	11.8 ± 0.6	12.7 ± 0.3	5.9 ± 0.4	23 ± 3
Benzo(a)anthracene	4.3 ± 0.2	3.8 ± 0.2	4.0 ± 0.2	2.3 ± 0.1	7.2 ± 0.9
Triphenylene/chrysene	4.8 ± 0.1	4.1 ± 0.2	4.4 ± 0.1	2.1 ± 0.1	8 ± 1
Benzo(b)fluoranthene	2.8 ± 0.2	2.8 ± 0.2	3.1 ± 0.1	0.83 ± 0.05	5.88 ± 0.04
Benzo(k)fluoranthene	2.7 ± 0.1	2.7 ± 0.1	2.91 ± 0.02	1.1 ± 0.1	4.8 ± 0.4
Benzo(a)pyrene	3.2 ± 0.2	3.4 ± 0.2	3.7 ± 0.1	1.6 ± 0.1	5.4 ± 0.1
Indeno(1,2,3-CD)pyrene	1.6 ± 0.1	1.9 ± 0.1	1.95 ± 0.04	0.72 ± 0.03	3.7 ± 0.1
Dibenz(a,h)anthracene	0.7 ± 0.0	0.6 ± 0.0	0.58 ± 0.01	0.23 ± 0.03	1.6 ± 0.1
Benzo(ghi)perylene	1.7 ± 0.1	1.8 ± 0.1	1.9 ± 0.1	0.66 ± 0.04	2.9 ± 0.1
Heterocylcic Compounds					
Benzo(b)thiophene	4.1 ± 0.1	4.1 ± 0.2	4.5 ± 0.1	3.4 ± 0.3	4.2 ± 0.1
Dibenzothiophene	3.7 ± 0.1	3.1 ± 0.2	3.3 ± 0.1	1.9 ± 0.3	4.4 ± 0.1
Dibenzofuran	4.0 ± 0.1	3.3 ± 0.3	3.60 ± 0.04	1.0 ± 0.1	18.5 ± 0.9
Carbazole	1.4 ± 0.1	1.1 ± 0.1	1.1 ± 0.1	0.31 ± 0.01	6.1 ± 0.2
Quinoline	*ND*	*ND*	*ND*	*ND*	2.8 ± 0.1
Phenolics					
Phenol	*ND*	*ND*	*ND*	*ND*	1.1 ± 0.1
o-Cresol	*ND*	*ND*	*ND*	*ND*	1.0 ± 0.1
m/p-Cresol	*ND*	*ND*	*ND*	*ND*	3.2 ± 0.1

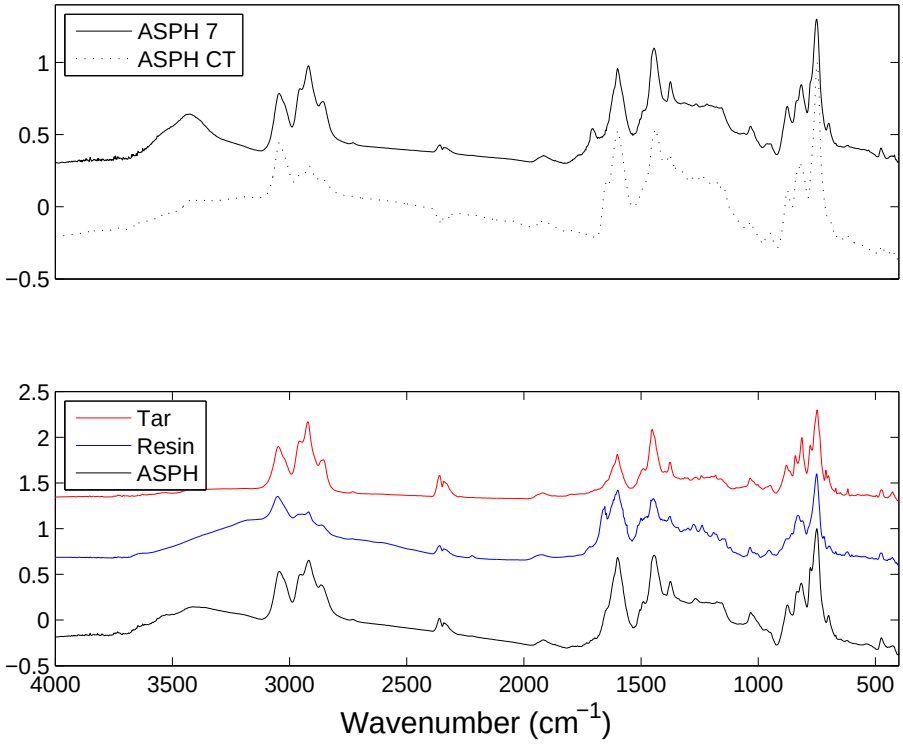

Figure 2.3: FTIR spectra comparing (a) asphaltenes from samples B1-09 and CT, and (b) tar, resin, and asphaltene fractions from sample P3.

Table 2.6: Results of IFT analysis. Units are mN/m. ± 95% CI.

Sample / pH	3	5	7	9	11
Tar					
P1	19.1 ± 0.1	21.6 ± 0.5	18.6 ± 0.3	10.9 ± 0.2	2.5 ± 0.2
P2	19.7 ± 0.1	20.5 ± 0.3	18.5 ± 0.1	10.7 ± 0.7	2.2 ± 0.2
P3	13.8 ± 0.3	20.2 ± 0.9	20 ± 2	15.5 ± 0.4	6 ± 1
P4	13.0 ± 0.5	18.8 ± 0.4	19.7 ± 0.3	13.3 ± 0.8	4.1 ± 0.2
P5	12.8 ± 0.4	18.5 ± 0.1	18.1 ± 0.4	12.9 ± 0.8	4.9 ± 0.8
B1-07	22 ± 1	22.8 ± 0.3	21.0 ± 0.4	11.1 ± 0.1	1.6 ± 0.2
B2	22.31 ± 0.09	22.2 ± 0.9	21 ± 1	12 ± 3	−−
B3	22.6 ± 0.6	22 ± 1	20.6 ± 0.4	10.5 ± 0.6	1.13 ± 0.04
CT	13.6 ± 0.2	20.3 ± 0.2	23.7 ± 0.1	24.5 ± 0.4	21.7 ± 0.4
Asphaltene DNAPL					
P1	20.1 ± 0.1	21.8 ± 0.1	20.8 ± 0.4	15.0 ± 0.7	2.0 ± 0.4
P3	14.91 ± 0.07	20.6 ± 0.3	20.6 ± 0.7	16.24 ± 0.08	6.9 ± 0.4
B1-07	20.2 ± 0.4	22.4 ± 0.4	18.7 ± 0.1	6.1 ± 0.4	0.092 ± 0.003
B3	24.8 ± 0.1	25.3 ± 0.5	22.8 ± 0.3	13 ± 2	0.047 ± 0.008
CT	10.8 ± 0.3	16.3 ± 0.4	19.6 ± 0.4	19.7 ± 0.2	15.7 ± 0.4
Resins DNAPL					
P1	17.0 ± 0.2	16.9 ± 0.6	13.6 ± 0.3	5.0 ± 0.5	0.3 ± 0.2
P3	14.4 ± 0.4	15.3 ± 0.2	13.8 ± 0.5	6.9 ± 0.2	2.3 ± 0.4
B1-07	18.5 ± 0.6	15.2 ± 0.2	7.0 ± 0.4	2.8 ± 1.6	0.13 ± 0.02
B3	13.3 ± 0.7	9.2 ± 0.3	0.12 ± 0.02	¡0.05	¡0.05
CT	16.1 ± 0.4	17.1 ± 0.2	17.33 ± 0.02	14.3 ± 0.4	8.2 ± 0.6

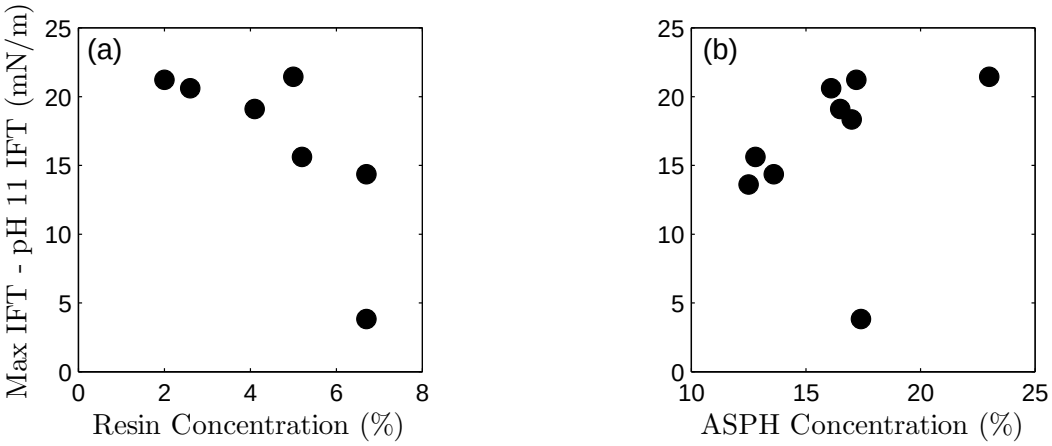

Figure 2.4: IFT reduction at high pH versus (a) resin concentration and (b) asphaltene concentration.

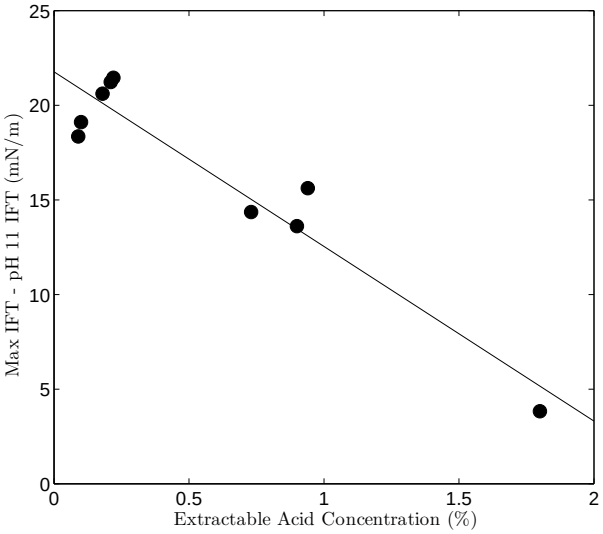

Figure 2.5: Relationship between the extractable acid concentration and the IFT reduction at high pH.

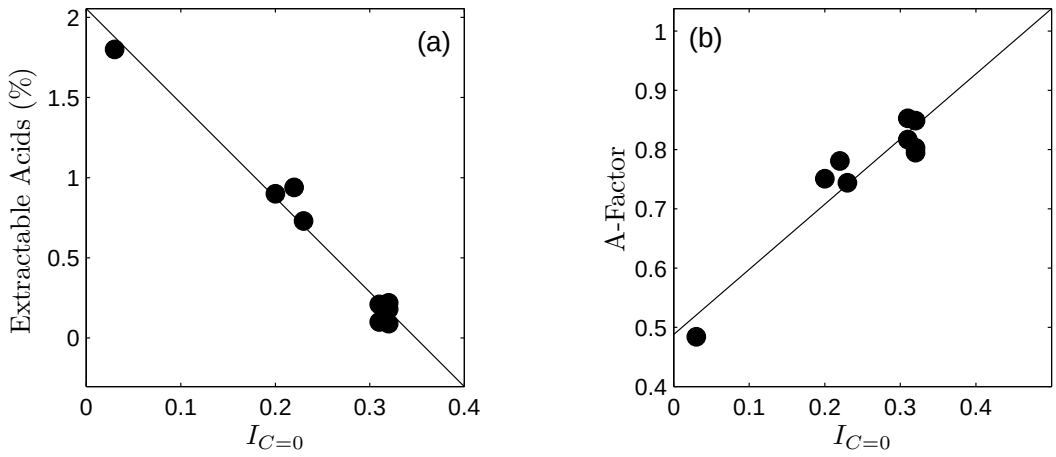

Figure 2.6: Relationships between $I_{C=O}$ and (a) extractable acid concentration and (b) A-factor.

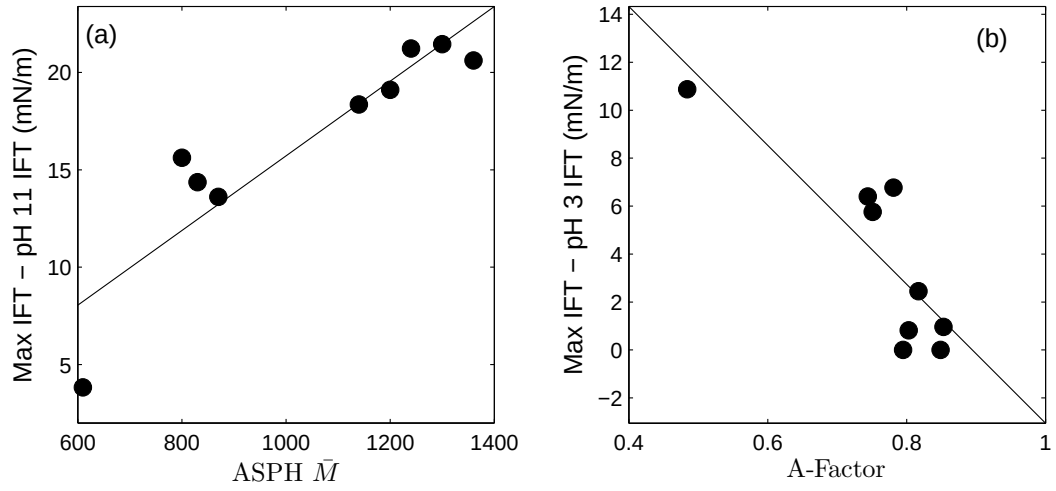

Figure 2.7: Relationship between (a) asphaltene $\bar{M}$ and the IFT reduction at high pH, and (b) the A-factor and the IFT reduction at low pH.

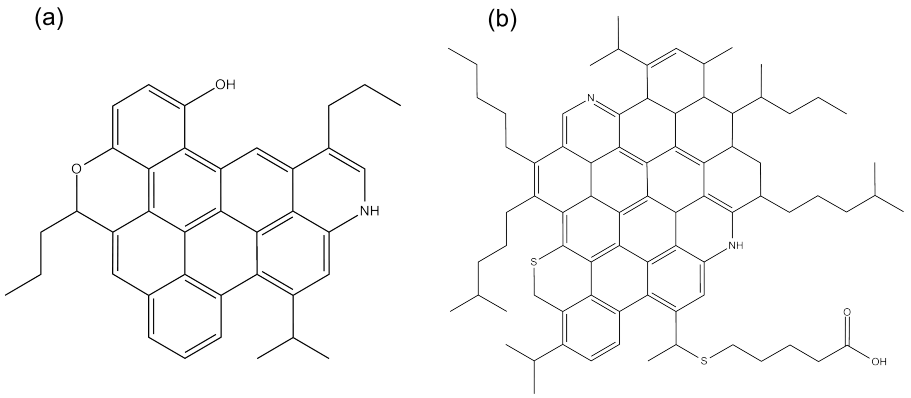

Figure 2.8: Hypothetical coal (a) and petroleum (b) asphaltene structures, based on [3, 22, 64, 87, 132, 138, 139, 177, 189, 201, 235], and consistent with the findings in this work.

CHAPTER 3

MOBILIZATION OF MANUFACTURED GAS PLANT TAR WITH ALKALINE FLUSHING SOLUTIONS[1]

3.1 Introduction

Former manufactured gas plants (FMGPs) were common in the U.S. and Europe between the early 1800s and the 1950s. These plants produced coke or town gas, a flammable gas that was used primarily for heating and lighting. The U.S. Environmental Protection Agency (EPA) estimated that there were between 36,121 and 55,001 FMGPs and related tar and gas processing facilities in the U.S. [217]. The vast majority of these sites are suspected to have had releases of solid and liquid waste products, including tars, cyanide-bearing purifier waste, slag, and coke [70, 128, 217]. The tars, which contain thousands of individual compounds, including many known or suspected carcinogens, are frequently the focus of remediation efforts at FMGPs [147]. Polycyclic aromatic hydrocarbons (PAHs), hydrocarbons composed of two or more fused aromatic rings, are the dominant class of compounds in tars [21, 228, 238, 239]. Asphaltenes, operationally defined as the short-alkane insoluble fraction, are another important component of tars and may account for up to 36% of total tar mass [18, 242]. Asphaltenes are suspected to play a key role in tar interfacial behavior [17, 88, 172, 240–243].

Once released into a porous medium system, tars migrate downward by grav-

[1]Reprinted (adapted) with permission from Hauswirth, S. C., et al. (2012) *Environmental Science and Technology* 46(1), 426–433. Copyright (2012) American Chemical Society.

ity, and because they are denser than water, can move down through the water table until reaching a confining layer (e.g., silt or clay). As the tar migrates through a porous medium, capillary forces act to trap isolated globules of tar in pores, creating a zone of residual saturation. FMGP tars' tendency toward NAPL-wetting conditions results in higher residual saturations than other denser-than-water NAPLs (DNAPLs), such as chlorinated solvents [128, 222]. FMGP tars are persistent in the environment due to their resistance to chemical and biological degradation and the relatively low solubilities of many of the chemical constituents in these complex mixtures. The U.S. EPA estimated the per site clean-up costs in the millions of dollars, and a cumulative total of $128 billion for all of the FMGP and related sites in the U.S. [217]. A number of strategies have been applied or investigated for MGP tar remediation including containment, excavation, natural or enhanced bioremediation, extraction by pumping (with or without the use of chemical additives), chemical oxidation, and thermal methods [15, 65, 79, 96, 120, 128, 134, 204, 211, 215, 217, 232].

Mobilization approaches are attractive alternatives for the remediation of NAPLs since they are less restricted by site access limitations than other methods. The basic principle behind such methods is to reduce the forces trapping the NAPL in the porous media. NAPL droplets are trapped in porous media when capillary forces are greater than the pressure acting on the drop. The capillary number (N_C) is a dimensionless number that represents the ratio of viscous forces to capillary forces, and for vertical flow it is defined as follows [160]:

$$N_C = \frac{q_\alpha \mu_\alpha}{\sigma_{\alpha n} \cos\theta}, \tag{3.1}$$

where q_α is the magnitude of the aqueous phase Darcy velocity, μ_α is the aqueous phase viscosity, θ is the contact angle, and $\sigma_{\alpha n}$ is the interfacial tension (IFT) between the aqueous and NAPL phases. When buoyancy forces are expected to be important, N_C may also be combined with the bond number (N_B) to arrive at the trapping number (N_T), which, for vertical flow, is defined as follows [160]:

$$N_T = \left| N_C + \frac{g k k_{r\alpha} \triangle \rho}{\sigma_{\alpha n} \cos\theta} \right| = \left| N_C + N_B \right|, \tag{3.2}$$

where k is the intrinsic permeability, $k_{r\alpha}$ is the relative water permeability, g is gravitational acceleration, and $\triangle\rho = \rho_\alpha - \rho_n$, where ρ_α and ρ_n are the aqueous and NAPL phase densities. When $\triangle\rho$ is small, as is the case for many FMGP tar-water systems, the contribution of N_B is negligible relative to N_C. It has been well established that residual saturation is a decreasing function of the trapping number [160, 170]. The goal for a mobilization-based remediation technique is to increase N_T, which is typically accomplished by reducing $\sigma_{\alpha n}$ by adding cosolvents or surfactants to the aqueous flushing solution, or by increasing the flow rate. The addition of polymers, such as xanthan gum (XG), to increase μ_α is common in the petroleum industry for enhanced oil recovery (EOR) applications [191], but has seen less use in the remediation field. Investigations of the effect of viscosity on remediation efficiency have tended to focus on the viscosity ratio ($\kappa = \mu_n/\mu_\alpha$) alone, rather than in relation to capillary forces. Giese and Powers [63] performed creosote and synthetic NAPL flushing experiments with XG solutions under NAPL-wet conditions, and found that solutions with $\kappa = 0.1$ resulted in final NAPL saturations roughly half those obtained when using solutions with

$\kappa \geq 1$. Tzimas et al. [212] reported a similarly strong impact for other NAPLs. Some researchers have found that $N_C \kappa^m$, where m is determined by fitting to experimental data, correlates with residual NAPL saturations better than N_C alone [124]. The proposed reason for this is that μ_n, which is not accounted for in the formulation of N_C, impacts NAPL entrapment processes (i.e., snap-off).

The use of alkaline agents to reduce IFT was developed by petroleum researchers for EOR applications. When exposed to high pH aqueous solutions, organic acids in crude oils become ionized, forming natural surfactants that significantly reduce the NAPL-water IFT [36, 37, 90, 237]. One of the major advantages of this approach is cost: commonly used alkaline chemicals, sodium hydroxide (NaOH) and sodium carbonate (Na_2CO_3), are readily available and inexpensive compared to other flushing chemicals such as surfactants [53, 205]. From a remediation perspective, an additional benefit is that both NaOH and Na_2CO_3 are designated as "generally recognized as safe" by the U.S. FDA and used widely as food additives [213]. The feasibility of applying such alkaline-based approaches to the remediation of FMGP tars has not been explicitly investigated; however, it has been shown that when exposed to high pH solutions, FMGP tars exhibit lower NAPL-water IFT and have a decreased tendency to wet porous media [17, 88, 172, 240–243]. This evidence suggests that acidic species are present that react to form surface active compounds, and that alkaline flushing may be effective for tars.

Two field trials of alkaline-surfactant-polymer (ASP) flushing have been conducted on wood-treating creosote, a DNAPL with similarities to, but important differences from, FMGP tars. One of the trials failed due to injection problems

and insufficient site characterization, while the other trial successfully removed 84.3% of the residual creosote [136, 169, 178]. The latter study, however, used a five-stage sequence of chemical flushing solutions and relied more on the use of surfactants than alkaline agents. The surfactant concentration in the main flushing solution was 1.4% while the pH was only 9.2; alkaline flushing solutions for EOR applications are typically above pH 12 [191].

The objectives of this work are: (1) to assess the impact of NaOH solutions on the IFT and contact angle of FMGP tars, (2) to conduct column experiments to assess the potential for the use of such solutions to remediate FMGP tars, and (3) to assess the impact of the remediation on dissolved phase concentrations of 15 PAHs.

3.2 Materials and Methods

All solvents used were ACS Reagent grade or better (Fisher) and water was distilled and deionized (DDI). Stock solutions of 10% NaOH (99.8%; Fisher Scientific) and 5% XG (MP Biomedicals) were prepared and used to make all subsequent solutions for IFT, contact angle, and flushing experiments. The buffer solution was made by dissolving appropriate quantities of NaH_2PO_4 and Na_2HPO_4 in DDI and titrating to pH 7 to produce a 100 mM stock solution. This solution was diluted to 1 mM, and NaCl was added to adjust the ionic strength to 10 mM. The tar used for this study was a tar, believed to be a carburetted water-gas tar, collected from a well at an FMGP in Baltimore, Maryland, USA. Measurements of pH were made with an Orion Research EA 940 expandable ion meter. All experiments were conducted at 22 ± 1 °C.

3.2.1 Fluid Characterization

To determine the tar composition, 0.05 g of tar was dissolved in 10 mL dichloromethane (DCM) containing 2-fluorobiphenyl and m-terphenyl as internal standards. Twenty-six compounds, including the 16 EPA priority pollutant PAHs, were quantified using a Hewlett-Packard 5890 gas chromatograph equipped with a flame ionization detector (GC-FID) and a Hewlett-Packard 7673 autoinjector system. Peak identification was confirmed with a gas chromatograph equipped with a mass spectrum detector (GC-MS). The GC-FID was calibrated with six standard solutions containing concentrations ranging from 0.3 to 500 mg/L.

Asphaltenes were extracted with n-pentane and reprecipitated from toluene. Acids and bases were extracted with 1 M NaOH and 10% H_2SO_4, respectively. Details of the methods used for the asphaltene, acid, and base extractions are provided in Supporting Information.

Density was measured with an Anton Paar DMA 48 density meter. Tar dynamic viscosity (μ_t) was measured with a TA Instruments AR-G2 rheometer at a shear rate of 1 s^{-1}. The viscosity of XG solutions with 0, 0.2, and 0.5% NaOH was measured over a shear rate ($\dot{\gamma}$) range of 10^{-4} to 10 s^{-1}. The solutions containing NaOH were analyzed within 1 hour of being produced.

3.2.2 IFT and Contact Angle

IFT was measured using the pendant drop method. An optical glass cell (Krüss) was filled with aqueous solution (0–1 wt.% NaOH), and a drop of tar was suspended from a stainless steel needle. A digital video camera captured images of

the drop, and Krüss's Drop Shape Analysis II (DSA2) software was used to determine the native IFT, for which $\triangle\rho = 1$ g/cm^3. The density of each phase was measured and used to determine the actual IFT. A schematic of the experimental apparatus is provided in Supporting Information.

Two needle sizes were used, a 16-gauge needle (1.6-mm outer diameter) for IFTs above 1 mN/m, and a 24-gauge needle (0.4-mm diameter) for IFTs between 1 mN/m and 0.05 mN/m, which was the lower limit of quantification for this method. The magnification of the optics system was adjusted as appropriate for each needle size. Optical scale calibration was performed directly by the DSA2 software using needle diameters measured to 0.001 mm with a digital micrometer. DCM-distilled water interfacial tensions were measured as a check of the accuracy of the measurements.

IFT was measured with and without prior equilibration. Equilibration entailed combining the tar and aqueous solution at a 1:3 volume ratio in a centrifuge tube, shaking periodically over a period of 7 days, and centrifuging at 3200 rpm (1700 g) for 20 minutes prior to measurement. This volume ratio was chosen based on an assumed residual tar saturation of 0.25 for the column experiments.

Contact angles were measured using the same instrumentation and software as for the IFT measurements. The measurements were conducted on a 25 mm $\times$ 25 mm quartz slide (Chemglass) placed in the glass cell. The interaction between the tar and the needle used to dispense the drop was found to greatly impact the drop shape, and therefore an inclined plate method was used to determine the advancing (θ_A) and receding (θ_R) contact angles. A drop was dispensed on the quartz slide and the stage was tilted until the drop just began to move along the

surface of the slide. Images captured immediately prior to the movement of the drop were used to measure the angle (through the aqueous phase) on each side of the drop. Contact angle measurements were conducted with the equilibrated tar and aqueous phases.

Between each sample, the glass cell and quartz slide were rinsed sequentially with methanol, n-methylpyrollidinone (NMP), DCM, methanol, and DDI water, followed by a 15 min soak in NaOH-saturated ethanol and a final, thorough DDI rinse.

3.2.3 Column Studies

Column studies were conducted in 2.5-cm inner diameter glass columns that were adjusted to 10 cm in length. The influent and effluent tubing, along with all associated fittings, were constructed of PTFE. Water and flushing solutions were pumped using Harvard Apparatus PHD 4400 programmable syringe pumps. A schematic of the column apparatus is provided in Supporting Information.

The columns were dry packed with a sieved fraction (#25 to #35 mesh) of a natural quartz and feldspar sand, using an air vibrator to ensure complete compaction. This sand was used since it is more representative of natural mineralogy and grain shapes than glass beads or pure quartz sand that are commonly used for this type of experiment. The intrinsic permeability was determined to be $2.2 \pm 0.4 \times 10^{-7}$ cm^2 for a representative column by measuring the head difference between the inlet and outlet over a range of flow rates. Further characterization of the original soil is presented elsewhere [16]. After packing, the column was flushed upward with carbon dioxide for 30 minutes at a rate of 20–30 mL/min to displace

the air from the column. This was followed by a several pore volume flush of pH 7 buffer to displace and dissolve the carbon dioxide. Porosity was calculated for each column based on the bulk density.

Tar was injected upward into the column to achieve a NAPL saturation (S_n) approaching 1. A water flood was conducted to create a residual tar saturation by flushing the pH 7 buffer downward until tar was no longer present in the effluent. Column experiments were conducted using 0.2, 0.35, and 0.5% NaOH solutions with and without the addition of 5000 ppm XG. An additional column was flushed with a 5000 ppm XG solution without NaOH. Chemical flushes were conducted in a downward direction and performed until no tar was present in the effluent. The column was then flushed with several pore volumes of the pH 7 buffer. Effluent samples of between 5 and 30 mL were collected during the water and chemical flushing. Tar removal was quantified by extracting the tar in the effluent samples with sequential portions of DCM, centrifuging and pipetting off the organic phase between each step, and analyzing the extract by GC-FID as described above. Internal standards were added directly to the effluent samples to account for extraction losses and matrix background. The mass of six individual compounds (naphthalene, 1- and 2-methylnaphthalene, acenaphthene, fluorene, phenanthrene) in each sample was determined and divided by the known mass fraction of that compound in the tar. These six values were averaged to provide an estimate of the tar mass in the sample. This approach was tested by adding a known mass of tar to DDI-filled centrifuge vials, and extracting as for the samples. These tests indicated that such an approach was accurate to within 0.4%.

Aqueous-phase concentrations of PAHs were measured before and after the

alkaline flushing for select columns. Aqueous effluent samples were collected in acetonitrile containing deuterated anthracene as an internal standard. The samples were filtered with 0.2 μm PTFE syringe filters (Fisher), allowing the first 1 mL to go to waste. Analysis was performed by high-performance liquid chromatography (HPLC) (Waters 600S controller, 616 pump, and 717 autosampler) equipped with a multi-wavelength fluorescence detector (Waters 2475) as described in [19].

At the completion of the flushing, the soil was split into four segments along the length of the column, each of which was homogenized and divided into three centrifuge vials. Internal standard and Na_2SO_4 (10 g) were added, and the tar was extracted with one 15-mL and three 10-mL portions of DCM. The vials were shaken and centrifuged between each step, and the supernatant from each sample was combined and diluted to 50 mL. The samples were then analyzed by GC-FID.

3.3 Results

The tar composition is presented in 3.1. The density of the tar was 1.0800 ± 0.0004 g/cm^3 (22°C), and the dynamic viscosity was 190 ± 10 (22°C, 1 s^{-1}). Rheological measurements of 5000 ppm XG solutions with 0.5% NaOH and without NaOH are shown in 3.1. The solution containing 0.2% NaOH yielded results very similar to those of the 0.5% solution. The addition of NaOH resulted in a significant reduction of the viscosity. At 0.75 s^{-1}, the shear rate ($\dot{\gamma}$) estimated to occur in the column using the equation of Hirasaki and Pope [84], the viscosity is a factor of 2.7 lower for the solution containing NaOH than the pure XG solution.

Table 3.1: Tar composition and properties. Compound concentrations are the average of 3 injections of 3 samples. All other values are the average of three analyses. All values are ± 95% CI

Compound	Concentration (mg/g)
indane	3.6 ± 0.1
indene	2.2 ± 0.1
naphthalene	95 ± 3
benzo(b)thiophene	3.9 ± 0.1
2-methylnaphthalene	34 ± 1
1-methylnaphthalene	24.4 ± 0.9
biphenyl	5.3 ± 0.2
2-ethylnaphthalene	4.5 ± 0.1
acenaphthylene	2.4 ± 0.1
acenaphthene	11.5 ± 0.4
dibenzofuran	4.1 ± 0.1
fluorene	10.9 ± 0.3
dibenzothiophene	5.5 ± 0.8
phenanthrene	33 ± 1
anthracene	8.9 ± 0.3
carbazole	3.0 ± 0.1
fluoranthene	13.0 ± 0.4
pyrene	14.7 ± 0.5
benzo(a)anthracene	5.3 ± 0.1
chrysene	6.0 ± 0.3
benzo(b)fluoranthene	3.5 ± 0.2
benzo(k)fluoranthene	3.5 ± 0.3
benzo(a)pyrene	4.5 ± 0.5
indeno(1,2,3-CD)pyrene	2.8 ± 0.2
dibenz(a,h)anthracene	1.2 ± 0.1
benzo(ghi)perylene	2.7 ± 0.3
sum	309 ± 4
asphaltenes	168 ± 3
extractable acids	1.8 ± 0.2
extractable bases	0.9 ± 0.3

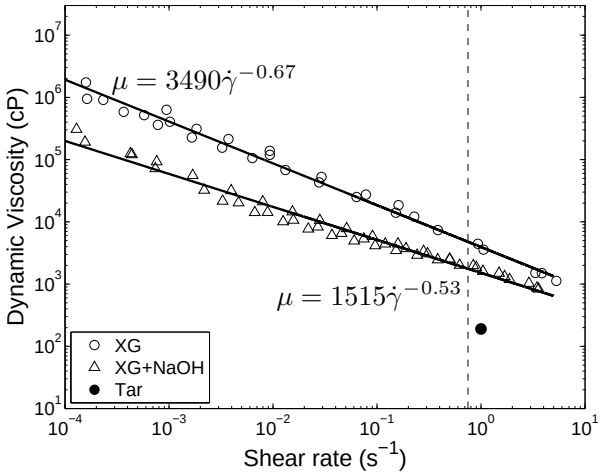

Figure 3.1: Rheology of XG solutions. The results of three analyses and the best-fit power law equation for each solution are shown. The dashed line represents a shear rate of 0.75 s^{-1}

3.3.1 IFT and Contact Angle

The measured IFT for DCM in DDI was 27.7 ± 0.6 mN/m (n=7), in good agreement with literature values, which ranged from 27.4–28.3 mN/m [14, 59, 86, 183, 184]. The IFT from [59] was measured at 20°C, while all other literature values were reportedly measured at room temperature.

The dynamic IFT for unequilibrated tar samples was measured for NaOH ranging from 0.1–1%. A 0.01% NaOH solution was also tested, but the initial IFT was below the quantitative limit of the method. The unequilibrated samples showed significant changes in IFT with time (3.2). Initially, the results show a trend of increasing IFT with increasing NaOH concentration. The trend begins to change at t ≈ 2 min; however, difficulties with drops releasing from the needle prevented measurement of IFT for some NaOH concentrations over longer time scales.

Equilibrium IFT was found to decrease steadily as the NaOH concentration

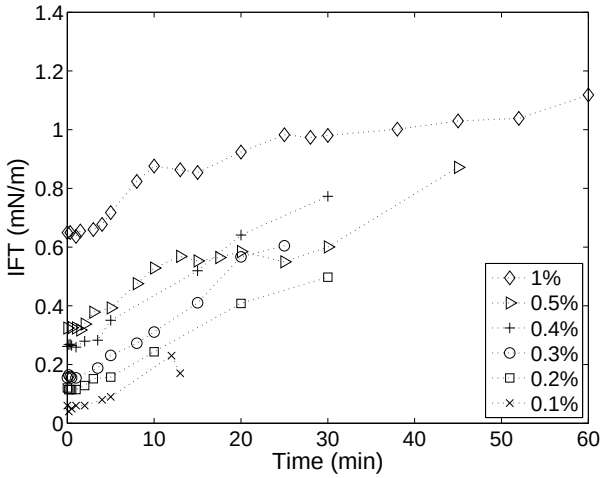

Figure 3.2: Dynamic tar-water IFT. Each point is the average of duplicate values.

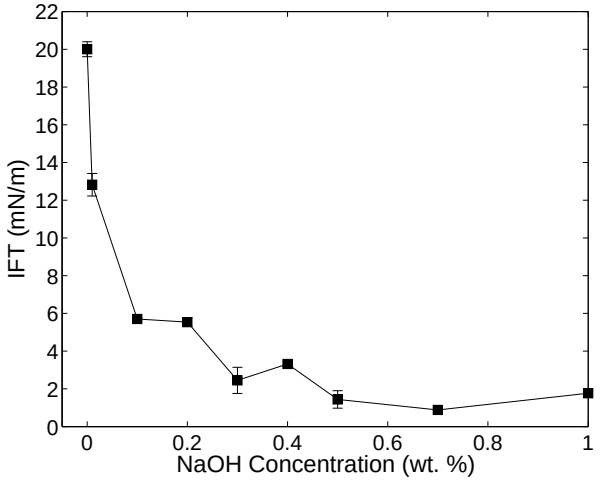

Figure 3.3: Equilibrated tar-water IFTs for a range of NaOH concentrations. Error bars are the 95% CI.

was increased from 0 to 0.5% (Figure 3.3). The IFT changed little between 0.5 and 1%. IFTs for equilibrated samples with NaOH concentrations of 0.1–0.4% were significantly higher than the corresponding non-equilibrated samples. The pH of the solutions was not significantly altered during the equilibration period, except for the 0.01% solution which exhibited a pH reduction from 11.40 to 9.88 (see figure in Supporting Information).

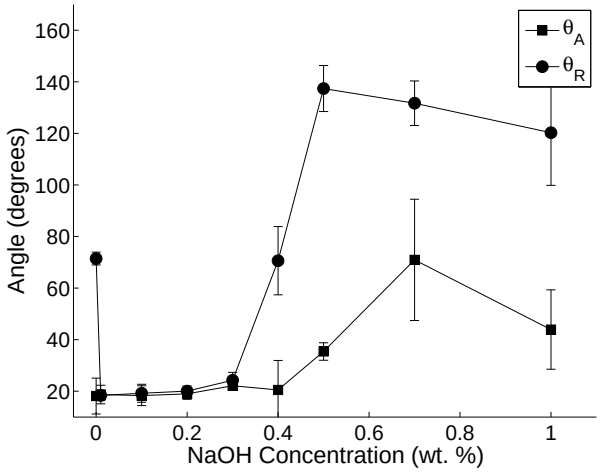

Figure 3.4: Contact angle measurements. Error bars are the 95% CI.

The results of the contact angle analyses are shown in 3.4. With the pH 7 buffer, contact angles were $\theta_R = 71 \pm 2°$and $\theta_A = 18 \pm 7°$. NaOH solutions of 0.01–0.3% resulted in much lower θ_R values, approximately 20°, while the θ_A values were similar to that of the buffer. At 0.4% NaOH, θ_A remained low, but θ_R increased significantly to about 70°. The maximum receding angle (137±9°) occurred at an NaOH concentration of 0.5%, with similarly high values measured for 0.7 and 1% NaOH solutions. Advancing angles for 0.5–1% NaOH solutions ranged from 35–70°. The results indicate that the lower NaOH concentrations (0.01–0.3%) reduce the NAPL-wetting tendency of the system, while the higher concentrations (0.4–1%) increase it. Drummond and Israelachvili [48] reported a similar shift toward

NAPL-wetting for crude oils at high pH and sodium concentrations. The reported cause of the shift is a combination of the reduction of IFT associated with the high pH and the reduction of repulsive forces between the NAPL and solid phase resulting from the high Na^+ concentration.

3.3.2 Column Studies

The results of the column experiments are summarized in Table 3.2 and plots of residual saturation versus pore volumes (PV) flushed for select columns are provided in Figure 3.5 (see Figures 3.9 and 3.10). The column experiments conducted without XG (C1–C3) resulted in relatively low removal efficiencies. The 0.2 (C1) and 0.5% (C3) NaOH solutions removed only 15 and 10% of the residual tar, respectively. The majority of the tar removed by these columns eluted during the first 2 PV of the alkaline flushing. The formation of a NAPL bank was observed in both of these columns immediately after the injection of alkaline solution, but appeared to stall near the top of the column. Column C2 (0.35% NaOH) resulted in a considerably higher tar removal (44%), but required approximately 7 PV to do so. The NAPL bank in this column was visibly more robust than those in C1 and C3, but also became unstable near the top of the column and failed to uniformly pass through the column.

Column C4 was conducted with 5000 ppm XG without NaOH to determine the impact of an increased flushing solution viscosity. This column resulted in the removal of 51% of the residual tar and a final tar saturation of 0.13.

Columns C5–C10 were all flushed with solutions containing an XG concentration of 5000 ppm and varying NaOH concentrations of 0.2% (C5–C6), 0.35%

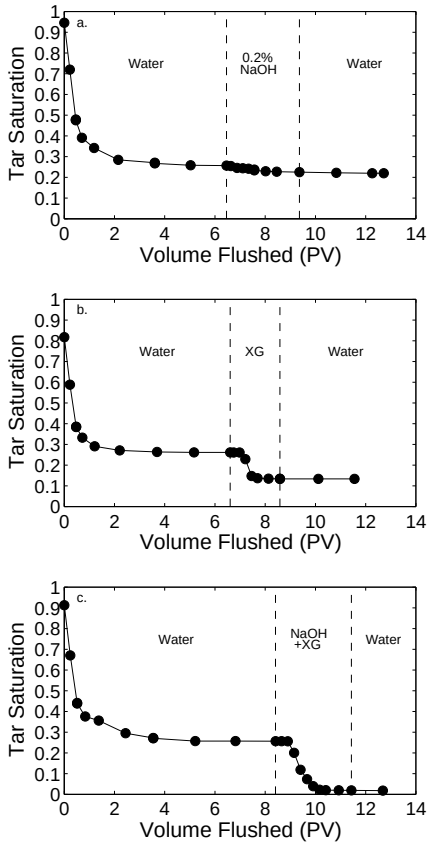

Figure 3.5: Results of select column flushing experiments illustrating the improved tar removal for a combined NaOH + XG solution versus either NaOH or XG alone: (a) C1, 0.2% NaOH; (b) C4, 5000 ppm XG; (c) C5, 0.2% NaOH + 5000 ppm XG.

(C7), and 0.5% (C8–C10). The viscosity ratio for these columns was about 0.1 at $\dot{\gamma} = 0.75$. The lowest final tar saturation (0.018, 93% removal) was obtained for a column flushed with a 0.2% NaOH solution (C5). A duplicate of this column (C6) resulted in a higher 0.037 tar saturation, apparently due to a small amount of tar trapped along the wall of the column. The columns flushed with 0.5% NaOH had somewhat higher final saturations, ranging from 0.043–0.048. Stable NAPL banks were observed in columns C5–C10, and were responsible for the large majority of the tar removal.

Table 3.2: Summary of column experiment results.

Column	Flushing Solution	PV Flushed	Residual S_n	Final S_n	% Removal
C1	0.2% NaOH	2.7	0.26	0.22	15 %
C2	0.35% NaOH	7.0	0.26	0.15	44 %
C3	0.5% NaOH	2.9	0.26	0.24	10 %
C4	5000 ppm XG	3.5	0.26	0.13	51 %
C5	0.2% NaOH + 5000 ppm XG	3.0	0.26	0.018	93 %
C6	0.2% NaOH + 5000 ppm XG	3.2	0.32	0.037	87 %
C7	0.35% NaOH + 5000 ppm XG	2.5	0.28	0.037	85 %
C8	0.5% NaOH + 5000 ppm XG	1.9	0.25	0.048	81 %
C9	0.5% NaOH + 5000 ppm XG	2.3	0.29	0.043	85 %
C10	0.5% NaOH + 5000 ppm XG	2.7	0.29	0.046	84 %

Aqueous phase concentrations of 15 PAHs were measured before and after alkaline flushing for columns C8–C10. Table 3.3 shows the results from column C9, which are typical of the results from the other columns. With the exception of naphthalene, statistically significant reductions in aqueous phase concentrations were not observed.

3.4 Discussion

Consistent with previous MGP tar studies, tar-aqueous IFTs were found to be significantly lower at higher pH than at neutral pH [17, 242]. This work, however, differs from previous studies in that a higher range of pH (7–13.4) was investigated.

Table 3.3: Aqueous phase concentrations before and after alkaline flushing. C_i^{eq} is the equilibrium concentration as calculated with Raoult's law. The pure compound aqueous solubilities (S_i^{aq}) are from [119] and the fugacity ratios (f^S/f^L) are from [51]. All units are μg/L. ± 95% CI.

Compound	S_i^{aq}	f^S/f^L	C_i^{eq}	Preflush	Postflush
naphthalene	31600	0.3	21200	15300 ± 300	11200 ± 800
acenaphthene	3800	0.2	370	264 ± 3	270 ± 50
fluorene	1900	0.16	210	140.3 ± 0.2	140 ± 20
phenanthrene	1200	0.28	210	139 ± 7	130 ± 50
anthracene	44	0.01	57	24.8 ± 0.3	30 ± 2
fluoranthene	210	0.21	17	12 ± 3	18 ± 7
pyrene	13.9	0.11	2.5	10 ± 2	18 ± 5
benzo(a)anthracene	9.3	0.04	1.3	1.4 ± 0.2	4 ± 1
chrysene	1.9	0.0097	1.2	1.2 ± 0.1	3 ± 3
benzo(b)fluoranthene	1.5	0.039	0.16	< 0.16	< 0.16
benzo(k)fluoranthene	8.0	0.013	2.10	0.3 ± 0.6	1.6 ± 0.80
benzo(a)pyrene	4.3	0.03	0.61	1 ± 2	3 ± 2
dibenz(a,h)anthracene	0.5	0.004	0.09	< 0.16	< 0.16
benzo(g,h,i)perylene	0.26	0.003	0.14	0.3 ± 0.1	< 0.16
indeno(1,2,3-cd)pyrene	0.2	0.045	0.01	0.5 ± 0.5	< 0.16

Instantaneous measurements indicated that, after a large decrease between pH 7 and 11.40, IFT generally increased with increasing NaOH concentration over this range. Measurements of equilibrated samples, however, showed that lower concentrations of NaOH resulted in relatively high IFTs. At an NaOH concentration of 0.1%, for example, there is a difference of two orders of magnitude between the instantaneous and equilibrium IFT. The difference between instantaneous and equilibrium IFT is much less for solutions with higher NaOH concentrations (0.5–1%). The change in pH during the equilibration period was minimal for all but the 0.01% NaOH solution, indicating that other mechanisms are responsible for the observed behavior.

A number of petroleum researchers have investigated the dynamic IFT behavior of crude oils or synthetic oil-acid mixtures contacted with alkaline solutions [31, 35, 36, 53, 143, 208, 224]. The basic mechanisms described in these studies are as follows. The organic acids (HA) present in the oil or tar are deprotonated

at the interface, resulting in a reduction of IFT. The ionized acids (A^-) may subsequently diffuse into the bulk aqueous phase or combine with Na^+ ions to form surface-inactive soap molecules (NaA). The rates and equilibria associated with these processes are responsible for dynamic IFT behavior. The differences between instantaneous and equilibrium IFT at different NaOH concentrations observed in this study could be explained by the higher ionic strength of the 0.5–1% NaOH solutions suppressing the diffusion of A^- away from the interface. However, the formation of NaA would simultaneously be expected to increase, leading to an increase in IFT. An alternate explanation relates to the presence of multiple acidic species within the tar. Chiwetelu et al. [35] showed that the dominant interfacially active species changed from a higher solubility, lower pK_a acid to a less soluble, higher pK_a acid as NaOH concentration was increased. A more recent study [237] found that higher molecular weight petroleum acid fractions required a higher alkaline concentration to produce an IFT reduction, but resulted in much less time-dependent IFTs as compared to the lower molecular weight fractions. It is likely that a similar range of species is present in FMGP tars and contributes to the observed differences in dynamic IFT behavior at different NaOH concentrations.

The columns conducted without XG indicate that the reduction of IFT does result in the mobilization of tar, but that the amount of removal is not correlated with either the instantaneous or equilibrium IFT values. The column flushed with 0.35% NaOH, which had intermediate equilibrium and instantaneous IFTs, resulted in a significantly lower final saturation than both the 0.2% NaOH column (with a lower instantaneous IFT) and the 0.5% NaOH column (with a lower equi-

librium IFT). NAPL-wet conditions are associated with reduced NAPL recovery, potentially explaining the low recovery for the 0.5% NaOH solution, which exhibited a high contact angle [49, 88]. The reason for the limited effectiveness of the 0.2% NaOH flushing solution is not immediately clear. A study investigating alkaline flushing for a heavy crude oil similarly reported that the solution producing the minimum IFT was ineffective and that a higher alkaline concentration was required [47]. Interactions between the alkaline solution and the solid phase (i.e., silica dissolution, ion exchange), and the increase of IFT as equilibration occurs likely play a role.

The addition of XG to the flushing solutions greatly improved tar removal, with final tar saturations below 0.05 for all NaOH concentrations. The final tar saturations for 0.2 and 0.35% NaOH were similar, ranging from 0.018 to 0.037. The slightly higher final saturation in the 0.5% NaOH columns may be due to the high contact angles observed at this NaOH concentration. The addition of XG not only increases the viscous forces acting on NAPL droplets, directly resulting in increased tar mobilization, but also greatly reduces instabilities in the flushing front, decreasing flow bypassing, and improving NAPL bank formation. Based on the results of the column experiments, it is clear that the combination of IFT reduction and increased flushing fluid viscosity results in much more effective tar removal than either mechanism alone.

The use of NaOH-XG flushing solutions successfully removed between 81–93% of the residual tar within about 1.5 PV without the use of costly surfactants. Although several obstacles exist, such a method may have a place in the remediation of MGP sites. As is the case with all mobilization-based methods, complete

removal of contaminants is not attained, with final saturations of 0.018–0.048. At these saturations, aqueous phase PAH concentrations would not be expected to be significantly reduced [230], and secondary remediation techniques, such as cosolvent flushing, *in situ* chemical oxidation (ISCO), or bioremediation would likely be required to achieve remediation goals.

3.5 Supporting Information

The information in this section was submitted to *Environmental Science and Technology* as Supporting Information to be made available online as a supplement to the paper.

Asphaltene Separation Procedure Asphaltenes were determined as the mass of tar that is insoluble in n-pentane. Others investigating FMGP tars have typically used ASTM D2007 to separate asphaltenes [10, 17, 162, 242]. Briefly, with this method n-pentane is added to the sample at a 10:1 ratio, the mixture is warmed, stirred, settled for 30 min, and filtered. An improved asphaltene method was developed based on combining several techniques described in the literature, which included extended precipitation times [200], the use of a sonication bath [6], and reprecipitation from toluene [199]. Specifically, asphaltene concentration was determined by adding 60 mL of n-pentane to 1.5 g of tar, sonicating for 15-minutes, and settling for 24 hours. The liquid portion was decanted through a vacuum filtration apparatus with a 0.2-μm nylon filter. The precipitate remaining in the flask was dissolved in toluene at a ratio of 10 mL per gram of solid, and sonicated until the solids were completely dissolved. The asphaltenes were then reprecipitated by adding n-pentane at a ratio of 50 mL per mL of toluene-

asphaltene, allowed to settle for 30 minutes, and vacuum filtered using the same filter as was used in the first stage. The flask and precipitate were rinsed with an additional 200 mL of n-pentane and dried under vacuum and weighed. This analysis was conducted for each of the samples in triplicate.

Acid and Base Extraction Acids were extracted by shaking 2 g of tar with 15 mL of 1 M NaOH, centrifuging to separate layers, then pipetting off the aqueous phase. The organic phase was rinsed with three additional 10-mL portions of 1 M NaOH and the aqueous extracts collected. The basic aqueous phase was washed twice with DCM to remove neutral organic compounds, then acidified with HCl. The organic acids were extracted with three 5-mL portions of DCM. The DCM was dried with Na_2SO_4, then evaporated under a gentle stream of N_2. The bases were extracted in the same manner using 10% H_2SO_4 containing 20 g/L Na_2SO_4.

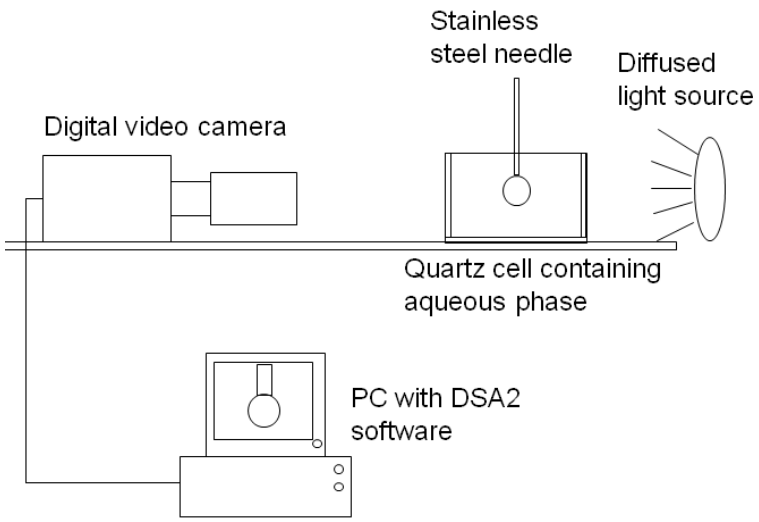

Figure 3.6: Diagram of the IFT and contact angle apparatus.

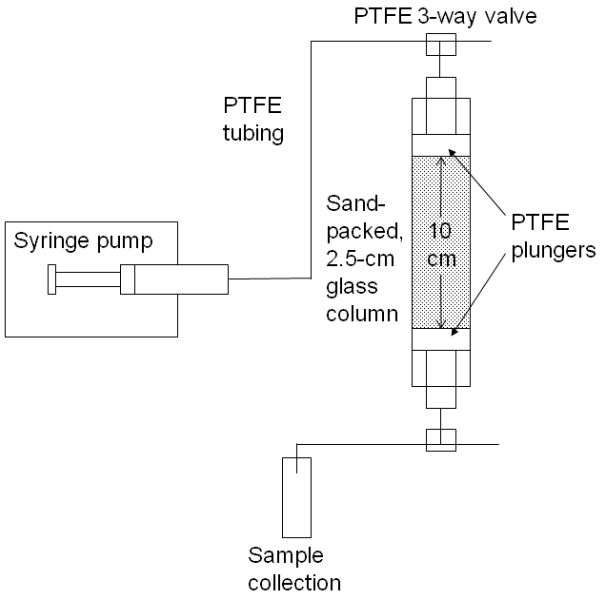

Figure 3.7: Diagram of the column apparatus.

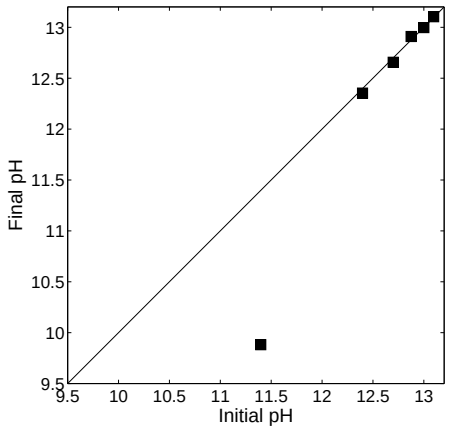

Figure 3.8: Alkaline solution pH before and after equilibration for IFT measurements

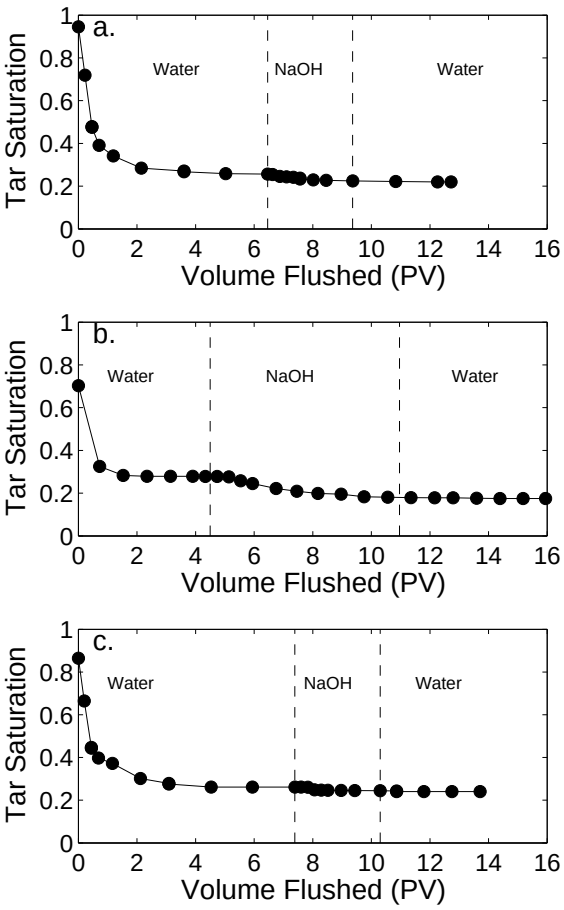

Figure 3.9: Results of column experiments conducted without XG: (a) 0.2% NaOH, (b) 0.35% NaOH, (c) 0.5% NaOH

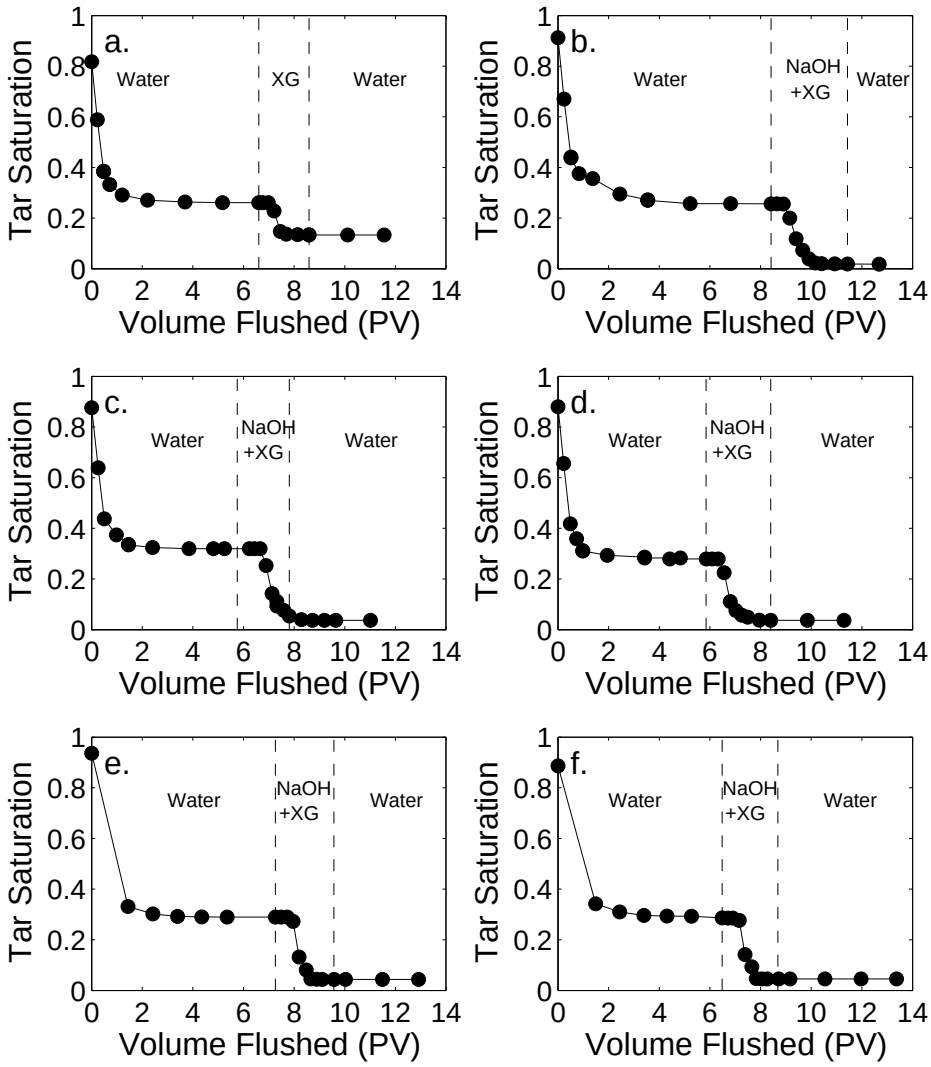

Figure 3.10: Results of column experiments conducted with XG: (a) C4, 5000 ppm XG, (b) C5, 0.2% NaOH + 5000 ppm XG, (c) C6, 0.2% NaOH + 5000 ppm XG, (d) C7, 0.35% NaOH + 5000 ppm XG,(e) C9, 0.5% NaOH + 5000 ppm XG,(f) C10, 0.5% NaOH + 5000 ppm XG

CHAPTER 4

A COMPARISON OF PHYSICOCHEMICAL METHODS FOR THE REMEDIATION OF POROUS MEDIUM SYSTEMS CONTAMINATED WITH TAR

4.1 Introduction

The remediation of former manufactured gas plant (FMGP) tars presents a number of challenges. These tars were generated during the historical gasification of coal and/or petroleum to produce "town gas," a flammable gas used for heating, cooking and lighting between the early 1800s and the 1950s [18]. Onsite disposal practices and leaks in plant infrastructure frequently resulted in the release of tars to the subsurface, and contaminated FMGP sites are estimated to number in the tens of thousands [70, 217]. FMGP tars are viscous, dense non-aqueous phase liquids (DNAPLs). They are mixtures of thousands of compounds, including mono- and polycyclic aromatic hydrocarbons (MAHs and PAHs), heterocyclic compounds, asphaltenes, and alkanes [18, 76, 128]. PAHs are the dominant compound class, but high molar mass, heterocyclic compounds, such as asphaltenes and resins, may account for up to 36% of the tar [17, 18, 76, 172, 242].

Once released to the subsurface tars may become trapped in porous media due to capillary forces, forming a residual. The residual saturation of tars is typically higher than that of other NAPLs due to their high viscosity and ability to alter the wettability of porous media [172]. Because tar components have low aqueous solubilities, they can persist in the subsurface for decades to centuries

under natural conditions, thereby acting as a long term source of groundwater contamination. Remediation through direct extraction or pump-and-treat have proven largely ineffective [2, 11, 130]. Where NAPL-contaminated source zones are readily accessible, direct removal by excavation, followed by *ex situ* treatment or offsite disposal, is often a preferred approach [128]. However, in many cases excavation may be precluded due to onsite structures, utilities, or roads, the depth of the contaminated zone, geologic limitations, or other considerations. In such situations, *in situ* techniques provide an alternative approach. *In situ* remediation involves containing, treating, or removing contaminants without excavation, and encompasses a wide-range of techniques, including surfactant or cosolvent flushing, *in situ* stabilization (ISS), enhanced bioremediation, vapor extraction, chemical oxidation or reduction, and thermal methods. We restrict our discussion here to chemical methods that result in removal of contaminants from the system through one of the following mechanisms: (1) mobilization of NAPL, (2) solubilization, and (3) chemical oxidation.

The application of *in situ* remediation techniques for FMGP tars has received relatively little study compared to petroleum, chlorinated solvents and other NAPLs. A summary of previous studies investigating mobilization- and solubilization-based methods for FMGP tars is provided in Table 4.1. A relatively early field trial used hot water flooding to remove 1,500 gal of FMGP tar from a site in Stroudsburg, PA, however, mobile tar remained after the project [96, 216]. Subsequent research on mobilization-based approaches has focused on modifying interfacial properties (contact angle and interfacial tension) by varying the aqueous phase pH [17, 75, 76, 88] or viscosity [63], or by adding surfactant

[46]. Of these studies, only Hauswirth, et al. (2012), which used a NaOH-xanthan gum (XG) solution (alkaline-polymer; AP solution), resulted in a large reductions of tar mass (80–93%), with final tar saturations of 0.018 to 0.048 [75].

Studies of the application of solubilization techniques for FMGP tars were initially directed at the use of cosolvents (Table 4.1), however, the mixed results and difficulty associated with injecting large volumes of potentially hazardous solvents at field sites shifted focus away from this approach [78, 128, 162, 179]. Although no studies have used surfactants to solubilize separate-phase tar, researchers have reported the removal of 60–80% of PAHs from FMGP soils, supporting the use of surfactants to solubilize tar components [99, 168, 232, 236].

A number of researchers have investigated the use of *in situ* chemical oxidation (ISCO) techniques for the remediation of FMGP soils, with widely varying results (Table 4.2). Fenton's reagent, H_2O_2 activated with ferrous iron, has been reported to degrade 30–100% of PAHs in FMGP soils [91, 98, 110, 118, 142, 174] . Similarly, PAH degradation as a result of persulfate ($S_2O_8^{-2}$) activated by ferrous iron, heat, or magnetite ranged from 0–100% [91, 106, 141, 167, 175, 219]. Only one study, Blanchard (2010), investigated the application of ISCO for separate-phase FMGP tar. This study indicated that combined H_2O_2-ozone with and without added surfactant was shown to reduce volatile organic compounds (VOCs) by 79% and naphthalene (NAP) by 31%, resulting in a large increase in the viscosity of the tar [20]. The reason for the wide range of reported PAH degradation is unclear, and highlights the need for additional research.

A major short-coming of the existing FMGP remediation literature is the lack of studies illustrating "complete" remediation of systems containing NAPL-phase

Table 4.1: Summary of Literature Studies of Mobilization and Solubilization Approaches Applied to FMGP Tars and Soils

Study	Major Findings	Ref.
Mobilization		
Johnson and Fahy, 1997	Hot water flushing removed 1,500 gal of tar from a field site, but significant quantities of mobile tar remained after the project.	[96, 216]
Barranco and Dawson, 1999	Tar-water IFT and quartz-water-tar contact angle are decreasing functions of pH.	[17]
Hugaboom and Powers, 2002	NAPL-wetting conditions observed at low pH, water-wet at high pH. IFT is decreasing function of pH. Tar saturations of 0.47, 0.30, and 0.29 reported for flushing solutions of pH 4.7, 7.2, and 9.2, respectively.	[88]
Giese and Powers, 2002	In tar-wet columns, increasing viscosity of water flushing solution ($\kappa = 0.1$) decreased tar saturation from ~ 0.45 to ~ 0.19. Tar saturation in water wet columns was ~ 0.19 regardless of flushing solution viscosity.	[63]
Dong, et al., 2004	Polaxamine surfactants reduced tar-water IFT and alter wetting behavior. Qualitatively shown to mobilize tar in sand-packed 2D cell.	[46]
Hauswirth, et al., 2012	NaOH + xanthan gum solutions mobilized >90% of residual tar in column studies, with final S_n of 0.018 –0.048.	[75]
Solubilization		
Peters and Luthy, 1993	Tar solubility greatly increased in n-butylamine, acetone, isopropanol.	[162]
Roy, et al. 1995	Flushing tar-contaminated sand columns (tar saturation = 0.04–0.25) with 80–100% n-butylamine removed large quantity of tar, but tar remained in effluent after 40 PV [179]	
Hayden and Van der Hoven, 1996	Field-collected, tar-contaminated soil columns flushed with 100% isopropanol, resulting in a maximum tar removal of 19.4%	[78]
Birak, et al. 2011	Field-collected, FMGP soil-packed columns flushed with 95% methanol resulted in 80–90% removal of total PAHs after 10 PV	[19]
Wu, et al., 2010	PAHs extracted from FMGP soil using biodiesel, Tween 80, and cyclodextrin. Biodiesel most effective, removing 80–100% of PAHs.	[232]
Pinto and Moore, 2000	Very high concentrations ($> 1000\times$ CMC) of Tween 80 resulted in removal of $> 50\%$ of PAHs from aged, PAH-contaminated soils in batch experiments.	[168]
Joshi and Lee, 1996	Nonionic surfactant (Igepal) at concentrations up to 10% removed up to 80% of PAHs from FMGP soil in column studies.	[99]
Yeom, et al., 1995	Nonionic surfactants (Brij 30, Triton X-100, Tween 80) at concentrations up to 3% removed a maximum of 25% of total PAHs from aged FMGP soil.	[236]

Table 4.2: Summary of Literature Studies of ISCO Approaches Applied to FMGP Tars and Soils

Study	Type	Oxidant/Activator	Removal	Comments	Ref.
Kulik, et al., 2006	Batch	H_2O_2 + Fe^{+2}	88.5% of 3- and 4-ring PAHs	Creosote-spiked sand	[110]
Nam, et al., 2001	Batch	H_2O_2+ Fe^{+2}	90–100% of NAP, FLE, PHE	Field-collected FMGP soil	[142]
Lemaire, et al., 2013	Column	H_2O_2+ Fe^{+2}, $S_2O_8^{-2}$+H_2O_2	18–35% total PAH	Field-collected, PAH-contaminated soil	[118]
Jonsson, et al., 2007	Batch	H_2O_2+ Fe^{+2}	9–43% PAHs	Field soils	[98]
Reddy and Chandhuri, 2009	Batch	H_2O_2+ Fe^{+2}	Field soil: 30–40% total PAH, spiked clay: 44–91% PHE	FMGP field soils, PHE-spiked clay	[174]
Isosaari, et al., 2007	3D Cell	H_2O_2+ Fe^{+2}, $S_2O_8^{-2}$+Fe^{+2}	H_2O_2: 26–30% total, $S_2O_8^{-2}$: 12–35%	FMGP contaminated clayey soil	[91]
Nadim, et al. (2006)	Batch	$S_2O_8^{-2}$+Fe^{+2}	75–100% of seven PAHs	PAH-contaminated field soil	[141]
Killian, et al. (2007)	Batch	$S_2O_8^{-2}$+Fe^{+2}	56–92% total PAH	FMGP soil, PAH degradation dependent on Fe^{+2} delivery	[106]
Peyton, et al., 1990	Column	$S_2O_8^{-2}$	52% total PAH	Field soil, no activator	[167]
Usman, et al., 2012	Batch	$S_2O_8^{-2}$ ± magnetite ± Fe^{+2}	0% for field soil	PAH-contaminated field soil	[219]
Richardson, et al., 2011	Batch, Column	$S_2O_8^{-2}$ + heat	Batch: 47%, Column: $\sim$ 0% total PAH	PAH-contaminated field soil	[175]
Blanchard (2010)	Batch	H_2O_2 + Ozone ± Surfactant	Without surfactant: 31% NAP, with surfactant: 25%	FMGP tar, viscosity increased after oxidation	[20]

tar. Although the success of a remediation project may in practice be defined by any number of regulatory or site specific criteria, two common, general remediation goals are: (1) a reduction of contaminant mass to a given value (e.g., soil clean-up levels, removal of mobile NAPL) and (2) reduction of contaminant concentrations in groundwater to regulatory or risk-based standards [44, 109, 197]. Few existing studies have investigated the remediation of tar-containing systems, and of these, only Hauswirth, et al. (2012) and Roy, et al. (1995) reported removal of a large percentage of residual tar. Hauswirth, et al. (2012) was also the only study, including those investigating remediation of FMGP soils, to assess the impact of the remediation on dissolved-phase PAH concentrations (which was found to be minimal). There is therefore a need to investigate remediation methods capable of removing large fractions of residual tar and significantly reducing aqueous-phase PAH concentrations.

The overall goals of this work are to identify effective remediation methods for porous medium systems containing FMGP tars and to improve understanding of the physicochemical mechanisms associated with these methods. Specific objectives are to (1) assess the magnitude and efficiency of tar mobilization using alkaline and surfactant flushing solutions in column studies, (2) assess tar solubilization with surfactant solutions in batch and column experiments, (3) determine the feasibilty of the use of base-activated persulfate for the oxidation of tar, (4) measure the impact of each flushing experiment on the dissolved-phase effluent concentrations of tar components, and (5) improve understanding of the mechanisms associated with mobilization, solubilization, chemical oxidation, and compositional dynamics of FMGP tars.

4.2 Background

4.2.1 NAPL Mobilization

The goal of mobilization-based remediation methods is to remove NAPL as a phase or an emulsion, by overcoming the capillary forces trapping NAPL within the porous media. The trapping number (N_T) represents the ratio of viscous to capillary and gravity forces, and is defined as [160]:

$$N_T = \sqrt{N_C^2 + 2N_C N_B \sin\beta + N_B^2} \tag{4.1}$$

where

$$N_C = \frac{q_\alpha \mu_\alpha}{\gamma_{\alpha n} \cos\theta} = \text{Capillary Number}, \tag{4.2}$$

$$N_B = \frac{g k k_{r\alpha} \triangle\rho}{\gamma_{\alpha n} \cos\theta} = \text{Bond Number}, \tag{4.3}$$

α and n subscripts represent aqueous and NAPL phases, respectively, β is the angle of flow from horizontal, q_α is the magnitude of the aqueous-phase Darcy velocity, μ_α is the aqueous-phase viscosity, $\gamma_{\alpha n}$ is the NAPL-aqueous interfacial tension (IFT), θ is the contact angle, g is gravitational acceleration, k is the intrinsic permeability, $k_{r\alpha}$ is the aqueous-phase relative permeability, and $\triangle\rho$ is the density difference between the phases. Residual NAPL saturation is a decreasing function of N_T, which can be increased by altering any of the variables in Equations (4.1–4.3). In practice, most schemes involve decreasing $\gamma_{\alpha n}$ and/or in-

creasing μ_α. The former is frequently accomplished with surfactants or cosolvents [131, 159, 160]. Viscosity is increased by adding viscosifying agents, which include xanthan gum (XG), guar gum, and synthetic polyacrylamide polymers. Increasing the viscosity of the flushing solution has the additional advantage of reducing the mobility ratio, defined as [63]:

$$M = \frac{\lambda_\alpha}{\lambda_n} = \frac{k_{r\alpha}\mu_n}{k_{rn}\mu_\alpha} = \frac{k_{r\alpha}}{k_{rn}}\kappa, \tag{4.4}$$

where λ is the fluid mobility and κ is the viscosity ratio (μ_n/μ_α). A decreased M reduces fingering, promotes a stable displacement front, and allows the flushing solution to enter less permeable zones in heterogeneous systems. While mobilization is capable of efficiently removing a large fraction of NAPL, complete removal is not obtained even under ideal conditions [95, 131, 197] . A mobilization approach, then, can lower the risk of future migration of NAPL and reduce the overall NAPL mass in the system. To significantly reduce contaminant groundwater concentrations, however, requires near complete NAPL removal, and therefore a mobilization approach alone will not generally achieve groundwater-based remediation goals [173, 230].

4.2.2 Tar Dissolution

The dissolution of tar components has been found to be reasonably well described by Raoult's law [113, 114, 163]:

$$C_i^{\alpha,eq} = \frac{\chi_i^n C_{i,p}^\alpha}{F_i}, \tag{4.5}$$

where $C_i^{\alpha,eq}$ is the equilibrium aqueous-phase concentration of species i, χ_i^n is the mole fraction of species i in the NAPL phase, $C_{i,p}^{\alpha}$ is the pure compound solubility, and F_i is the solid-liquid fugacity ratio. The pure-compound solubility of tar components varies by several orders of magnitude, which results in selective depletion of more soluble, lower molecular weight compounds as they dissolve into groundwater. This phenomenon increases the viscosity of the tar, and with sufficient time may result in the formation of a semi-solid [97, 122, 161, 164]. Solubilization-based remediation techniques may accelerate this process [179]. As the viscosity increases, intra-NAPL diffusion rates and, therefore tar-water mass transfer rates, will decrease. This will impact both mass flux from source zones and the effectiveness of remediation strategies dependent on mass transfer [154]. Equilibrium aqueous-phase concentrations of individual components are also affected by compositional dynamics. Changes in χ_i^n of several orders of magnitude may occur as higher solubility compounds become depleted from the tar, resulting in proportional changes in compound solubility (decreasing for high solubility compounds, increasing for low) [122].

4.2.3 NAPL Solubilization

Solubilization techniques involve increasing the solubility of NAPL components (or compounds sorbed to soil) in the aqueous phase, allowing for greatly increased contaminant removal through groundwater extraction. Increasing solubility can be accomplished with cosolvents or surfactants. The increase in solubility for

cosolvents follows the log-linear relationship [234]:

$$\log C_i^{cs} = \log C_i^{\alpha,eq} + \sigma_i^{cs} f_c \tag{4.6}$$

where C_i^{cs} is the equilibrium solubility of species i in cosolvent, C_i^{α} is the solubility in pure water, σ_i^{cs} is the cosolvency power, and f_c is the volume fraction of cosolvent.

Surfactants increase the solubility of hydrophobic compounds by forming micelles above a critical surfactant concentration (critical micelle concentration; $C_{ss,m}$). The micelles form due to the amphiphilic nature of surfactant molecules; the molecules associate such that the hydrophobic portion of the molecule orient toward the interior of the micelle, forming a hydrophobic core into which compounds can partition. Above the critical micelle concentration, the increase in solubility follows the relationship [52]:

$$C_i^{ss} = C_i^{\alpha,eq} + \mathrm{MSR}(C_{ss} - C_{ss,m}) \tag{4.7}$$

where C_i^s is the apparent solubility of species i in the surfactant solution, MSR is the molar solubilization ratio (moles i dissolved per mole of surfactant above $C_{ss,m}$), and C_{ss} is the surfactant concentration. Solubilization-based approaches are inherently less efficient than mobilization since they are limited by interphase mass transfer processes [67, 73, 158]. In field applications, difficulties arise due to porous media heterogeneity: aqueous flushing solutions preferentially flow into high permeability materials, bypassing contaminants present in low permeability

units [136, 197]. Recent research, however, has shown that preferential flow due to heterogeneity can be reduced by increasing the viscosity of the flushing solution with natural, food-grade polymers (i.e., XG) [40, 43, 127, 153, 176, 194, 195, 206, 207, 233, 244].

4.2.4 Chemical Oxidation

ISCO involves the injection of chemical oxidants to degrade organic contaminants in the subsurface. A number of oxidants have been applied for ISCO remediation, including permanganate, ozone, H_2O_2, and persulfate. The effectiveness of a given oxidant is dependent on the contaminants of interest, groundwater chemistry, soil oxidant demand, contaminant distribution, and site geology [192, 193]. Permanganate, for example, cannot oxidize benzene, a common component of petroleum, industrial solvents, and FMGP tars. Iron-activated H_2O_2 is highly reactive and non-selective, and therefore tends to be short-lived in porous media, especially where there is a high concentration of organic matter [166]. Other oxidants, including persulfate, are longer lived in the subsurface [202]. Because oxidation reactions occur primarily in the aqueous phase, mass transfer may be a limiting factor when large quantities of NAPL are present, especially when in the form of pools. As a result, ISCO is most often prescribed for dissolved or sorbed contaminants or when low residual NAPL saturations are present [192, 193].

4.3 Methods and Materials

4.3.1 Materials

All reagents were obtained from Fisher Scientific and were ACS Reagent grade or better. Standards for the 16 Priority Pollutant PAHs were obtained from Spex Certiprep. Additional compound standards were made from neat compounds obtained from Fisher Scientific. The tar sample used in this study was collected from a well at an FMGP in Baltimore, Maryland. The composition is presented in Table 4.3; detailed tar characterization data is available elsewhere (Sample B1-07 in [76]). The sand used in the column experiments was 20/30-mesh Accusand, which has an mean grain diameter of 0.713 mm and an intrinsic permeability (k) of 2.3×10^{-6} cm^2 [188]. Triton X-100, (TX100) was used as the surfactant.

4.3.2 Analytical Methods

Density was measured with an Anton Paar DMA 48 and pH was measured with an Oakton PC700 pH meter. Interfacial tension ($\gamma_{n\alpha}$) and advancing and receding contact angles (θ_A and θ_R) on quartz were measured using the pendant drop inclined plate methods, repsectively, as described elsewhere [75, 76]. Tar was equilibrated with aqueous solution (1:3 tar-aqueous ratio) for 3 days prior to interfacial tension and contact angle measurements. Viscosity was measured with a TA Instruments AR-G2 rheometer. All measurements were conducted at 22±1°C.

The dissolved-phase concentrations of 15 PAHs (see Table 4.3) were measured by high-performance liquid chromatography (HPLC) using a Waters 600S

controller, 616 pump, and 717 autosampler equipped with a Waters 2475 multi-wavelength fluorescence detector. The solvent flow and wavelength programs were designed to maximize peak separation and detector sensitivity. All samples were filtered with a 0.22-μm syringe filter prior to analysis. Calibration was performed with 15-compound standards at five concentrations, with deuterated anthracene (AD10) as an internal standard. The sum of the 15 PAHs is hereafter referred to as "SPAH".

Dichloromethane (DCM) extracts of effluent samples and sand from the column experiments were analyzed with a Hewlett-Packard 5890 gas chromatograph with a flame ionization detector (GC-FID). The column was a 30-m, fused silica DB-5 (95% methyl- 5% phenyl-methylsiloxane) capillary column with an inner diameter of 0.25 mm and a 0.5-μm film thickness. The chromatographic conditions were as follows: injector 300°C, detector 310°C, constant helium carrier flow of 1 mL per minute, splitless injection, initial oven temperature 40°C, hold 2 minutes, increased linearly at 4°C per minute to 310°C, hold 5 minutes. Twenty-six PAHs and heterocyclic compounds were quantified (Table 4.3). Standard solutions of the 26 compounds at six concentration levels, using 2-fluorobiphenyl and m-terphenyl as internal standards, were used for calibration. The sum of the 26 PAHs is hereafter referred to as "TPAH".

4.3.3 Batch Experiments

Batch tests were conducted to determine the solubility of PAHs in TX100. 30 mL of TX100 solution, at concentrations of 0, 0.1, 0.2, 0.35, 0.7, 0.9, and 1.0 wt.%, was combined with 1 g of tar in centrifuge vials and tumbled at 22°C for 5 days.

Table 4.3: PAHs included in this study, their concentration in the tar (C_i^{tar}) and pure phase solubility(S_i).

Compound	Abbr.	PAHs by HPLC[a]	C_i^{tar} (mg/g)[b]	S_i (mg/L; 25°C)[c]
Indane	INA		3.9 ± 0.1	109.1
Indene	INE		3.0 ± 0.2	332.4
Naphthalene	NAP	X	93.0 ± 1.9	31.6
Benzo(b)thiophene	Bbt		4.1 ± 0.1	130
2-Methylnaphthalene	2MN		32.9 ± 0.7	25.4
1-Methylnaphthalene	1MN		23.7 ± 0.6	28.045
Biphenyl	BiPh		4.6 ± 0.1	7
2-Ethylnaphthalene	2EN		4.4 ± 0.1	8
Acenaphthylene	ACY		1.8 ± 0.1	16
Acenaphthene	ACE	X	11.6 ± 0.4	3.8
Dibenzofuran	DBF		4.0 ± 0.1	4.75
Fluorene	FLE	X	9.0 ± 0.3	1.9
Dibenzothiophene	DBT		3.7 ± 0.1	1.47
Phenanthrene	PHE	X	22.9 ± 0.8	1.2
Anthracene	ANT	X	6.1 ± 0.2	0.044
Fluoranthene	FLU	X	10.0 ± 0.3	0.21
Pyrene	PYR	X	12.0 ± 0.4	0.0139
Benzo(a)anthracene	BaA	X	4.3 ± 0.2	0.0093
Triphenylene/chrysene	CHR	X	4.8 ± 0.1	0.0019
Benzo(b)fluoranthene	Bbf	X	2.8 ± 0.2	0.002
Benzo(k)fluoranthene	BkF	X	2.7 ± 0.1	0.0008
Benzo(a)pyrene	BaP	X	3.2 ± 0.2	0.0043
Indeno(1,2,3-CD)pyrene	IND	X	1.6 ± 0.1	0.0002
Dibenz(a,h)anthracene	DaA	X	0.7 ± 0.0	0.0005
Benzo(ghi)perylene	BgP	X	1.7 ± 0.1	0.00026

a. PAHs quantified by HPLC
b. Ref. [76]
c. Ref. [119]

The vials were then centrifuged, and the aqueous phase was sampled using a gas-tight syringe. The aliquot was diluted to 10 mL with isopropanol (IPA) and AD10 was added. The solution was filtered with a 0.2-μm PTFE syringe filter and analyzed by HPLC to determine the aqueous-phase PAH concentrations. Batch experiments were conducted in triplicate at 22±1°C.

4.3.4 Column Experiments

The column experiments were conducted in 2.5-cm inner diameter glass columns (Ace Glass) with bed lengths that are adjustable using PTFE plungers. The columns were packed using two different procedures depending on the desired initial tar saturation (S_n). For experiments with high initial tar saturations, the column was packed using the method described in Ref. [75]. Briefly, dry sand was added to the column, vibrated, then flushed with CO_2 followed by DDI to achieve an initially water saturated condition. Tar was injected upward such that S_n approached 1. DDI was then flushed downward until tar was no longer present

in the effluent, thereby producing a residual tar saturation. For experiments with a low initial tar saturation (OX1-OX3, OX2C, OX3C), after adding sand to the column, the desired volume of tar was injected directly into the sand. The plungers were positioned to allow several cm of headspace and the column was shaken vigorously by hand for 5 min to evenly coat the sand grains with tar. The plungers were then pushed together, vibrating with an air vibrator several times to compact the sand, and CO_2 and DDI flushes were conducted to saturate the column with water. Flushing for all experiments was performed with programmable Harvard Apparatus syringe pumps, and all tubing and fittings were PTFE. Oxidant flushes were performed at 2 mL/h; all other flushes were conducted downward at a rate of 5 mL/h. Flushes for mobilization were conducted until no tar was present in the effluent. All experiments were conducted at 22±1°C.

During flushing, effluent samples were collected continually in 40 mL centrifuge vials. Samples containing tar were extracted with DCM and the extract was analyzed by GC-FID, as described elsewhere [75]. The mass of tar was calculated based on the mass of six PAHs (NAP, 1MN, 2MN, ACE, FLE, and PHE) in the sample and the concentration of each compound in the tar. This method was found to be accurate to within 0.4% [75]. For experiments using surfactant, the samples were centrifuged at 1500 g for 5 min prior to extraction by DCM, and the aqueous phase was sampled, diluted and analyzed by HPLC. Both solubilized PAHs and mobilized tar were quantified.

To assess the impact of each remediation method on dissolved-phase PAH concentrations, aqueous samples were collected and analyzed at the end of each stage. Prior to collecting the samples, the remediation solutions were flushed out of

the column. Solutions containing XG were displaced with a series of six solutions with decreasing XG concentrations to minimize viscous fingering, followed by a DDI flush. Once XG and remediation fluids were removed from the column, a 12-h stop flow was conducted prior to sampling. Aqueous samples (5 mL) were then collected in 10-mL volumetric flasks containing pre-weighed IPA (5 mL) and an appropriate concentration of AD10. The flasks were brought up to volume with IPA, filtered through a 0.22-μm syringe filter, and analyzed by HPLC. Sampling was performed for a minimum of 2 PV.

At the end of each experiment, the column sand was divided into segments of equal length, and each segment was placed in a 40-mL centrifuge vial. Anhydrous sodium sulfate and internal standards (2-fluorobiphenyl and m-terphenyl) were added, and the sand was extracted with successive additions of DCM. The extractant was analyzed for 26 PAHs by GC-FID.

Table 4.4: Experimental Summary. HBRM columns are from Ref. [75]

Column	L (cm)	S_n^0	Soln.	NaOH	TX100	persulfate	XG	PV Flushed
HBRM-C1[a]	10.00	0.26	ALK	0.2%	–	–	–	2.7
HBRM-C4[a]	9.80	0.26	XG	–	–	–	0.5%	3.5
HBRM-C5[a]	9.15	0.26	AP	0.2%	–	–	0.5%	3.0
HBRM-C6[a]	10.05	0.32	AP	0.2%	–	–	0.5%	2.1
OX1	9.50	0.028	Ox-L	0.2 M	–	50 g/L	–	52.1
OX2	10.65	0.031	Ox-H	0.2 M	–	274 g/L	–	19.1
OX2C	10.51	0.030	CTRL	0.2 M	–	–	–	20.9
OX3	13.95	0.037	S-Ox	0.2 M	0.5%	274 g/L	–	32.5
OX3C	13.90	0.037	S-CTRL	0.2 M	0.5%	–	–	33.4
MSR1A - Stage 1	11.70	0.20	ASP	0.2%	0.5%		0.5%	3.0
MSR1A - Stage 2			Ox-H	0.2 M	–	274 g/L		10.0
MSR1B	11.35	0.20	ASP	0.2%	0.5%		0.5%	2.9
MSR1C - Stage 1	11.75	0.18	ASP	0.2%	0.5%		0.5%	2.9
MSR1C - Stage 2			DDI	–	–	–	–	50
MSR2 - Stage 1	11.71	0.21	AP	0.2%	–	–	0.5%	2.3
MSR2 - Stage 2			SP	–	0.5%	–	0.5%	6.6
MSR2 - Stage 3			Ox-H	0.2 M	–	274 g/L	–	9.6
MSR3	11.70	0.19	SP	–	0.5%	–	0.5%	20.9
MSR4	11.62	0.20	SP	–	0.5%	–	0.5%	20.2

a. HBRM data from Ref. [75]

The experimental details of the column experiments are summarized in Table 4.4. The general approach was to initially perform a mobilization stage to reduce the tar saturation, followed by a secondary, and in some cases tertiary treatment

using solubilization and/or ISCO methods. Mobilization was conducted with one of three flushing solutions: (1) AP: 0.2 wt.% NaOH, 0.5% XG, which was the most effective solution tested in Ref. [75], (2) SP: 0.5% TX100 surfactant, 0.5% XG, or (3) ASP: 0.2% NaOH, 0.5% TX100, 0.5% XG. XG was added to all solutions to increase viscous forces, create a favorable viscosity ratio, and ensure a stable displacement. Solubilization experiments used a 0.5% TX100, 0.5% XG solution. The XG was used in this case for front stability and due to the recent interest in using viscosifying agents for improved chemical delivery [176, 194, 244]. Chemical oxidation with base-activated persulfate was investigated, using one of three oxidant solutions: (1) 50 g/L persulfate, 0.2 M NaOH (OX-L), (2) 274 g/L persulfate, 0.2 M NaOH (OX-H), and (3) 274 g/L persulfate, 0.2 M NaOH, and 0.5% TX100 (S-OX).

4.4 Results

4.4.1 Fluid Properties

Table 4.5 shows the physical properties of the fluids used in this study. The flushing solutions are denser than DDI in all cases; only the 0.2% NaOH, 0.5% XG solution and solutions containing 0.2 M NaOH are denser than the tar. The 0.5% XG solutions had a viscosity of 2000 cP, roughly 10 times that of the tar ($\kappa \approx 0.1$). NaOH and TX100 reduced the tar-aqueous interfacial tension significantly, as shown in Figure 4.1. NaOH alone reduced the IFT from a value of 20.0 $\pm$ 0.4 mN/m for DDI to 5.70 $\pm$ 0.05 mN/m for 0.1% NaOH. The IFT was similar for 0.2% NaOH (5.5 $\pm$ 0.2 mN/m), then decreased to 1.4 $\pm$ 0.5 mN/m as the

NaOH concentration was increased to 0.5%. TX100 produced similar results, with an IFT of 5.5 ± 0.1 mN/m at a concentration of 0.1% and 3.0 ± 0.1 mN/m at 0.5%. A combined 0.1% TX100, 0.2% NaOH solution had a higher IFT (6.5 ± 0.5 mN/m) than 0.2% NaOH alone, but as the TX100 concentration was increased to 0.2% then to 0.5% (holding the NaOH concentration constant at 0.2%), the IFT fell below values for either additive alone, with a minimum of 0.56 ± 0.06 mN/m.

Table 4.5: Physical properties of fluids used in this study. All values at 22 ± 1°C.

Fluid	ρ (g/cm^3)	pH	μ (cP)	$\gamma_{\alpha n}$ (mN/m)	θ_A	θ_R
DDI	0.9977	–	0.95[a]	20.0 ± 0.4	18 ± 7	71 ± 2
Tar	1.0080	–	190	–	–	–
XG	0.9990	6.7	2000	–	–	–
ALK	1.0014	12.7	–	5.5 ± 0.2[b]	34 ± 7	36 ± 6
AP	1.0097	12.7	2000	5.5 ± 0.2[b,c]	–	–
SP	0.9992	–	2000	3.0 ± 0.1[c]	103 ± 3	138 ± 8
ASP	1.0049	12.7	2000	0.56 ± 0.06[c]	60[d]	60[d]
Ox-H	1.1871	13.2	–	–	–	–
S-CTRL	1.0152	13.3	–	–	–	–

a. Ref. [104]
b. Ref. [75]
c. $\gamma_{\alpha n}$ measured for solution without XG
d. Estimated value, see text.

Wetting behavior varied significantly between solutions. NaOH resulted in water-wetting conditions and nearly equal advancing and receding contact angles. Conversely, TX100 resulting in NAPL-wetting conditions with a significantly greater θ_R. Difficulties were encountered during measurement of the contact angles for the combined NaOH-TX100 solution due to the dark coloration of the aqueous phase and the tendency of the tar drop to move on the quartz slide when the stage was tilted even slightly off-level. A sufficiently clear image of the drop was obtained to estimate a value of 60°for both θ_A and θ_R.

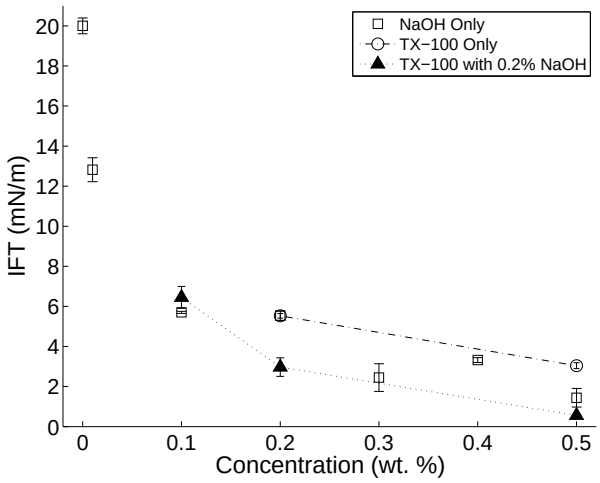

Figure 4.1: Interfacial tension as a function of aqueous-phase composition. Data for "NaOH Only" from Ref. [75].

4.4.2 Surfactant Batch Test

The data from the surfactant batch tests was used to calculate the MSR using Equation 4.7 by fitting a line to $(C_i^s - C_i^{\alpha,eq})$ versus $(C_s - C_{s,m})$ (Table 4.6). The micellar partitioning coefficient (K_m) was calculated using the equation [52]:

$$K_m = \frac{\chi_i^m}{\chi_i^\alpha} = \frac{MSR}{(1 + MSR)C_i^{\alpha,eq}\bar{V}_\alpha}, \tag{4.8}$$

where χ_i^m is the mole fraction of the component in the micelles, χ_i^α is the mole fraction of the component in water, $C_i^{\alpha,eq}$ is the equilibrium aqueous-phase concentration given in Equation 4.5, and V_α is the molar volume of water. Absolute solubility in surfactant solution was generally inversely proportional to PAH molecular mass, while the opposite was true for the ratio of $C_i^{ss}/C_i^{\alpha,eq}$. For the 0.5% TX100 solution, the results of the surfactant batch experiments indicated PAH solubility enhancements of 1–5 orders of magnitude (Figure 4.2).

Table 4.6: Solubilization of PAHs in TX100 solutions in batch studies

PAH	MSR	R^2	$\log K_m$
NAP	4.44×10^{-1}	0.99	4.96
ACE	3.86×10^{-2}	0.95	6.08
FLE	1.95×10^{-2}	0.97	6.28
PHE	5.46×10^{-2}	0.99	6.72
ANT	1.20×10^{-2}	0.98	6.84
FLU	1.55×10^{-2}	0.99	7.51
PYR	1.14×10^{-2}	0.99	7.55
BaA	5.40×10^{-3}	0.97	7.28
CHY	5.20×10^{-3}	0.97	7.51
BbF	3.30×10^{-3}	0.96	7.39
BkF	1.60×10^{-3}	0.96	7.51
BaP	3.30×10^{-3}	0.95	7.29
IND	6.00×10^{-4}	0.94	7.26
DaA	1.30×10^{-3}	0.96	6.69
BgP	1.80×10^{-3}	0.97	7.93

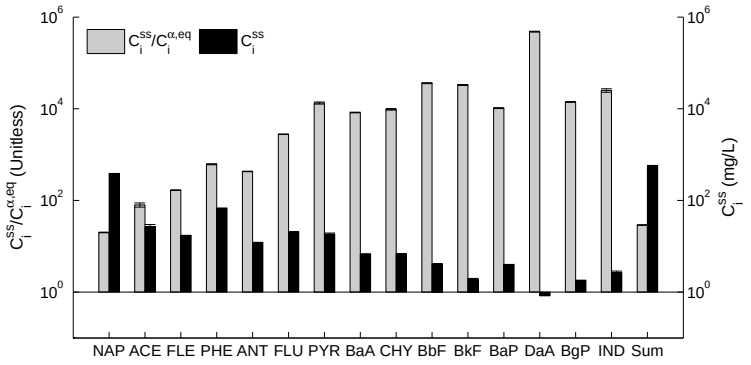

Figure 4.2: Solubility of tar components in 0.5% TX100 solution and the ratio of the solubility in surfactant solution to aqueous solubility.

4.4.3 Mobilization and Solubilization

The results of mobilization experiments are summarized in Table 4.7. Column experiments conducted as part of a previous study (HBRM-C1, HBRM-C4, HBRM-C5, HBRM-C6) indicated that a 0.2% NaOH, 0.5% XG solution mobilized 88.4–92.9% of residual tar by lowering interfacial tension and increasing viscous forces (HBRM-C5 and HBRM-C6) [75]. A 0.2% NaOH solution alone resulted in a much lower 14.5% removal due to flow instabilities resulting in fingering and bypassing of tar-filled pores (HBRM-C1). A 0.5% XG solution removed 50.4% of residual tar due to increased viscous forces alone (HBRM-C4).

Columns MSR1A-C were initially flushed with the ASP solution to investigate the effect of added surfactant on alkaline flushing solutions. Based on effluent

Table 4.7: Results of mobilization and solubilization experiments. HBRM columns are from Ref. [75]

Column	Solution	%Rem. Tot.[a]	%Mob[a,b]	%Sol[a,b]	S_n^{end}	SPAH[c]	TPAH[c]
HBRM-C1	ALK	14.5%	100%	0%	0.22	–	–
HBRM-C4	XG	50.6	100	0	0.13	–	–
HBRM-C5	AP	92.9	100	0	0.018	–	–
HBRM-C6	AP	88.4	100	0	0.037	–	–
MSR1A	ASP	94.1	99.7	0	0.012	22.6	35.9
MSR1B	ASP	95.6	95.8	4.2	0.009	17.7	28.0
MSR1C	ASP	95.0	95.5	4.5	0.009	–	–
MSR2-Stage1	AP	77.3	100	0	0.051	–	–
MSR2-Stage2	SP	92.5[d]	34.8	65.2	0.0005	5.8	9.5
MSR3	SP	99.3	62.2	37.8	0.0016	5.4	7.4
MSR4	SP	99.3	65.9	34.1	0.0014	8.9	12.5

ALK= NaOH, AP = alkaline-polymer (NaOH, XG), SP = surfactant-polymer (TX100, XG), ASP = alkaline-surfactant-polymer (NaOH, TX100, and XG)
a. Tar mass determined from effluent sample analysis by GC for mobilization and HPLC for solubilization.
b. % Mob and % Sol are the percentage of total removal by mobilization and solubilization, respectively.
c. Concentration of SPAH (15 PAHs) and TPAH (26 PAHs) in sand as measured by GC-FID following sand extraction, mg/kg.
d. % Removal of residual from Stage 1. Total removal for both stages of MSR2 = 98.3%

sampling, tar removal was 94.1–95.6%, with final $S_{\alpha n}$ of 0.009–0.012, representing a significant improvement over AP solutions. Tar was mobilized as a sharp tar bank that eluted within 1.6 PV (Figure 4.3). Despite the presence of surfactant, solubilization was minimal for these columns, accounting for only around 4% of the removal (Figure 4.4). MSR1B was extracted after the mobilization flush without receiving secondary treatment. The mass of extracted SPAH was 1.7 mg (by GC-FID), consistent with the visual appearance of the column, but well below the 50.5 mg calculated based on the analysis of the effluent samples. While apparently large, the difference in fact represents less than 0.25% of the initial, pre-water flush mass of tar in the column, and is likely the result of cumulative error in the effluent sample analysis.

To investigate changes in composition due to solubilization, a pseudo-mass fraction was defined:

$$\omega_i^* = \frac{M_i^s}{\sum_{n=1}^{26} M_n^s}, \tag{4.9}$$

where M_i^s is the mass of species i in the sand and $\sum_{n=1}^{26} M_n^s$ is the sum of the

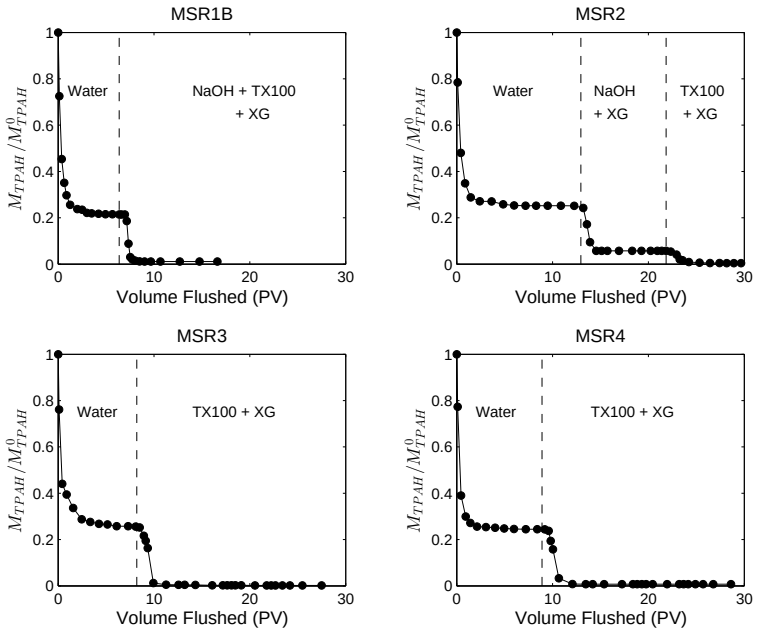

Figure 4.3: Fraction SPAH remaining as a function of PV flushed for MSR1B–4. The mass of PAHs was calculated solely by analysis of the effluent.

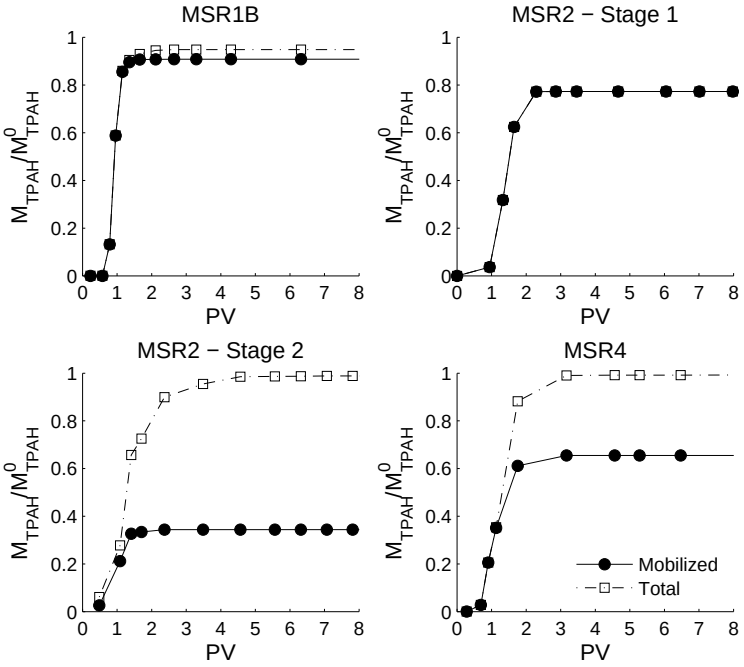

Figure 4.4: Cumulative tar mass removed as a function of PV flushed for columns MSR1–MSR4 showing the fraction removed by mobilization and solubilization mechanisms. Portions of the post-treatment DDI flushes are also shown.

masses of the 26 PAHs measured by GC-FID. This approach is necessary due to the fact that the majority (73%) of the tar is not quantified, and therefore the final total tar mass is uncertain. Changes in composition were assessed through a ratio of final $\omega_i^{*,f}$ to the initial $\omega_i^{*,0}$ (Figure 4.5). For all columns, NAP was significantly reduced, while higher molar mass species (PHE and above), were relatively enriched (Figure 4.5). Columns MSR1A and 1C were flushed with oxidant and additional DDI, respectively, after the ASP flush, as discussed later in this section.

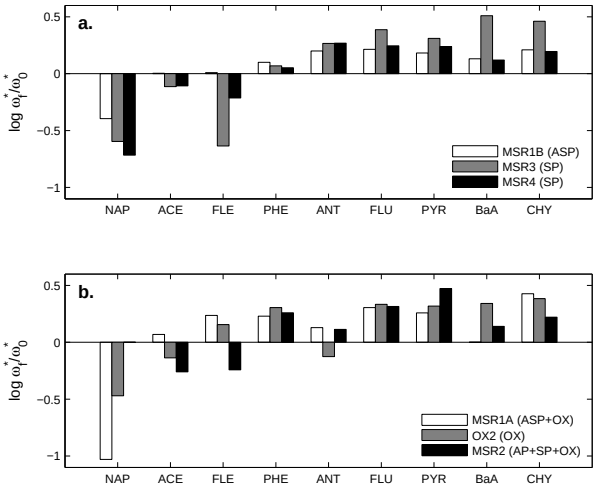

Figure 4.5: Change in ω^* for (a) mobilization and solubilization experiments and (b) oxidation experiments.

Column MSR2 was flushed in two stages: first with the same AP solution as HBRM-C5–6, then with the SP solution. The first stage resulted in the removal of 77.3% of the residual tar and a reduction in S_n from 0.22 to 0.051, representing both lower tar removal and a higher final saturation than for the HBRM columns. Since the same fluids and procedures were used for both sets of experiments, the difference in results is likely related to the sands used to pack the columns. The previous study used a sieved fraction of a natural, field

collected sand (d=0.50–0.71mm, porosity=0.40–0.42), whereas the current experiments used 20/30-mesh Accusand (d=0.59–0.84, porosity=0.35–0.37). The differences in pore geometry and wettability (due to mineralogical considerations), likely account for the observed differences in both initial residual saturations (0.26–0.32 for HBRM columns and 0.19–0.22 for MSR columns) and the removal by alkaline flushing. The pattern of removal for the first stage of MSR2, however, was similar to those of the HBRM columns, with the tar bank breaking through prior to the flushing solution, and completion of mobilization within 2 PV (Figure 4.3).

The second stage of MSR2 used the SP solution to mobilize and solubilize the tar remaining in the system after the alkaline flush. This stage removed 1.20 g of the 1.21 g remaining in the column (98.9%), resulting in a calculated tar saturation of 0.0006. The lower γ_{on} of the surfactant solution (3.04 mN/m) as compared to the alkaline solution (5.53 mN/m) resulted in the mobilization of additional tar within the first 1.5 PV of the flush, accounting for 34.8% of the removal of this stage. Solubilization accounted for the remaining 65.2%. Dissolved tar in the effluent was minimal while mobilization was occurring, peaked immediately behind the tar bank, and then tailed for several pore volumes (Figures 4.4 and 4.6). The peak concentration was 5,060 mg/L, a factor of 210 times the pure water solubility of SPAH (24.37 mg/L) as caclulated with Equation 4.5. The total removal for both stages of flushing was 98.3%. MSR2 received tertiary treatment in the form of ISCO, as discussed later in the following section.

MSR3 and MSR4 were duplicate columns flushed with SP solution for both primary mobilization and solubilization. The flushes removed 99.3% of the residual

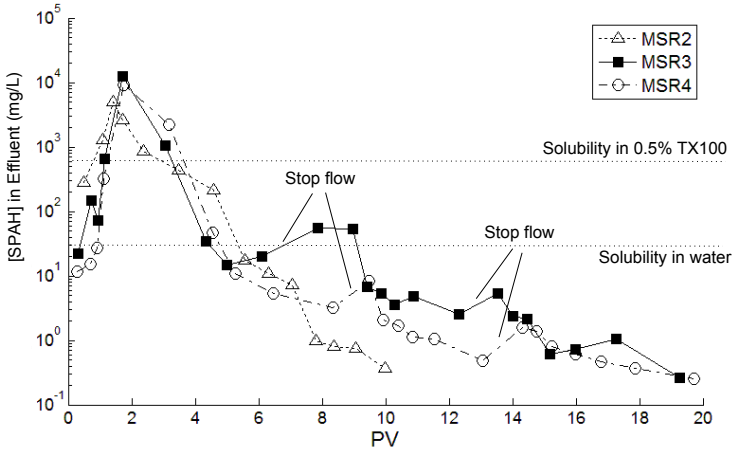

Figure 4.6: Effluent concentration of SPAH during surfactant flushing for MSR2, MSR3, and MSR4.

tar over 20.9 and 20.2 PV, respectively, with 99% of the removal occurring during the first 4 PV (Table 4.7, Figure 4.3). Mobilization constituted 62 and 66% of the total removal, while solubilization accounted for 38 and 34% for MSR3 and 4, respectively (Figure 4.4). Figure 4.6 shows the dissolved SPAH concentration for MSR3 and MSR4. The pattern of effluent concentrations closely followed that of MSR2 for the first 6 PV. Peak SPAH concentrations were 12,400 and 9,300 mg/L, respectively. Stop flows (48 h) were performed as indicated in Figure 4.6, and effluent concentrations subsequently increased, suggesting that the dissolution was rate limited. The greater concentrations for MSR3 during the initial and post-stop flow peaks may be related to the lesser mass recovered by mobilization and therefore greater mass available to be solubilized. Sand extractions indicated that 0.52 and 0.84 mg SPAH remained in MSR3 and MSR4, respectively; the masses remaining based on effluent samples were 5.9 and 21 mg, respectively. A similar pattern of composition change as for MSR1B, with greater magnitude, was observed for these columns (Figure 4.5).

4.4.4 Oxidation

ISCO is frequently used as a "polishing" step during site remediation to degrade contaminants remaining after primary remediation. Base-activated persulfate was applied in this manner to columns MSR1A and MSR2, however, because there is uncertainty in the mass of the PAHs present in the column at the start of the oxidation, columns were also conducted for which oxidation was the only remediation stage (OX1–3).

Columns OX1–OX3 had initial tar saturations of 2.5–4%, representing a post-AP tar saturation. Results of these columns are shown in Figure 4.7. Column OX1 was flushed with 52.1 PV (1 L) of OX-L solution for a total contact time of 20.8 days and resulted in removal of 53% of quantified PAHs. The removal of individual compounds was generally correlated with solubility, with the exception of ACE, ACY, and ANT, which were more degraded than other compounds with similar solubility and molar mass. OX2 was flushed with 20 PV (contact time = 8.6 days) of a solution with a higher persulfate concentration (274 g/L; OX-H) along with a parallel control column flushed with the NaOH activator solution. The oxidant column resulted in a 57% reduction in total PAHs, with the reduction of individual PAHs again roughly correlating with solubility. The mass of PAHs was reduced by 24% in the control column.

Due to the relatively low overall degradation, and the observed correlation between removal and compound solubility, an additional set of columns (OX3 and OX3C) were conducted using a combined surfactant-oxidant (S-OX) flush. These columns were flushed with 32.5 and 33.4 PV, with total contact times of

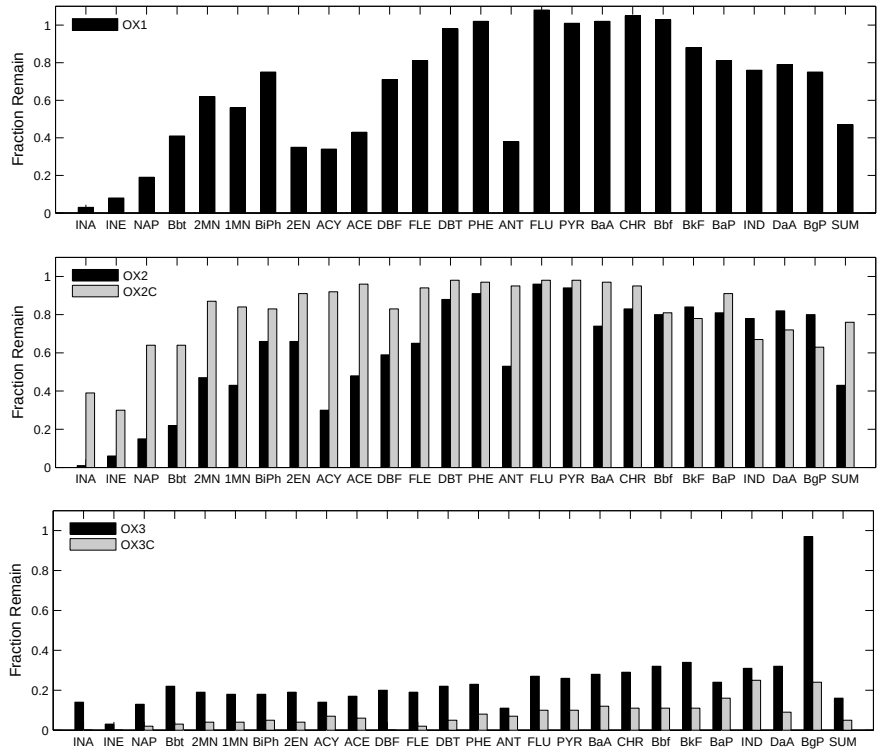

Figure 4.7: Fraction of PAHs remaining in sand at the end of oxidation column experiments.

18.4 and 18.7 days, respectively. Total PAH removal in column OX3 was 84%, while 95% of total PAHs was removed from OX3C, which was flushed with an NaOH+TX100 solution. The reduction in PAH mass in these columns is primarily the result of solubilization. Figure 4.8 shows the cumulative effluent PAH mass for columns OX3 and OX3C. The PAH removal in column OX3C is entirely ascribed to solubilization by the surfactant solution, with a stage of rapid removal in the first 5 PV of the TX-100 flush (between 15-20 PV on Figure 4.8), followed by tailing as less accessible tar is slowly dissolved. The effluent from the oxidant column contained very low concentrations of PAHs until a visible solubilized-tar front moved through the system at 35 PV. For OX3, 19% of the initial total

PAHs remained in the sand at the completion of the flush; 43% was removed by solubilization and 38% was destroyed by oxidation (as calculated by difference). The mass of total PAHs oxidized was 77 and 78 mg for columns OX2 and OX3, respectively.

Columns MSR1A and MSR2 were flushed with 10 and 9.6 PV of the OX-H solution after mobilization and solubilization stages. The mass of SPAH at the beginning of the oxidant flush was 41.3 and 13.6 mg (based on effluent analysis) for MSR1A and MSR2, respectively. Based on the sand extractions, the final SPAH mass was 2.2 and 0.56 mg, reductions of 95 and 96%, respectively. It should be noted that the effluent-based calculations significantly overestimated the post-mobilization/solubilization PAH mass for columns MSR1B and MSR3–4, and, therefore there is considerable uncertainty in the pre-oxidation PAH mass for MSR1A and MSR2. Furthermore, the final PAH mass in MSR1B (1.8 mg), which received the same ASP flush as MSR1A without secondary ISCO treatment, was slightly lower than that of MSR1A. Similarly, the final SPAH mass for MSR2 was similar to that of MSR3 and 4, which were flushed with the same SP solution. Changes in the relative concentrations of the remaining PAHs, however, do suggest that some oxidation has occurred. Comparing $\omega_i^*/\omega_i^{*,0}$ for columns receiving oxidation versus solubilization (Figure 4.5), a clear difference can be observed for phenanthrene and anthracene. In the solubilization columns, $\omega_i^*/\omega_i^{*,0}$ is lower for PHE than ANT, which would be expected based on the much higher solubility of PHE. This trend is reversed for the oxidant columns, consistent with the results of columns OX1–3, which indicated that ANT was much more readily oxidized than ANT.

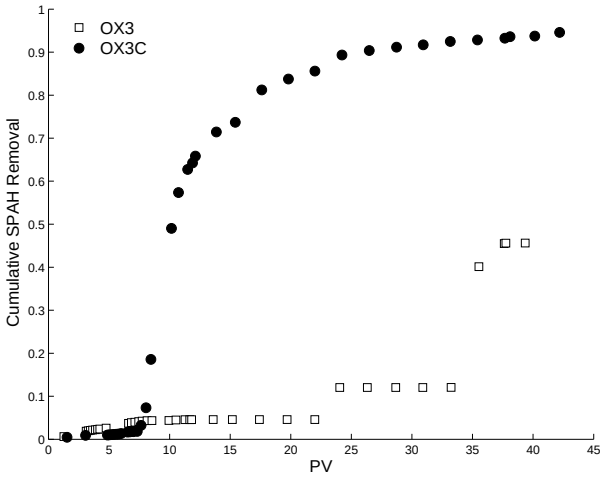

Figure 4.8: Cumulative mass of SPAHs in effluent from OX3 and OX3C, indicating significant removal by solubilization. Oxidant and control flushes started at 6.61 and 6.52 PV, respectively.

4.4.5 Dissolved PAH Concentrations

Aqueous samples were collected before and after each stage of remediation for MSR1–MSR4 and OX1 to assess each remediation method's impact on dissolved-phase concentrations. Figure 4.9 shows the ratio of post-treatment dissolved-phase concentration to the initial concentration prior to any treatment. The concentrations used for the calculation were an average of multiple consecutive samples once a quasi-steady-state concentration was reached. Analysis was limited to nine of the 15 PAHs analyzed, due to the fact that the higher molecular mass compounds were frequently at or below detection limits for many of the columns.

The effect of mobilization-based methods (AP and ASP) on dissolved-phase concentrations was relatively limited. MSR1A (ASP) showed little change, except for NAP, which was lower than the initial concentration by a factor of 5. A greater reduction in NAP, along with decreases of ACE, FLE, PHE, and ANT, was observed for MSR1B, which was also flushed with the ASP solution. MSR2,

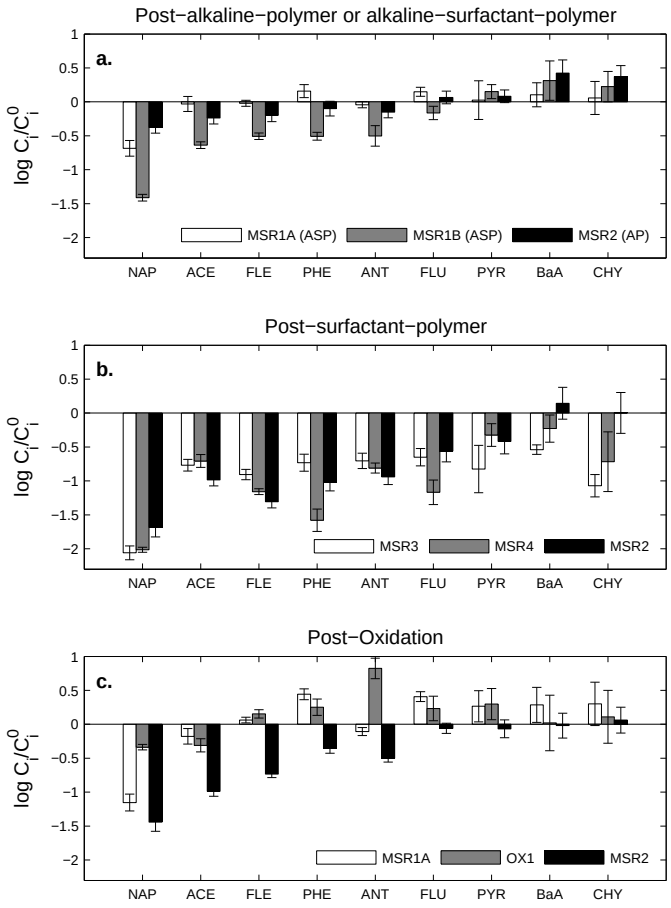

Figure 4.9: Ratio of post-treatment to pre-treatment dissolved-phase concentrations after (a) AP or ASP, (b) SP, and (c) oxidation flushes.

flushed with the AP solution, exhibited lesser decreases of NAP, ACE, FLE, PHE, and ANT concentrations than either MSR1A or MSR1B. Small but significant increases of BaA and CHY were observed for MSR1B and MSR2.

Solubilization methods had a larger impact on dissolved PAH concentrations. NAP was reduced by nearly two orders of magnitude for all three columns receiving an SP flush (MSR2–4). The concentrations of ACE through PYR were reduced by 0.5–1.5 orders of magnitude for all columns. Reductions in BaA and CHY were observed for MSR3 and 4, while little change in the concentrations of these compounds were observed for MSR2. Column MSR1C was flushed with

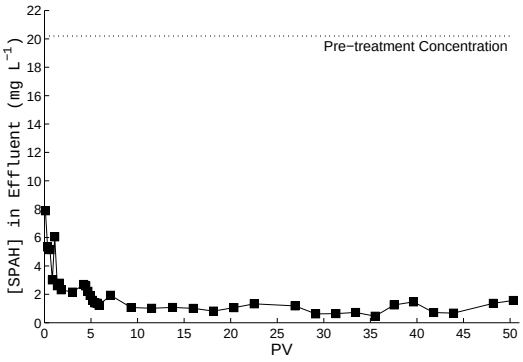

Figure 4.10: Post-treatment effluent concentrations during 50 PV DDI flush of MSR1C.

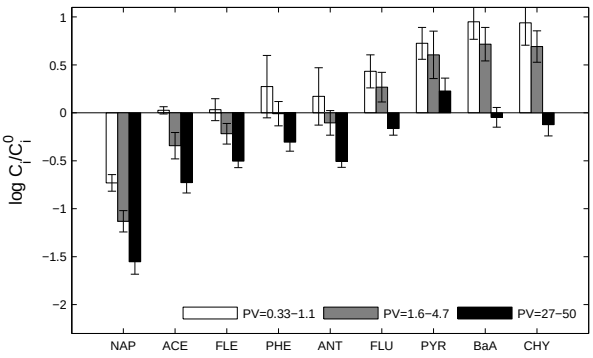

Figure 4.11: Change in ratio of post-treatment to pre-treatment dissolved-phase concentrations during MSR1C water flush.

50 PV of DDI after the ASP flush; the results are shown in Figure 4.10. The SPAH concentration decreased over the first 5 PV, then remained relatively constant to 50 PV. The concentration of individual compounds changed significantly over the course of the DDI flush (Figure 4.11). At the beginning of the flush, dissolved-phase concentrations were generally similar to those of MSR1A and MSR1B, with the exception of FLU–CHY, which were significantly higher. As the flush proceeded, all compounds decreased in concentration, with the final C_i/C_i^0 values falling between those of ASP and SP flushing.

Dissolved-phase concentrations after oxidation are shown in Figure 4.9c. For MSR1A, NAP was decreased from the post-AP concentration, but several other

Table 4.8: Ratios of measured to calculated dissolved-phase PAH concentrations after each stage of treatment for MSR2. $C_i^{\alpha,eq}$ is calculated with Raoult's law (Eq. 4.5) using the mole fraction in the original tar (Ref. [75]), S_i from Ref. [119], and FR from Ref. [51]. ± 95% CI

		$C_i^{\alpha}/C_i^{\alpha,eq}$			
PAH	$C_i^{\alpha,eq}$(μg/L)	Initial	Post AP	Post SP	Post Ox
NAP	19100	0.44 ± 0.04	0.18 ± 0.03	0.009 ± 0.003	0.016 ± 0.005
ACE	620	0.24 ± 0.02	0.14 ± 0.02	0.024 ± 0.004	0.024 ± 0.003
FLE	170	0.51 ± 0.05	0.32 ± 0.06	0.025 ± 0.005	0.094 ± 0.006
PHE	130	0.60 ± 0.09	0.47 ± 0.09	0.06 ± 0.01	0.26 ± 0.02
ANT	31	0.52 ± 0.05	0.37 ± 0.06	0.06 ± 0.01	0.16 ± 0.01
FLU	12	0.72 ± 0.09	0.8 ± 0.1	0.20 ± 0.07	0.6 ± 0.1
PYR	1.52	6.1 ± 0.7	7 ± 1	2.3 ± 0.9	5 ± 1
BaA	1.0	0.7 ± 0.3	1.8 ± 0.4	1.0 ± 0.4	0.7 ± 0.1
CHY	0.92	0.8 ± 0.3	1.8 ± 0.2	0.8 ± 0.5	0.9 ± 0.2
BbF	0.1	3 ± 1	8 ± 1	7 ± 3	3 ± 1
BkF	0.08	3 ± 1	7 ± 2	7 ± 2	1.8 ± 0.7
BaP	0.43	0.9 ± 0.7	2.2 ± 0.5	1.8 ± 0.8	0.4 ± 0.2
DaA	0.002	40 ± 20	70 ± 220	100 ± 50	59 ± 20
BgP	0.18	1.6 ± 0.9	5 ± 2	2.6 ± 0.9	2.3 ± 0.7

compounds increased, including PHE and FLU. For column OX1, NAP and ACE were reduced, and FLE, PHE, FLU, and PYR increased. Despite a decrease in ω^*_{ANT} (Figure 4.5), ANT exhibited a large increase for reasons that are not clear. In MSR2, NAP through ANT were below initial concentrations, but higher than post-SP/pre-oxidation concentrations. The full set of 15 PAHs for each stage of remediation for column MSR2 is given in Table 4.8.

4.5 Discussion

4.5.1 Mobilization

These experiments illustrate that large reductions in tar saturation may be achieved using several methods. Five different solutions were used to mobilize residual tar, and, accounting only for the mass removed by mobilization, the effectiveness of these solutions follows the order: ALK < XG < SP < AP < ASP. This ordering is generally consistent with N_T. XG alone resulted in a lower final S_n than NaOH alone, because viscosity is increased by three orders of magnitude versus a one

order of magnitude reduction of IFT. The ASP solution has an order of magnitude lower IFT than either SP or AP, consistent with studies of enhanced oil recovery [123, 143, 144, 209], and therefore results in greater tar mobilization. The SP solution is apparently less effective than AP, however, the concurrent solubilization confounds this analysis since some portion of the mobilized tar may dissolve in the surfactant solution. Overall, the final S_n, calculated using only mobilized tar mass, was found to be a strong linear function of log N_T (Figure 4.12a). The slope of the fitted line differs between the experiments conducted as part of this work and those of Hauswirth, et al. (2012). This finding is explained by the different media used in the experiments. The permeability of the media differ by an order of magnitude (HBRM sand = 2.2×10^{-7} cm^2 [75], MSR sand =2.3×10^{-6} cm^2 [188]), resulting in proportional differences in N_B, which is important at low N_C (i.e., the water flushing points where the greatest deviation is observed). Furthermore, S_n–N_T relationships themselves are dependent on media properties [33, 49, 160].

Previous studies have reported a critical N_T (N_T^c), defined as the minimum value required to initiate NAPL mobilization, below which S_n is constant, of between 1×10^{-5} and 5×10^{-5} [34, 49, 112, 135, 146, 159, 160]. Above N_T^c, S_n has been found to decrease sharply to a value of N_T of about 1×10^{-3}, at which point a lower plateau is reached (N_T^∞). Figure 4.12a shows that neither upper nor lower plateaus of S_n were observed over the range of N_T used in this study (1.8×10^{-6} to 2.0×10^{-2}), which extended an order of magnitude lower and higher than previously reported N_T^c and N_T^∞. The reason for this is not clear, but major difference include the NAPL used in the experiments and the use of polymer solutions. The previous studies focused on chlorinated solvents, which

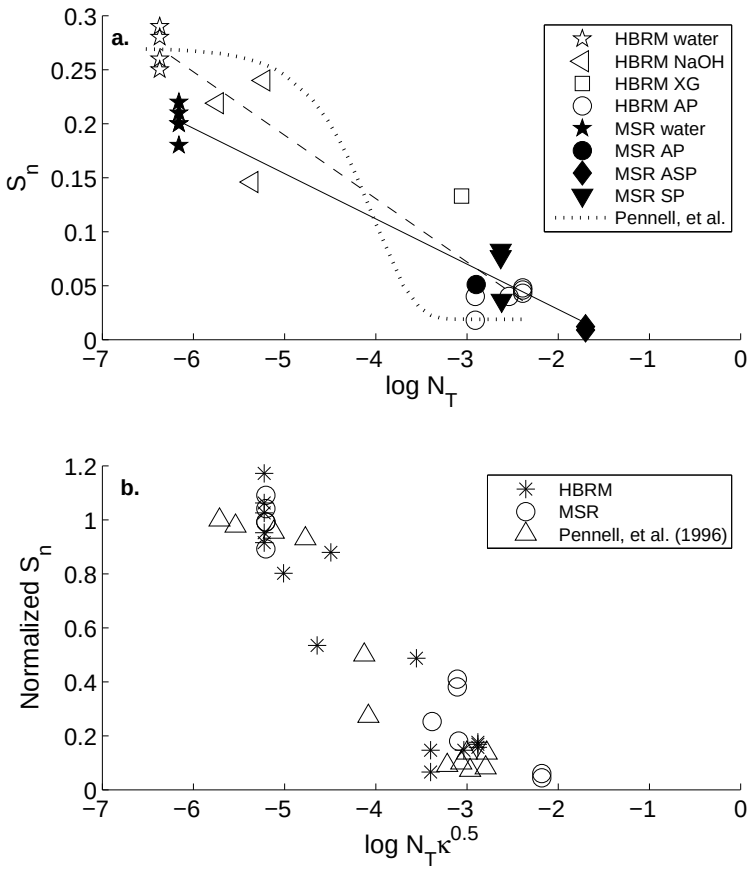

Figure 4.12: Relationship between (a) S_n and $\log N_T$, and (b) normalized S_n and $\log N_T \kappa^{0.5}$. N_T was calculated using Equations 4.1–4.3 for HBRM and MSR. HBRM data from Ref. [75]. S_n and $N_T \kappa^{0.5}$ for Pennell, et al. (1996) were determined based on estimated values from Figure 4a and viscosity data in Table 1 in Ref. [160].

have much lower viscosity than the tar used in this work. In the development of N_T, it was assumed that shear forces are negligible, however, that may not be the case for highly viscous NAPLs. Abrams (1975) and Longino and Kueper (1999) suggested incorporating NAPL viscosity as follows:

$$N_C^* = N_C \kappa^m \tag{4.10}$$

where m is a fitted parameter (0.5 for Longino and Kueper, -0.4 for Abrams)[1, 124]. Figure 4.12b shows normalized S_n data from this work plotted against a

modified form of Equation 4.10 that uses N_T in place of N_C. The dataset from this work is not well suited to fitting m since there were only two values of κ (with and without XG), and therefore the value of Longino and Kueper was used. To allow direct comparison between studies, S_n, N_T, and viscosity values were extracted from Pennell, et al. (1996) [160], $N_T\kappa^{0.5}$ was calculated, and the data was plotted in Figure 4.12b. Because the Pennell study used perchlorothylene (PCE), which has a viscosity of 0.89 cP, and did not use viscosifying agents, κ was near unity for all points, and therefore $N_T\kappa^{0.5}$ was only slightly changed relative to N_T. The incorporation of κ^m effectively shifts the MSR and HBRM data to within the range observed in the Pennell, et al. study, suggesting that it can serve as a scaling term allowing for comparison of systems with widely varying viscosities of both NAPL and aqueous phases.

The reason for the scatter in the data Figure 4.12a is not clear, but we note that there is some uncertainty in the values used for calculating N_T. The IFT measurement used in this study was determined after a 3 day equilibration period; however, Hauswirth, et al. (2012) found that the instantaneous tar-alkaline solution IFT may be an order of magnitude lower than the equilibrated value [75]. That study also observed differences in the temporal evolution of IFT with time depending on the NaOH concentration. These findings suggest that the IFT may vary in time and space in an alkaline flushing scenario, making identification of a representative IFT value difficult. The contact angle may similarly be expected to vary in time and space [71, 181]. In addition to chemical reaction kinetics, contact angle hysteresis presents a difficulty since Equations 4.1–4.3 allow for only a single contact angle, and θ_A and θ_R may vary by up to 100°for tar-alkaline solution

systems [17, 75]. While dynamic IFT and contact angle for surfactant and alkaline-surfactant solutions were not measured in this study, previous studies conducted with petroleum suggest that such effects may be significant [5, 12, 143, 144, 208].

4.5.2 Solubilization

SP flushes resulted in both mobilization and solubilization of tar components. When considering both mechanisms, SP floods resulted in the greatest overall tar removal of the methods tested. Although some tailing of dissolved-phase concentration was observed (Figure 4.6), greater than 99% of the removal occurred within 7 PV for all SP columns. The dissolved-phase concentration (SPAH) in effluent (Figure 4.6) at the peak was over an order of magnitude higher than equilibrium concentrations for the same TX100 concentration as measured in the batch experiment (Figure 4.2) for all three SP columns (MSR2–4). Peak effluent concentrations for the ASP columns were approximately three times greater than the batch concentration. The reason for this is not clear. Dwarakanath, et al (1999) reported that the use of a polymer resulted in higher dissolved-phase concentrations in surfactant flushing , with the hypothesized reason that NAPL-surfactant contact was increased due to the increased viscosity [50]. In that study, however, effluent concentrations remained below the equilibrium concentration. The batch tests in this work did not use XG in the surfactant solutions, presenting two possible explanations for the apparent supra-equilibrium concentrations in effluent. First, the XG may itself increase the solubility of PAHs by one of two mechanisms: (1) the large XG molecules ($\sim 2 - 20 \times 10^6$ g/mol [61]) may act as colloids onto which molecules may adsorb, similar to findings of enhanced

solubility due to natural colloids and humic acids [129], or (2) XG may become incorporated into surfactant micelle structures and thereby increase the micellar volume available for partitioning. The effect of polymers on the solubility of hydrophobic compounds has received little study, and further research is required to better understand these potential processes. The second explanation is that the elevated concentrations are the result of an analytical artifact. Both the batch and column effluent samples were centrifuged prior to sampling the aqueous phase, however, the high viscosity of the XG-containing effluent samples may have prevented the settling of small tar droplets, effectively increasing macroemulsion stability [210]. This explanation would also explain why SP flushes resulted in lower-than-expected removal by mobilization, since some portion of separate phase tar would be counted as solubilized tar.

4.5.3 Oxidation

ISCO using base-activated persulfate without surfactant resulted in removal of 53–57% of total PAHs. It is significant that the degradation was similar for OX1 and OX2 despite the > 5 times higher persulfate concentration and double total persulfate mass of the OX2 flush. This fact, combined with the preferential degradation of low molar mass, high solubility compounds, provides evidence that the oxidation is mass transfer limited. That several compounds, including ACY and ANT, were degraded to a greater degree than compounds with similar or even greater solubilities, however, suggests an interplay of chemical and mass transfer kinetics. Further research is required to elucidate the mechanisms responsible for these observations. The addition of surfactant to the oxidant solution (OX3)

greatly increased removal of tar compounds, however, most of that increase was the result of solubilization. Oxidation was responsible for only 38% of the overall removal, as compared to 33% for OX2. Furthermore, the removal by solubilization was significantly lower than that for the control column (OX3C). The likely explanation for these results is that the surfactant is oxidized by the persulfate, resulting in competition with PAHs for oxidant and reduction of the surfactant concentration.

4.5.4 Aqueous-Phase Concentrations

Assessment of the reduction of dissolved-phase concentrations is complicated by the compositional complexity of the tar. Preferential dissolution of more soluble compounds results in shifts in composition that produce corresponding changes in C_i^{eq} according to Equation 4.5. Removal of high solubility compounds increases the mole fraction of lower solubility compounds and thereby their equilibrium aqueous-phase concentrations. As solubilization proceeds, increasingly high molar mass compounds are depleted from the tar. In comparing changes in aqueous concentrations (Figure 4.9) and changes in composition Figure 4.5, the results of the AP (MSR2), ASP (MSR1A–C), and DDI (MSR1C) flushes are qualitatively consistent with this mechanism. The SP flushes, however, result in reduced aqueous concentrations of all measured PAHs despite increases in $\omega_i^*/\omega_i^{*,0}$ for higher molar mass compounds. The likely reason for this is that the high molar mass fraction of the tar (i.e., asphaltenes), which was not quantified in either effluent sample or sand extracts, is relatively enriched in the post-treatment tar. Preferential retention of this fraction would result in reduced mass fractions for all PAHs,

accounting for the observed dissolved-phase concentrations.

The observation that, for MSR2, oxidation reduced the aqueous-phase concentrations of high molar mass PAHs (BbF through BgP) and increased concentrations of several lower molar mass compounds (FLE through PYR) relative to post-SP concentrations (Table 4.8) is not as easily explained. This result would suggest that high molar mass compounds are preferentially oxidized, which is not consistent with either the results presented in Figure 4.7 or the general assumption that oxidation reactions occur in the aqueous phase. Further research is required to confirm this result and to determine the mechanisms responsible.

4.6 Conclusion

The effectiveness of an *in situ* NAPL remediation technique can be assessed by: (1) the reduction NAPL/contaminant mass in the system or (2) the reduction of contaminant concentrations or fluxes in the water passing through the contaminated region [103, 109, 173, 197]. In terms of mass removal, the overall effectiveness of individual remediation methods follows the order OX (30–50% removal) < AP (77–93%) < ASP (94–96%) < SP (>99%). SP flushes removed 99% of the tar residual within about 4 PV, with effluent PAH concentrations reaching pure water solubility within about 5 PV (Figure 4.6). ASP flushes were very efficient, removing 95% of the tar within about 2 PV. The ASP flushes were stopped when NAPL-phase tar was no longer visible in the effluent, and a longer flush or a secondary SP flush would likely have further reduced the mass of PAHs through dissolution, although whether this would improve efficiency over a solely SP flush is uncertain. It is also noted that the volume of ASP solution injected

likely exceeded the volume required to achieve the same removal by mobilization. The width of the tar bank for MSR1B, for example, is about 0.6 PV (Figure 4.4), suggesting that a plug of ASP solution of considerably less volume than 2 PV may have achieved the same final saturation. While it was previously shown that AP flushing could efficiently remove over 90% of residual tar [75], the effectiveness was considerably lower in this study, potentially due to sensitivity to the solid-phase properties. Conducting an AP flush prior to SP flushing (MSR2) provided little advantage over SP alone in terms of the final mass of PAHs, the removal efficiency, or reductions in dissolved-phase concentrations. Tar removal by mobilization was generally consistent with the trapping number concept, but it was found that incorporating the NAPL viscosity through κ ($N_T\kappa^m$) resulted in better agreement with other studies using less viscous NAPLs.

Base-activated persulfate was shown to degrade PAHs, primarily low molar mass compounds, however, the overall mass reduction, even using very high persulfate concentrations, was low compared to other methods. Furthermore, the impact on dissolved-phase PAH concentrations was minimal whether used alone (OX1–2), with surfactant (OX3), or in conjunction with other methods (MSR1A and MSR2). The limited effectiveness of base-activated persulfate in this study suggests that this activator-oxidant system is not well-suited for degrading NAPL-phase FMGP tar.

Dissolved concentrations of the lower molar mass PAHs (i.e., NAP and ACE), which often drive groundwater remediation at contaminated sites, were reduced significantly for all flushing solutions. The SP solution was the most effective at reducing post-treatment groundwater concentrations, with a 98.8–99.1% re-

duction of the total PAH concentration (SPAH) and 0.5–2 orders of magnitude for all individual compounds included in the analysis (NAP–CHY). Optimization of combined ASP–SP flushing schemes may allow for equivalent results with increased efficiency. For example, using a 0.5 PV ASP flush to mobilize 95% of the residual tar followed by an SP flush, may reduce the overall volume of fluids required to attain the desired reductions in tar mass and effluent concentrations.

The combination of efficient NAPL removal and significant reductions in dissolved concentrations results illustrate the potential for *in situ* remediation of MGP tars under ideal conditions in one-dimensional systems. Field-scale remediation, however, involves three-dimensional systems with inherently more complexity than laboratory column studies. Heterogeneity in terms of both geology and NAPL distribution, and concerns regarding the downward migration of mobilized tar, present major challenges to implementation of mobilization and solubilization approaches. The use of viscosifying agents, a carefully designed remediation scheme, and potentially an emplaced brine-based barrier [82, 133, 231], however, may partially alleviate these challenges and allow for successful application.

Nomenclature

Roman Letters

C	Concentration, subscript indicates species, superscript indicates phase
f_c	Cosolvent volume fraction
g	Gravitational acceleration
k	Intrinsic permeability
k_r	Relative permeability
K_m	Micellar partition coefficient
M	Mobility ratio
N_T	Trapping number
N_T^c	Critical trapping number below which no mobilization occurs
N_T^∞	Trapping number corresponding to minimum S_n
N_C	Capillary number
N_B	Bond number
S_n	NAPL saturation
q	Magnitude of the Darcy velocity
$\bar{V}$	Molar volume of water

Greek Letters

μ	Dynamic viscosity
σ	Cosolvency power
θ	Contact angle
β	Angle between flow direction and horizontal
ρ	Density
λ	Fluid mobility
κ	Viscosity ratio, μ_n/μ_α
χ	Mole fraction
γ	Interfacial tension
ω^*	Pseudo-mass fraction based mass of quantified PAH

Subscripts and Superscripts

α	Qualifier for aqueous phase
i	General species indicator
n	Qualifier for NAPL phase
eq	Equilibrium qualifier
s	Qualifier for solid phase
ss	Qualifier for surfacant solution
$n\alpha$	Qualifier for NAPL-water interface
cs	Qualifier for cosolvent
m	Qualifier for micelle pseudophase

Abbreviations

AP	Alkaline-polymer solution
ASP	Alkaline-surfactant-polymer solutio
DDI	Distilled, deionized water
FMGP	Former manufactured gas plant
IPA	Isopropanol
ISCO	*In situ* chemical oxidation
MAH	Monocyclic aromatic hydrocarbon
MSR	Molar solubilization ratio
NAPL	Non-aqueous phase liquid
PAH	Polycyclic aromatic hydrocarbon
PV	Pore volume
SP	Surfactant-polymer solution
SPAH	Sum of 15 PAHs quantified by HPLC
TPAH	Sum of 26 PAHs quantified by GC
TX100	Triton X-100 surfactant
XG	Xanthan gum

CHAPTER 5

CONCLUSIONS AND RECOMMENDATIONS

The "town gas" industry of the mid-nineteenth through early-twentieth century has left a legacy of environmental concerns. Waste by-products, most notably tar, were released, intentionally or incidentally, into the environment at thousands of former manufactured gas plants (FMGPs) throughout the U. S. In many cases, these wastes persist in the subsurface, presenting continued risks to humans and ecological systems. FMGP tars contain high concentrations of harmful and carcinogenic compounds that may leach into groundwater and potentially contaminate surface water bodies and drinking water sources. The characterization and remediation of the tars has received considerable attention over the last several decades, however, significant gaps in understanding, and challenges to remediation, remain.

Tars are complex mixtures that can vary greatly between FMGPs and even within a single site due to differences in the processes or source materials used at the plant and due to subsequent environmental modification. Variations in composition result in corresponding variations in physical properties, including density, viscosity, and interfacial behavior. The last of these, which includes interfacial tension (IFT) and wetting behavior (i.e., contact angle), are parameters of primary importance in the flow and entrapment of non-aqueous phase liquids (NAPLs) in porous medium systems. Understanding these properties is therefore critical for

both predicting the movement of tars in the subsurface and designing remediation techniques. The overall goals of this work were to (1) improve understanding of the interfacial properties of FMGP tars and their relationship to composition, and (2) to develop improved methods for remediating tar-contaminated sites. These objectives were addressed by characterizing tars and measuring their interfacial properties as a function of aqueous composition, and conducting a series of one-dimensional column experiments to assess the ability of remedial flushing solutions to remove residual tar.

Consistent with previous studies, tar-water IFT was found to be a strong function of pH, with the highest values obtained at neutral pH, and, for all samples except the coal tar, minimum values at high pH [17, 242]. The pH dependence of IFT has previously been associated with asphaltenes, an operationally defined, high molar mass fraction of tars; however, the results of this work indicated that the low IFT values at low and high pH were related to the concentrations of aqueous-extractable base compounds and high molar mass carboxylic acids, respectively. These compositional features, along with the concentration of extractable acids, the aromaticity of the tar and the average molecular mass of the asphaltenes, were further related to the gas plant processes from which the tars were produced. These findings provide valuable knowledge regarding the interrelationships between gas plant process, composition, and interfacial behavior. The large differences observed between tars in terms of composition and properties can significantly impact the behavior of tars in porous media, and are important to take into consideration when investigating and remediating FMGP sites.

The potential exploitation of the pH dependence of IFT was investigated by

flushing tar-contaminated sand columns with alkaline (NaOH) solutions. Alkaline solutions alone removed a maximum of only 44% of residual tar, however, the addition of xanthan gum polymer (XG) to increase the viscosity of the flushing solution resulted in tar removals of 81-93% within 2–3 pore volumes (PV). The use of XG not only increased the viscous forces acting to mobilize the tar, but also minimized viscous fingering, resulting in a more efficient displacement and the formation of a stable tar bank. Despite the large fraction of residual tar removed by these alkaline-polymer (AP) solutions, dissolved phase polycyclic aromatic hydrocarbon (PAH) concentrations were not significantly reduced, indicating the need for additional treatment to meet typical remediation goals.

Additional column experiments were conducted to identify methods capable of removing a sufficient fraction of tar and tar components to reduce dissolved-phase PAH concentrations. An alkaline-surfactant-polymer solution produced a significantly lower tar-water IFT than AP solutions, removed 94–96% of residual tar within 2 PV, and reduced the concentration of low molar mass PAHs in the aqueous phase. Surfactant-polymer solutions, through a combination of mobilization and solubilization, removed a larger fraction of the tar ($> 99\%$) and resulted in greater reduction of dissolved-phase PAHs, but required a larger flushing volume to do so (6–20 PV). The use of base-activated persulfate to chemically oxidize tar components resulted in the degradation of only 30–50% of total PAHs and had a minimal effect on dissolved-phase PAH concentrations.

Consistent with previous studies, the final tar saturation achieved by mobilization methods was generally a decreasing function of trapping number (N_T) [34, 49, 112, 135, 146, 159, 160]. However, incorporation of the NAPL-aqueous

viscosity ratio (κ) into a modified trapping number ($N_T\kappa^m$) allowed for better comparison between studies using NAPLs and aqueous solutions with widely varying viscosities. This finding suggests that the commonly used form of N_T developed by Pennell, et al. (1996) [160] is insufficient for describing disparate systems, and that further theoretical and computational research is required to better understand the mechanisms of NAPL mobilization.

In comparing the effectiveness of these methods, the surfactant-polymer (SP) solution resulted in the greatest total tar removal and the lowest post-remediation dissolved-phase PAH concentrations. The alkaline-surfactant-polymer (ASP) solution, however, was significantly more efficient in terms of the volume of solution required. An optimized remediation strategy may take advantage of both ASP and SP methods: an initial, low volume ASP flush to rapidly mobilize the bulk of the tar, followed by SP to solubilize the remaining tar. The results of the chemical oxidation experiments strongly suggested that base-activated persulfate is not an effective method of degrading tar components when even low saturations of separate-phase tar are present.

The results of these studies are promising and support the application of *in situ* flushing techniques for the remediation of FMGP tars. It is important to acknowledge, however, that these experiments were conducted in one-dimensional columns packed with homogenous sand. Real systems are three-dimensional and inherently more complex. Geologic heterogeneity can significantly reduce the effectiveness of such methods, and downward migration of mobilized tar into previously uncontaminated zones is a major concern. Future studies should focus on heterogeneous systems of higher dimensionality to assess the effects of these

complicating factors and to develop strategies to minimize them.

BIBLIOGRAPHY

[1] Abrams, A. (1975). The influence of fluid viscosity interfacial tension and flow velocity on residual oil saturation left by waterflood. *Society of Petroleum Engineers Journal*, 15(05):437–447.

[2] Abriola, L. M. and Bradford, S. A. (1998). Experimental investigations of the entrapment and persistence of organic liquid contaminants in the subsurface environment. *Environmental health perspectives*, 106(Suppl 4):1083.

[3] Acevedo, S., Castro, A., Negrin, J. G., Fernandez, A., Escobar, G., and Piscitelli, V. (2007). Relations between asphaltene structures and their physical and chemical properties: The rosary-type structure. *Energy & Fuels*, 21:2165–2175.

[4] Aczel, T., Williams, R. B., Chamberlain, N. F., and Lumpkin, H. E. (1981). *Composition of asphaltenes from coal liquids*, pages 237–251. Advances in Chemistry Series No. 195. American Chemical Society.

[5] Akhlaq, M. S., Götze, P., Kessel, D., and Dornow, W. (1997). Adsorption of crude oil colloids on glass plates: measurements of contact angles and the factors influencing glass surface properties. *Colloids and Surfaces A: Physicochemical and Engineering Aspects*, 126(1):25–32.

[6] Alboudwarej, H., Beck, J., Svrcek, W. Y., Yarranton, H. W., and Akbarzadeh, K. (2002). Sensitivity of asphaltene properties to separation techniques. *Energy & Fuels*, 16(2):462–469.

[7] Allen, D. T., Grandy, D. W., Jeong, K.-M., and Petrakis, L. (1985). Heavier fractions of shales oils, heavy crudes, tar sands, and coal liquids: Comparison of structural profiles. *Industrial Engineering Chemistry Process Design and Development*, 24:737–742.

[8] Andersen, S. I. and Speight, J. G. (2001). Petroleum resins: Separation, character, and role in petroleum. *Petroleum Science and Technology*, 19(1–2):1–34.

[9] Apostoluk, W. and Drzymala, J. (2003). An improved estimation of water-organic liquid interfacial tension based on linear solvation energy relationship approach. *Journal of Colloid and Interface Science*, 262:483–8.

[10] ASTM (2008). Standard test method for characteristic groups in rubber extender and processing oils and other petroleum-derived oils by the clay-gel absorption chromatographic method, D2007-03(2008). Technical report, American Society for Testing and Materials, Philadelphia, PA.

[11] Atteia, O., Estrada, E. D. C., and Bertin, H. (2013). Soil flushing: A review of the origin of efficiency variability. *Reviews in Environmental Science and Biotechnology*, 12(4):379–389.

[12] Ayirala, S. C., Vijapurapu, C. S., and Rao, D. N. (2006). Beneficial effects of wettability altering surfactants in oil-wet fractured reservoirs. *Journal of Petroleum Science and Engineering*, 52(14):261 – 274. Reservoir Wettability 8th International Symposium on Reservoir Wettability.

[13] Badre, S., Goncalves, C. C., Norinaga, K., Gustavson, G., and Mullins, O. C. (2006). Molecular size and weight of asphaltene and asphaltene solubility fractions from coals, crude oils and bitumen. *Fuel*, 85:1–11.

[14] Bahramian, A. and Danesh, A. (2004). Prediction of liquid–liquid interfacial tension in multi-component systems. *Journal of Fluid Phase Equilibria*, 221(1-2):197–205.

[15] Baker, R. S., Brogan, D., and Lotti, M. (2006). Demonstration of tailored levels of in-situ heating for remediation of a former MGP site. *Land Contamination and Reclamation*, 14:335–339.

[16] Ball, W. P., Liu, C., Xia, G., and Young, D. F. (1997). A diffusion-based interpretation of tetrachloroethene and trichloroethene concentration profiles in a groundwater aquitard. *Water Resources Research*, 33(12):2741–2757.

[17] Barranco, F. T. and Dawson, H. E. (1999). Influence of aqueous pH on the interfacial properties of coal tar. *Environmental Science & Technology*, 33(10):1598–1603.

[18] Birak, P. S. and Miller, C. T. (2009). Dense non-aqueous phase liquids at former manufactured gas plants: Challenges to modeling and remediation. *Journal of Contaminant Hydrology*, 105(3–4):81–98.

[19] Birak, P. S., Newman, A. P., Richardson, S. D., Hauswirth, S. C., Pedit, J. A., Aitken, M. D., and Miller, C. T. (2009). Cosolvent flushing for the remediation of PAH's from former manufactured gas plants. *In review.*

[20] Blanchard, C. (2010). Applying chemical oxidation technologies at NAPL-impacted sites to facilitate risk-based closure. *Remediation Journal*, 20(2):77–91.

[21] Blanco, C. G., Blanco, J., Bernard, P., and Guillen, M. D. (1991). Capillary gas chromatographic and combined gas chromatography–mass spectrometric study of the volatile fraction of a coal tar pitch using OV-1701 stationary phase. *Journal of Chromatography A*, 539(1):157–167.

[22] Bockrath, B. C. and Schweighardt, F. K. (1981). *Coal-derived asphaltenes. History and some current observations.*, chapter Coal-derived asphaltenes: History and some current observations, pages 29–38. Advances in Chemistry Series No. 195. American Chemical Society, Washington D.C.

[23] Bone, B. D., Barnard, L. H., Boardman, P. J., Carey, C. D., Jones, H. M., MacLeod, C. L., and Tyrer, M. (2004). Review of scientific literature on the use

of stabilisation/solidification for the treatment of contaminated soil, solid waste and sludges. Technical Report Science Report SC980003/SR2, Environment Agency U.K.

[24] Bonnar, R. V., Dimbat, M., and Stross, F. H. (1958). *Number Average Molecular Weights*. Wiley-Interscience, New York.

[25] Bradford, S. A., Abriola, L. M., and Rathfelder, K. M. (1998). Flow and entrapment of dense nonaqueous phase liquids in physically and chemically heterogeneous aquifer formations. *Advances in Water Resources*, 22(2):117–132.

[26] Bradford, S. A., Rathfelder, K. M., Lang, J., and Abriola, L. M. (2003). Entrapment and dissolution of DNAPLs in heterogeneous porous media. *Journal of Contaminant Hydrology*, 67:133–157.

[27] Brown, D. G., Gupta, L., Kim, T. H., Moo-Young, H. K., and Coleman, A. J. (2006). Comparative assessment of coal tars obtained from 10 former manufactured gas plant sites in the eastern United States. *Chemosphere*, 65(9):1562–1569.

[28] Buckley, J. S. (1994). Chemistry of the crude oil/brine interface. In Morrow, N. R., editor, *Proceedings of the 3rd International Symposium on Evaluation of Reservoir Wettability and Its Effect on Oil Recovery*, pages 33–38, Laramie, WY.

[29] Buckley, J. S. (2001). Effective wettability of minerals exposed to crude oil. *Current Opinion in Colloid and Interface Science*, 6:191–196.

[30] Buckley, J. S. and Lord, D. L. (2003). Wettability and morphology of mica surfaces after exposure to crude oil. *Journal of Petroleum Science and Engineering*, 39:261–273.

[31] Chatterjee, J. and Wasan, D. T. (1998). A kinetic model for dynamic interfacial tension variation in an acidic oil/alkali/surfactant system. *Chemical Engineering Science*, 53(15):2711–2725.

[32] Chevalier, L. R. (2006). Use of optimization to develop a correlation model for predicting residual NAPL saturation. *Civil Engineering and Environmental Systems*, 23(2):65–72.

[33] Chevalier, L. R. and Fonte, J. M. (2000). Correlation model to predict residual immiscible organic contaminants in sandy soils. *Journal of Hazardous Materials*, B72:39–52.

[34] Childs, J. D., Acosta, E., Knox, R., Harwell, J. H., and Sabatini, D. A. (2004). Improving the extraction of tetrachloro ethylene from soil columns using surfactant gradient systems. *Journal of Contaminant Hydrology*, 71(1-4):27–45.

[35] Chiwetelu, C. I., Hornof, V., and Neale, G. H. (1990a). A dynamic-model for the interaction of caustic reagents with acidic oils. *Aiche Journal*, 36(2):233–241.

[36] Chiwetelu, C. I., Hornof, V., and Neale, G. H. (1990b). Mechanisms for the interfacial reaction between acidic oils and alkaline reagents. *Chemical Engineering Science*, 45(3):627–638.

[37] Chiwetelu, C. I., Hornof, V., Neale, G. H., and George, A. (1994). Use of mixed surfactants to improve the transient interfacial tension behaviour of heavy oil/alkaline systems. *The Canadian Journal of Chemical Engineering*, 72:534–540.

[38] Choudhary, G., Citra, M. J., McDonald, A. R., and Quinones-Rivera, A. (2002). Toxicological profile for wood creosote, coal tar creosote, coal tar, coal tar pitch, and coal tar pitch volatiles. Technical report, Agency for Toxic Substances and Disease Registry, U.S. Department of Health and Human Services.

[39] Cohen, R. M. and Mercer, J. W. (1993). DNAPL site evaluation. Technical Report EPA/600/SR-93/022, U.S. Environmental Protection Agency, Robert S. Kerr Environmental Research Laboratory, Ada, OK.

[40] Comba, S., Dalmazzo, D., Santagata, E., and Sethi, R. (2011). Rheological characterization of xanthan suspensions of nanoscale iron for injection in porous media. *Journal of Hazardous Materials*, 185(2-3):598–605.

[41] Cratin, P. D. (1993). Mathematical modeling of some pH-dependent surface and interfacial properties of stearic acid. *Journal of Dispersion Science and Technology*, 14(5):559–602.

[42] Danielli, J. F. (1937). The relations between surface pH, ion concentrations and interfacial tension. *Proceedings of the Royal Society of London B*, 122:155–174.

[43] Darwish, M. I., McCray, J. E., Currie, P. K., and Zitha, P. L. (2003). Polymer-enhanced DNAPL flushing from low-permeability media: An experimental study. *Ground Water Monitoring & Remediation*, 23(2):92–101.

[44] DiFilippo, E. L. and Brusseau, M. L. (2008). Relationship between mass-flux reduction and source-zone mass removal: Analysis of field data. *Journal of Contaminant Hydrology*, 98(1):22–35.

[45] Domenico, P. A. and Schwartz, F. W. (1998). *Physical and Chemical Hydrogeology*. John Wiley & Sons, New York.

[46] Dong, J. F., Chowdhry, B., and Leharne, S. (2004). Investigation of the wetting behavior of coal tar in three phase systems and its modification by poloxamine block copolymeric surfactants. *Environmental Science & Technology*, 38(2):594–602.

[47] Dong, M., Ma, S., and Liu, Q. (2009). Enhanced heavy oil recovery through interfacial instability: A study of chemical flooding for brintnell heavy oil. *Fuel*, 88:1049–1056.

[48] Drummond, C. and Israelachvili, J. (2002). Surface forces and wettability. *Journal of Petroleum Science and Engineering*, 33:123–133.

[49] Dwarakanath, V., Jackson, R. E., and Pope, G. A. (2002). Influence of wettability on the recovery of NAPLs from alluvium. *Environmental Science and Technology*, 36:227–231.

[50] Dwarakanath, V., Kostarelos, K., Pope, G. A., Shotts, D., and Wade, W. H. (1999). Anionic surfactant remediation of soil columns contaminated by non-aqueous phase liquids. *Journal of Contaminant Hydrology*, 38(4):465–488.

[51] Eberhardt, C. and Grathwohl, P. (2002). Time scales of organic contaminant dissolution from complex source zones: Coal tar pools vs. blobs. *Journal of Contaminant Hydrology*, 59(1-2):45–66.

[52] Edwards, D. A., Luthy, R. G., and Liu, Z. (1991). Solubilization of polycyclic aromatic hydrocarbons in micellar nonionic surfactant solutions. *Environmental Science & Technology*, 25(127–133).

[53] Elkamel, A., Al-Sahhaf, T., and Suttar Ahmed, A. (2002). Studying the interaction between an Arabian heavy crude oil and alkaline solutions. *Petroleum Science and Technology*, 20(7, 8):789–807.

[54] EPRI (1993). *Chemical and physical characteristics of tar samples from selected manufactured gas plant (MGP) sites*. Electric Power Research Institute, Palo Alto, Calif.

[55] Falta, R. W., Lee, C. M., Brame, S. E., Roeder, E., Wood, L., and Enfield, C. (1999). *Innovative Subsurface Remediation: Field Testing of Physical, Chemical, and Characterization Technologies*, chapter Design and Performance of a Field Cosolvent Flooding Test for Nonaqueous Phase Liquid Mobilization, pages 102–117. American Chemical Society.

[56] Fei, Y. Q., Sakanishi, K., Sun, Y. N., Yamashita, R., and Mochida, I. (1990). Concentration of pyrroles and phenols from coal tar pitch by organic solvent extraction. *Fuel*, 69:261–262.

[57] Fountain, J. C., Klimek, A., Beikirch, M. G., and Middleton, T. M. (1991). The use of surfactants for in situ extraction of organic pollutants from a contaminated aquifer. *Journal of Hazardous Materials*, 28(3):295–311.

[58] Freeze, R. A. and Cherry, J. A. (1989). What has gone wrong. *Ground Water*, 27(4):458–464.

[59] Freitas, A. A., Quina, F. H., and Carroll, F. A. (1997). Estimation of water-

organic interfacial tensions. A linear free energy relationship analysis of interfacial adhesion. *Journal of Physical Chemistry B.*, 101:7488–7493.

[60] Ganz, H. H. and Kalkreuth, W. (1991). Ir classification of kerogen type, thermal maturation, hydrocarbon potential and lithological characteristics. *Journal of Southeast Asian Earth Sciences*, 5(1–4):19–28.

[61] Garcıa-Ochoa, F., Santos, V., Casas, J., and Gomez, E. (2000). Xanthan gum: production, recovery, and properties. *Biotechnology advances*, 18(7):549–579.

[62] Gerstein, B. C., Murphy, P. D., and Ryan, L. M. (1982). *Aromaticity in coal*, pages 87–129. Academic Press.

[63] Giese, S. W. and Powers, S. E. (2002). Using polymer solutions to enhance recovery of mobile coal tar and creosote DNAPLs. *Journal of Contaminant Hydrology*, 58(1-2):147–167.

[64] Groenzin, H. and Mullins, O. C. (2001). Molecular size and structure of asphaltenes. *Petroleum Science and Technology*, 19(1-2):219–230.

[65] Grosscurth, M., Osten, M., and Kilger, R. (2006). Clean-up of the Grasbrook Gasworks in the Hafencity of Hamburg. *Land Contamination & Reclamation*, 14(2):185–188.

[66] Guillen, M. D., Iglesias, M. J., Dominguez, A., and Blanco, C. G. (1992). Polynuclear aromatic hydrocarbon retention indices on se-54 stationary phase of the volatile components of a coal tar pitch. *Journal of Chromatography*, 591:287–295.

[67] Gupta, D. K. and Mohanty, K. K. (2001). A laboratory study of surfactant flushing of DNAPL in the presence of macroemulsion. *Environmental Science & Technology*, 35(13):2836–2843.

[68] Haeseler, F., Blanchet, D., Druelle, V., Werner, P., and Vandecasteele, J. P. (1999). Analytical characterization of contaminated soils from former manufactured gas plants. *Environmental Science & Technology*, 33(6):825–830.

[69] Hamper, M. J. (2006). Manufactured gas history and processes. *Environmental Forensics*, 7(1):55–64.

[70] Harkins, S. M., Truesdale, R. S., Hill, R., Hoffman, P., and Winters, S. (1988). *U.S. production of manufactured gases: Assessment of past disposal practices.* Prepared by Research Triangle Institute for the U.S. Environmental Protection Agency, Hazardous Waste Engineering Research Laboratory, Cincinnati, OH.

[71] Harrold, G., Gooddy, D. C., Lerner, D. N., and Leharne, S. A. (2001). Wettability changes in trichloroethylene-contaminated sandstone. *Environmental Science & Technology*, 35(7):1504–1510.

[72] Hartridge, H. and Peters, R. A. (1922). Interfacial tension and hydrogen ion concentration. *Proceedings of the Royal Society of London A*, 101:348–367.

[73] Harwell, J. H., Sabatini, D. A., and Knox, R. C. (1999). Surfactants for ground water remediation. *Colloids and Surfaces A – Physicochemical and Engineering Aspects*, 151(1-2):255–268.

[74] Hatheway, A. W. (2002). Geoenvironmental protocol for site and waste characterization of former manufactured gas plants; worldwide remediation challenge in semi-volatile organic wastes. *Engineering Geology*, 64(4):317–338.

[75] Hauswirth, S. C., Birak, P. S., Rylander, S. C., and Miller, C. T. (2012a). Mobilization of manufactured gas plant tar with alkaline flushing solutions. *Environmental Science & Technology*, 46(1):426–33.

[76] Hauswirth, S. C., Schultz, P. B., and Miller, C. T. (2012b). Compositional and pH effects on the interfacial tension between complex tar mixtures and aqueous solutions. *Environmental Science & Technology*, 46:10214–10221.

[77] Havre, T. E., Sjöblom, J., and Vindstad, J. E. (2003). Oil/water-partitioning and interfacial behavior of naphthenic acids. *Journal of Dispersion Science and Technology*, 24(6):789–801.

[78] Hayden, N. J. and Van der Hoven, E. J. (1996). Alcohol flushing for enhanced removal of coal tar from contaminated soils. *Water Environment Research*, 68(7):1165–1171.

[79] Heasman, I. and Westcott, F. J. (2006). Remediation of a gasworks site for residential development: the wharf lane site, solihull, uk. *Land Contamination & Reclamation*, 14(2):189–193.

[80] Hemmingsen, P. V., Silset, A., Hannisdal, A., and Sjoblom, J. (2005). Emulsions of heavy crude oils. I: Influence of viscosity, temperature, and dilution. *Journal of Dispersion Science and Technology*, 26(5):615–627.

[81] Herrenkohl, M. J., Lunz, J. D., Sheets, R. G., and Wakeman, J. S. (2001). Environmental impacts of PAH and oil release as a NAPL or as contaminated pore water from the construction of a 90-cm in situ isolation cap. *Environmental Science and Technology*, 35:4927–4932.

[82] Hill, E. H., Moutier, M., Alfaro, J., and Miller, C. T. (2001). Remediation of DNAPL pools using dense-brine barrier strategies. *Environmental Science & Technology*, 35(14):3031–3039.

[83] Hill, J. B. (1923). Determination of phenols in coal-tar oils and crude carbolic acid. *Industrial & Engineering Chemistry*, 15(8):799–800.

[84] Hirasaki, G. J. and Pope, G. A. (1974). Analysis of factors influencing mobility and adsorption in the flow of polymer solution through porous media.

Society of Petroleum Engineers Journal, 14:337–346.

[85] Hoeiland, S., Barth, T., Blokhus, A. M., and Skauge, A. (2001). The effect of crude oil acid fractions on wettability as studied by interfacial tension and contact angles. *Journal of Petroleum Science and Engineering*, 30:91–103.

[86] Hool, K. and Schuchardt, B. (1992). A new instrument for the measurement of liquid-liquid interfacial tension and the dynamics of interfacial tension reduction. *Measurement Science and Technology*, 3(5):451.

[87] Hortal, A. R., Hurtado, P., Martinez-Haya, B., and Mullins, O. C. (2007). Molecular-weight distributions of coal and petroleum asphaltenes from laser desorption/ionization experiments. *Energy & Fuels*, 21:2863–2868.

[88] Hugaboom, D. A. and Powers, S. E. (2002). Recovery of coal tar and creosote from porous media: The influence of wettability. *Ground Water Monitoring and Remediation*, 22(4):83–90.

[89] Huling, S. G. and Pivetz, B. E. (2006). In-situ chemical oxidation. Technical report, U. S. EPA.

[90] Islam, M. R. and Chakma, A. (1991). Mathematical modelling of enchanced oil recovery by alkali solutions in the presence of cosurfactant and polymer. *Journal of Petroleum Science and Engineering*, 5:105–126.

[91] Isosaari, P., Piskonen, R., Ojala, P., Voipio, S., Eilola, K., Lehmus, E., and Itävaara, M. (2007). Integration of electrokinetics and chemical oxidation for the remediation of creosote-contaminated clay. *Journal of Hazardous Materials*, 144(1):538–548.

[92] ITRC (2005). Overview of in situ bioremediation of chlorinated ethene DNAPL source zones. Technical report, Interstate Technology & Regulatory Council, Washington, D.C.

[93] Jackson, R. E., Dwarakanath, V., Meinardus, H. W., and Young, C. M. (2003). Mobility control: How injected surfactants and biostimulants may be forced into low-permeability units. *Remediation*, Summer:59–66.

[94] Jang, L. K., Sharma, M., Chang, Y. I., Chan, M., and Yen, T. F. (1982). *Correlation of petroleum component properties for caustic flooding*, volume 78 of *AIChE Symposium Series*, pages 97–104. American Institute of Chemical Engineers.

[95] Johnson, D. N., Pedit, J. A., and Miller, C. T. (2004). Efficient, near-complete removal of DNAPL from three-dimensional, heterogeneous porous media using a novel combination of treatment technologies. *Environmental Science & Technology*, 38(19):5149–5156.

[96] Johnson, L. A. and Fahy, L. J. (1997). *In situ treatment of manufactured gas*

plant contaminated soils demonstration program. U.S. Department of Energy.

[97] Johnston, N., Sadler, R., Shaw, G., and Connell, D. (1993). Environmental modification of pah composition in coal tar containing samples. *Chemosphere*, 27(7):1151–1158.

[98] Jonsson, S., Persson, Y., Frankkl, S., van Bavel, B., Lundstedt, S., Haglund, P., and Tysklind, M. (2007). Degradation of polycyclic aromatic hydrocarbons (PAHs) in contaminated soils by Fenton's reagent: A multivariate evaluation of the importance of soil characteristics and PAH properties. *Journal of Hazardous Materials*, 149(1):86–96.

[99] Joshi, M. M. and Lee, S. (1996). Optimization of surfactant-aided remediation of industrially contaminated soils. *Energy Sources*, 18(3):291–301.

[100] Juyal, P., Merino-Garcia, D., and Andersen, S. I. (2005). Effect on molecular interactions of chemical alteration of petroleum asphaltenes. i. *Energy & Fuels*, 19:1272–1281.

[101] Kanicky, J. R., Poniatowski, A. F., Mehta, N. R., and Shah, D. O. (2000). Cooperativity among molecules at interfaces in relation to various technological processes: Effect of chain length on the pk_a of fatty acid salt solutions. *Langmuir*, 16:172–177.

[102] Kanicky, J. R. and Shah, D. O. (2002). Effect of degree, type, and position of unsaturation on the pk_a of long-chain fatty acids. *Journal of Colloid and Interface Science*, 256:201–207.

[103] Kavanaugh, M. C., Rao, P. S. C., and Wood, A. L. (2003). The DNAPL remediation challenge: Is there a case for source depletion? Technical Report EPA 600/R-03-143, U.S. Environmental Protection Agency.

[104] Kestin, J., Sokolov, M., and Wakeham, W. A. (1978). Viscosity of liquid water in the range -8°C to 150°C. *Journal of Physical and Chemical Reference Data*, 7(3):941–946.

[105] Khadim, M. A. and Sarbar, M. A. (1999). Role of asphaltenes and resin in oil field emulsions. *Journal of Petroleum Science and Engineering*, 23:213–221.

[106] Killian, P. F., Bruell, C. J., Liang, C., and Marley, M. C. (2007). Iron (II) activated persulfate oxidation of MGP contaminated soil. *Soil & Sediment Contamination*, 16(6):523–537.

[107] Klein, G. C., Kim, S., Rodgers, R. P., and Marshall, A. G. (2006). Mass spectral analysis of asphaltenes. II. Detailed compositional comparison of asphaltene deposit to its crude oil counterpart for two geographically different crude oils by ESI FT-ICR MS. *Energy & Fuels*, 20:1973–1979.

[108] Kostarelos, K., Pope, G. A., Rouse, B. A., and Shook, G. M. (1998). A new

concept: The use of neutrally-buoyant microemulsions for DNAPL remediation. *Journal of Contaminant Hydrology*, 34(4):383–397.

[109] Krembs, F. J., Siegrist, R. L., Crimi, M. L., Furrer, R. F., and Petri, B. G. (2010). ISCO for groundwater remediation: Analysis of field applications and performance. *Groundwater Monitoring & Remediation*, 30(4):42–53.

[110] Kulik, N., Goi, A., Trapido, M., and Tuhkanen, T. (2006). Degradation of polycyclic aromatic hydrocarbons by combined chemical pre-oxidation and bioremediation in creosote contaminated soil. *Journal of Environmental Management*, 78(4):382–391.

[111] Lai, W.-C. and Song, C. (1995). Temperature-programmed retention indices for G.C. and G.C.-M.S. analysis of coal- and petroleum-derived liquid fuels. *Fuel*, 74(10):1436–1451.

[112] Lake, L. W. (1996). *Enhanced Oil Recovery*. Prentice Hall.

[113] Lane, W. F. and Loehr, R. C. (1992). Estimating the equilibrium aqueous concentrations of polynuclear aromatic hydrocarbons in complex mixtures. *Environmental Science & Technology*, 26(5):983–990.

[114] Lane, W. F. and Loehr, R. C. (1995). Predicting aqueous concentrations of polynuclear aromatic hydrocarbons in complex mixtures. *Water Environment Research*, 67(2):169–173.

[115] Langevin, D., Poteau, S., Hénaut, I., and Argillier, J. (2004). Crude oil emulsion properties and their application to heavy oil transportation. *Oil and Gas Science and Technology*, 59(5):511–521.

[116] Layrisse, I., Rivas, H., Intevep, S. A., and Acevedo, S. (1984). Isolation and characterization of natural surfactants present in extra heavy crude oils. *Journal of Dispersion Science and Technology*, 5:1–18.

[117] Lee, M. L., Vassilaros, D. L., White, C. M., and Novotny, M. (1979). Retention indexes for programmed-temperature capillary-column gas-chromatography of polycyclic aromatic-hydrocarbons. *Analytical Chemistry*, 51(6):768–774.

[118] Lemaire, J., Laurent, F., Leyval, C., Schwartz, C., Buès, M., and Simonnot, M.-O. (2013). PAH oxidation in aged and spiked soils investigated by column experiments. *Chemosphere*, 91(3):406–414.

[119] Lide, D. R. (2011). *CRC Handbook of Chemistry and Physics, Ninety-First Edition*. CRC Press, Cleveland, OH, 91st edition edition.

[120] Lingle, J. W. and Brehm, K. L. (2003). Application of source removal and natural attenuation remediation strategies at MGP sites in Wisconsin. *Remediation Journal*, 13(4):29–39.

[121] Link, A. (2000). Effect of nonionic surfactants on dissolution of polycyclic aromatic hydrocarbons from coal tar. *Practice Periodical of Hazardous, Toxic, and Radioactive Waste Management*, 4(2):78–81.

[122] Liu, L. H., Endo, S., Eberhardt, C., Grathwohl, P., and Schmidt, T. C. (2009). Partition behavior of polycyclic aromatic hydrocarbons between aged coal tar and water. *Environmental Toxicology and Chemistry*, 28(8):1578–1584.

[123] Liu, Q., Dong, M., Ma, S., and Tu, Y. (2007). Surfactant enhanced alkaline flooding for Western Canadian heavy oil recovery. *Colloids and Surfaces A: Physicochemical and Engineering Aspects*, 293:63–71.

[124] Longino, B. L. and Kueper, B. H. (1999). Effects of capillary pressure and use of polymer solutions on dense, non-aqueous-phase lliquid retention and mobilization in a rough-walled fracture. *Environmental Science and Technology*, 33:2447–2455.

[125] Lord, D. L., Demond, A. H., and Hayes, K. F. (2000). Effects of organic base chemistry on interfacial tension, wettability, and capillary pressure in multiphase subsurface waste systems. *Transport in Porous Media*, 38:79–92.

[126] Lundstedt, S., Haglund, P., and Oberg, L. (2003). Degradation and formation of polycyclic aromatic compounds during bioslurry treatment of an aged gasworks soil. *Environmental Toxicology and Chemistry*, 22(7):1413–1420.

[127] Lunn, S. R. D. and Kueper, B. H. (1999). Risk reduction during chemical flooding: Preconditioning DNAPL density in situ prior to recovery by miscible displacement. *Environmental Science & Technology*, 33(10):1703–1708.

[128] Luthy, R. G., Dzombak, D. A., Peters, C. A., Roy, S. B., Ramaswami, A., Nakles, D. V., and Nott, B. R. (1994). Remediating tar-contaminated soils at manufactured gas plant sites. *Environmental Science & Technology*, 28(6):266A–276A.

[129] MacKay, A. A. and Gschwend, P. M. (2001). Enhanced concentrations of PAHs in groundwater at a coal tar site. *Environmental Science & Technology*, 35(7):1320–1328.

[130] Mackay, D. M. and Cherry, J. A. (1989). Groundwater contamination: Pump-and-treat remediation. *Environmental Science & Technology*, 23(6):630–636.

[131] Mercer, J. W. and Cohen, R. M. (1990). A review of immiscible fluids in the subsurface: Properties, models, characterization and remediation. *Journal of Contaminant Hydrology*, 6(2):107–163.

[132] Merdrignac, I. and Espinat, D. (2007). Physiochemical characterization of petroleum fractions: the state of the art. *Petroleum Science and Technology – Rev. IFP*, 62(1):7–32.

[133] Miller, C. T., Hill, E. H., and Moutier, M. (2000). Remediation of DNAPL-contaminated subsurface systems using density-motivated mobilization. *Environmental Science & Technology*, 34(4):719–724.

[134] Mival, K., Pump, W., and Dixon, G. (2006). From wasteland to green parkland, the remediation of the former West Melbourne Gasworks, Victoria, Australia. *Land Contamination & Reclamation*, 14(2):194–199.

[135] Morrow, N. R. and Chatzis, I. (1982). Measurement and correlation of conditions for entrapment and mobilization of residual oil: First annual report. Technical Report DOE/BC/10310-20, U.S. Department of Energy, Oak Ridge, TN.

[136] Mulligan, C. N., Yong, R. N., and Gibbs, B. F. (2001). Surfactant-enhanced remediation of contaminated soil: a review. *Engineering Geology*, 60(1-4):371–380.

[137] Mulligan, M. J., Thomas, K. M., and Tytko, A. P. (1987). Functional group fractionation and characterization of tars and pitches. *Fuel*, 66:1472–1480.

[138] Murata, S., Kidena, K., and Nomura, M. (2005). *Construction of chemical structural model of Arabian asphaltene and its density simulation*, pages 75–94. ACS Symposium Series No. 895. American Chemical Society.

[139] Murgich, J., Rodriguez, J., and Aray, Y. (1996). Molecular recognition and molecular mechanics of micelles of some model asphaltenes and resins. *Energy & Fuels*, 10:68–76.

[140] Murphy, B. L., Sparacio, T., and Shields, W. J. (2005). Manufactured gas plants – processes, historical development, and key issues in insurance coverage disputes. *Environmental Forensics*, 6(2):161–173.

[141] Nadim, F., Huang, K.-C., and Dahmani, A. M. (2006). Remediation of soil and ground water contaminated with PAH using heat and Fe (II)-EDTA catalyzed persulfate oxidation. *Water, Air, & Soil Pollution: Focus*, 6(1-2):227–232.

[142] Nam, K., Rodriguez, W., and Kukor, J. J. (2001). Enhanced degradation of polycyclic aromatic hydrocarbons by biodegradation combined with a modified fenton reaction. *Chemosphere*, 45(1):11–20.

[143] Nasr-El-Din, H. A., Hawkins, B. F., and Green, K. A. (1992). Recovery of residual oil using the alkali/surfactant/polymer process: effect of alkali concentration. *Journal of Petroleum Science and Engineering*, 6:381–401.

[144] Nasr-El-Din, H. A. and Taylor, K. C. (1998). The role of surfactants in enhanced oil recovery. In Shah, D. O., editor, *Micelles, Microemulsions and Monolayers: Science and Technology*. CRC Press, New York.

[145] Neuhauser, E. F., Ripp, J. A., Azzolina, N. A., Madsen, E. L., Mauro, D. M., and Taylor, T. (2009). Monitored natural attenuation of manufactured gas plant tar mono- and polycyclic aromatic hydrocarbons in ground water: A 14-year field study. *Ground Water Monitoring and Remediation*, 29(3):66–76.

[146] Ng, K. M., Davis, H. T., and Scriven, L. E. (1978). Visualization of blob mechanics in flow through porous media. *Chemical Engineering Science*, 33:1009–1017.

[147] NIOSH (1977). *Criteria for a Recommended Standard: Occupational Exposure to Coal Tar Products*. U.S. Dept. of Health, Education, and Welfare, Public Health Service; Center for Disease Control; National Institute for Occupational Safety and Health, Cincinnati.

[148] Novotny, M., Strand, J. W., Smith, S. L., Wiesler, D., and Schwende, F. J. (1981). Compositional studies of coal-tar by capillary gas chromatography-mass spectrometry. *Fuel*, 60(3):213–220.

[149] NRC (1993). *In Situ Bioremediation: When Does It Work?* National Research Council, National Academy Press, Washington, D.C.

[150] NRC (2005). *Contaminants in the subsurface: Source zone assessment and remediation*. National Research Council, Committee on Source Removal of Contaminants in the Subsurface, National Academies Press, Washington, D.C.

[151] Okuda, I., McBride, J. F., Gleyzer, S. N., and Miller, C. T. (1996). An investigation of physicochemical transport processes affecting the removal of residual DNAPL by nonionic surfactant solutions. *Environmental Science & Technology*, 30(6):1852–1860.

[152] Oostrom, M., Hofstee, C., Walker, R. C., and Dane, J. H. (1999). Movement and remediation of trichloroethylene in a saturated heterogeneous porous medium, 1. Spill behavior and initial dissolution. *Journal of Contaminant Hydrology*, 37:159–178.

[153] Oostrom, M., Wietsma, T., Covert, M., and Vermeul, V. (2007). Zero-Valent Iron Emplacement in Permeable Porous Media Using Polymer Additions. *Ground Water Monitoring & Remediation*, 27(1):122–130.

[154] Ortiz, E., Kraatz, M., and Luthy, R. G. (1999). Organic phase resistance to dissolution of polycyclic aromatic hydrocarbon compounds. *Environmental Science & Technology*, 33(2):235–242.

[155] Palermo, M., Maynord, S., Miller, J., and Reible, D. (1998). Guidance for in-situ subaqueous capping of contaminated sediments. Technical report, U.S. EPA Great Lakes National Program Office. EPA 905-B96-004.

[156] Paterson, I. F., Chowdhry, B. Z., and Leharne, S. A. (1999). Polycyclic aromatic hydrocarbon extraction from a coal tar-contaminated soil using aqueous

solutions of nonionic surfactants. *Chemosphere*, 38(13):3095–3107.

[157] Payatakes, A. C. (1982). Dynamics of oil ganglia during immiscible displacement in water-wet porous media. *Annual Reviews of Fluid Mechanics*, 14:365–393.

[158] Pennell, K. D., Abriola, L. M., and Weber, W. J. (1993). Surfactant-enhanced solubilization of residual dodecane in soil columns. 1. Experimental investigation. *Environmental Science & Technology*, 27(12):2332–2340.

[159] Pennell, K. D., Jin, M., Abriola, L. M., and Pope, G. A. (1994). Surfactant enhanced remediation of soil columns contaminated by residual tetrachloroethylene. *Journal of Contaminant Hydrology*, 16(1):35–53.

[160] Pennell, K. D., Pope, G. A., and Abriola, L. M. (1996). Influence of viscous and buoyancy forces on the mobilization of residual tetrachloroethylene during surfactant flushing. *Environmental Science & Technology*, 30(4):1328–1335.

[161] Peters, C. A., Knightes, C. D., and Brown, D. G. (1999). Long-term composition dynamics of PAH-containing NAPLs and implications for risk assessment. *Environmental Science & Technology*, 33(24):4499–4507.

[162] Peters, C. A. and Luthy, R. G. (1993). Coal tar dissolution in water-miscible solvents: Experimental evaluation. *Environmental Science & Technology*, 27:2831–2843.

[163] Peters, C. A., Mukherji, S., Knightes, C. D., and Weber, J. W. J. (1997). Phase stability of multicomponent NAPLs containing PAHs. *Environmental Science & Technology*, 31(9):2540–2546.

[164] Peters, C. A., Wammer, K. H., and Knightes, C. D. (2000). Multicomponent NAPL solidification thermodynamics. *Transport in Porous Media*, 38(1-2):57–77.

[165] Peters, R. A. (1931). Interfacial tension and hydrogen-ion concentration. *Proceedings of the Royal Society of London A*, 133:140–155.

[166] Petri, B. G., Watts, R. J., Teel, A. L., Huling, S. G., and Brown, R. A. (2011). *In Situ Chemical Oxidation for Groundwater Remediation*, chapter Fundametnals of ISCO Using Hydrogen Peroxide, pages 33–88. SERDP and ESTCP Remediation Technology Monograph Series. Springer. Siegrist, R. L. and Crimi, M. and Simpkin, T. J., eds.

[167] Peyton, G. R., LeFaivre, M. H., and Smith, M. A. (1990). Treatability of contaminated ground water and aquifer solids at "town gas" sites using photolytic ozonation and chemical in situ reclamation. Technical report, Hazardous Waste Reseach and Information Center, Illinois State Water Survey, Champaign, IL.

[168] Pinto, L. J. and Moore, M. M. (2000). Release of polycyclic aromatic hydrocarbons from contaminated soils by surfactant and remediation of this effluent by penicillium spp. *Environmental Toxicology and Chemistry*, 19(7):1741–1748.

[169] Pitts, M., Wyatt, K., Sale, T., and Piontek, K. R. (1993). Utilization of chemical-enhanced oil recovery technology to remove hazardous oily waste from alluvium. In *SPE International Symposium on Oilfield Chemistry*, pages 33–44, New Orleans, LA, USA. Society of Petroleum Engineers.

[170] Pope, G. A. and Wade, W. H. (1995). Lessons from enhanced oil recovery research for surfactant-enhanced aquifer remediation. In Sabatini, D. A., Knox, R. C., and Harwell, J., editors, *Surfactant-Enhanced Subsurface Remediation: Emerging Technologies*, pages 142–160. American Chemical Society, Washington, D.C.

[171] Powers, S. E., Abriola, L. M., and Weber, J. W. J. (1992). An experimental investigation of nonaqueous phase liquid dissolution in saturated subsurface systems: Steady state mass transfer rates. *Water Resources Research*, 28(10):2691–2705.

[172] Powers, S. E., Anckner, W. H., and Seacord, T. F. (1996). Wettability of NAPL-contaminated sands. *Journal of Environmental Engineering - ASCE*, 122(10):889–896.

[173] Rao, P. S. C., Jawitz, J. W., Enfield, C. G., Falta Jr, R. W., Annable, M. D., and Wood, A. L. (2001). Technology integration for contaminated site remediation: Clean-up goals and performance criteria. *Groundwater Quality: Natural and Enhanced Restoration of Groundwater Pollution*, 275:571–578.

[174] Reddy, K. R. and Chandhuri, K. S. (2009). Fenton-like oxidation of polycyclic aromatic hydrocarbons in soils using electrokinetics. *Journal of Geotechnical and Geoenvironmental Engineering*, 135(10):1429–1439.

[175] Richardson, S. D., Lebron, B. L., Miller, C. T., and Aitken, M. D. (2011). Recovery of phenanthrene-degrading bacteria after simulated in situ persulfate oxidation in contaminated soil. *Environmental Science & Technology*, 45(2):719–725.

[176] Robert, T., Martel, R., Conrad, S., Lefebvre, R., and Gabriel, U. (2006). Visualization of TCE recovery mechanisms using surfactant-polymer solutions in a two-dimensional heterogeneous sand model. *Journal of Contaminant Hydrology*, 86(1-2):3–31.

[177] Rogel, E. (2000). Simulation of interactions in asphaltene aggregates. *Energy & Fuels*, 14:566–574.

[178] Roote, D. S. (1998). Technology status report: In situ flushing. Technical report, Ground-Water Remediation Technologies Analysis.

[179] Roy, S. B., Dzombak, D. A., and Ali, M. A. (1995). Assessment of in situ solvent extraction for remediation of coal tar sites: Column studies. *Water Environment Research*, 67(1):4–15.

[180] Ruberto, R. G. and Cronauer, D. C. (1978). *Oxygen and oxygen functionalities in coal and coal liquids*, pages 50–70. ACS Symposium Series No. 71. American Chemical Society.

[181] Ryder, J. L. and Demond, A. H. (2008). Wettability hysteresis and its implications for DNAPL source zone distribution. *Journal of Contaminant Hydrology*, 102(1-2):39–48.

[182] Sabatini, D. A., Knox, R. C., and Harwell, J. H. (1995). Emerging technologies in surfactant-enhanced subsurface remediation. In Sabatini, D. A., Knox, R. C., and Harwell, J., editors, *Surfactant-Enhanced Subsurface Remediation: Emerging Technologies*, pages 142–160. American Chemical Society, Washington, D.C.

[183] Sah, H. (1999). Protein behavior at the water/methylene chloride interface. *Journal of Pharmaceutical Sciences*, 88(12):1320–1325.

[184] Sah, H., Choi, S.-K., Choi, H.-G., and Yong, C.-S. (2002). Relation of dynamic changes in interfacial tension to protein destabilization upon emulsification. *Archives of Pharmacal Research*, 25:381–386. 10.1007/BF02976643.

[185] Samanta, A., Ojha, K., and Mandal, A. (2011). Interactions between acidic crude oil and alkali and their effects on enhanced oil recovery. *Energy & Fuels*, 25:1642–1649.

[186] Sayyouh, M., Hemeida, A. M., Al-Blehed, M. S., and Desouky, S. M. (1991). Role of polar compounds in crude oils on rock wettability. *Journal of Petroleum Science and Engineering*, 6:225–233.

[187] Schneider, M. H., Andrews, A. B., Mitra-Kirtley, S., and Mullins, O. C. (2007). Asphaltene molecular size by fluorescence correlation spectroscopy. *Energy & Fuels*, 21:2875–2882.

[188] Schroth, M. H., Ahearn, S. J., Selker, J. S., and Istok, J. D. (1996). Characterization of Miller-similar silica sands for laboratory hydrologic studies. *Soil Science Society of America Journal*, 60(5):1331–1339.

[189] Schwager, I., Farmanlan, P. A., Kwan, J. T., Weinberg, V. A., and Yen, T. F. (1983). Characterization of the microstructure and macrostructure of coal-derived asphaltene by nuclear magnetic resonance spectrometry and x-ray diffraction. *Analytical Chemistry*, 55:42–45.

[190] Seifert, W. K. and Howells, W. G. (1969). Interfacially active acids in a California crude oil: Isolation of carboxylic acids and phenols. *Analytical Chemistry*, 41(4):554–562.

[191] Sheng, J. J. (2011). *Modern Chemical Enhanced Oil Recovery*. Gulf Professional Publishing (Elsevier), Burlington, MA.

[192] Siegrist, R. L., Crimi, M., and Brown, R. A. (2011a). In situ chemical oxidation technology: Description and status. In *In Situ Chemical Oxidation for Groundwater Remediation*, pages 1–32. Springer.

[193] Siegrist, R. L., Palaia, T. A., Clayton, W., and Lewis, R. W. (2011b). Site characterization and ISCO treatment goals. In *In Situ Chemical Oxidation for Groundwater Remediation*. Springer.

[194] Silva, J. A. K., Liberatore, M., and McCray, J. E. (2013). Characterization of Bulk Fluid and Transport Properties for Simulating Polymer-Improved Aquifer Remediation. *Journal of Environmental Engineering*, 139(2):149–159.

[195] Silva, J. A. K., Smith, M. M., Munakata-Marr, J., and McCray, J. E. (2012). The effect of system variables on in situ sweep-efficiency improvements via viscosity modification. *Journal of Contaminant Hydrology*, 136-137:117–30.

[196] Sobkowiak, M. and Painter, P. (1995). A comparison of drift and KBr pellet methodologies for the quantitative analysis of functional groups in coal by infrared spectroscopy. *Energy & Fuels*, 9:359–363.

[197] Soga, K., Page, J. W. E., and Illangasekare, T. H. (2004). A review of NAPL source zone remediation efficiency and the mass flux approach. *Journal of Hazardous Materials*, 110(1–3):13–27.

[198] Speight, J. G. (2001). Petroleum resins: separation, character, and role in petroleum. *Petroleum Science and Technology*, 19(1&2):1–34.

[199] Speight, J. G. (2004). Petroleum asphaltenes part 1: Asphaltenes, resins and the structure of petroleum. *Oil & Gas Science and Technology*, 59(5):467–477.

[200] Speight, J. G., Long, R. B., and Trowbridge, T. D. (1984). Factors influencing the separation of asphaltenes from heavy petroleum feedstocks. *Fuel*, 63:616–620.

[201] Speight, J. G. and Moschopedis, S. E. (1981). *On the molecular nature of petroleum asphaltenes*, pages 1–16. Advances in Chemistry Series No. 195. American Chemical Society.

[202] Sra, K. S., Thomson, N. R., and Barker, J. F. (2010). Persistence of persulfate in uncontaminated aquifer materials. *Environmental Science & Technology*, 44(8):3098–3104.

[203] Srivastava, V. J. (1993). Manufactured gas plant sites: Characterization of wastes and IGT's innovative remediation alternatives. In *Symposium for Hazardous and Environmentally Sensitive Waste Management in the Gas Industry*, Albequerque, New Mexico. Institute of Gas Technology.

[204] Switzer, C., Pironi, P., Gerhard, J. I., Rein, G., and Torero, J. L. (2009). Self-sustaining smoldering combustion: A novel remediation process for non-aqueous-phase liquids in porous media. *Environmental Science & Technology*, 43(15):5871–5877.

[205] Taylor, K. C. and Hawkins, B. F. (1992). Emulsions in enhanced oil recovery. In Schramm, L. L., editor, *Emulsions: Fundamentals and Applications in the Petroleum Industry*, pages 263–294. American Chemical Society, Washington, D.C.

[206] Tiraferri, A. and Sethi, R. (2009). Enhanced transport of zerovalent iron nanoparticles in saturated porous media by guar gum. *Journal of Nanoparticle Research*, 11(3):635–645.

[207] Tosco, T. and Sethi, R. (2010). Transport of non-Newtonian suspensions of highly concentrated micro-and nanoscale iron particles in porous media: a modeling approach. *Environmental Science & Technology*, 44(23):9062–9068.

[208] Touhami, Y., Hornof, V., and Neale, G. H. (1998). Dynamic interfacial tension behavior of acidified oil/surfactant-enhanced alkaline systems 1. Experimental studies. *Colloids and Surfaces A: Physiochemical and Engineering Aspects*, 132:61–74.

[209] Touhami, Y., Rana, D., Hornof, V., and Neale, G. H. (2001). Effects of added surfactant on the dynamic interfacial tension behavior of acidic oil/alkaline systems. *Journal of colloid and interface science*, 239(1):226–229.

[210] Traynor, M., Burke, R., Frias, J. M., Gaston, E., and Barry-Ryan, C. (2013). Formation and stability of an oil in water emulsion containing lecithin, xanthan gum and sunflower oil. *International Food Research Journal*, 20(5):2173–2183.

[211] Troxler, W. L. and Brankley, T. W. (2006). Factors affecting soil clean-up levels achievable by thermal desorption technologies at mgp sites. *Land Contamination & Reclamation*, 14(2):209–217.

[212] Tzimas, G., Matsuura, T., Avraam, D., Van der Brugghen, W., Constantinides, G. N., and Payatakes, A. (1997). The combined effect of the viscosity ratio and the wettability during forced imbibition through nonplanar porous media. *Journal of Colloid and Interface Science*, 189:27–36.

[213] U.S. Department of Health and Human Services (2002). CFR title 21, part 184 direct food substances generally recognized as safe.

[214] U.S. EPA (1985). Survey of town gas and by-product production and locations in the u.s. (1880–1950). Technical Report EPA-600/7-85-004, U.S. EPA. EPA-600/7-85-004.

[215] U.S. EPA (1999). Waste research strategy. Technical Report EPA/600/R-98/154, U.S. Environmental Protection Agency, Washington, DC.

[216] U.S. EPA (2000). Western research institute contained recovery of oily wastes (CROW) process: Innovative technology report. Technical Report EPA/540/R-00/500, U.S. Environmental Protection Agency, Washington, D. C.

[217] U.S. EPA (2004). Cleaning up the nation's waste sites: Markets and technology trends. Technical Report EPA/542/R-04/015, U.S. Environmental Protection Agency, Cincinnati, OH. EPA/542/R-04/015.

[218] USGS (2009). Estimated use of water in the United States in 2005. Technical report, U. S. Geological Survey. Circular 1344.

[219] Usman, M., Faure, P., Ruby, C., and Hanna, K. (2012). Application of magnetite-activated persulfate oxidation for the degradation of PAHs in contaminated soils. *Chemosphere*, 87(3):234–240.

[220] Vassilaros, D. L., Kong, R. C., Later, D. W., and Lee, M. L. (1982). Linear retention index system for polycyclic aromatic-compounds – critical-evaluation and additional indexes. *Journal of Chromatography*, 252(Dec):1–20.

[221] Villaume, J. F. (1984). Coal tar wastes: Their environmental fate and effects. In Majumdar, S. K. and Miller, E. W., editors, *Hazardous and Toxic Wastes: Technology, Management, and Health Effects*, pages 362–375. The Pennsylvania Academy of Science.

[222] Villaume, J. F. (1985). Investigations at sites contaminated with dense non-aqueous phase liquids. *Ground Water Monitoring Review*, 5(2):60–74.

[223] Wang, Z., Li, K., Lambert, P., and Yang, C. (2007). Identification, characterization and quantitation of pyrogenic polycylic aromatic hydrocarbons and other organic compounds in tire fire products. *Journal of Chromatography A*, 1139(1):14–26.

[224] Wasan, D. T. (1994). Surfactant-enhanced alkaline flooding for light oil recovery: Annual report 1992-1993.

[225] West, C. C. and Harwell, J. H. (1992). Surfactants and suburface remediation. *Environmental Science & Technology*, 26(12):2324–2330.

[226] Whitehurst, D. D. (1978). *A primer on the chemistry and constitution of coal*, pages 1–35. ACS Symposium Series No. 71. American Chemical Society.

[227] Willson, C. S., Hall, J. L., Imhoff, P. T., and Miller, C. T. (1999). Factors affecting bank formation during surfactant-enhanced mobilization of residual NAPL. *Environmental Science & Technology*, 33(14):2440–2446.

[228] Wise, S., Sander, L., Chang, H., Markides, K., and Lee, M. (1988a). Shape selectivity in liquid and gas chromatography: Polymeric octadecylsilane (c18) and liquid crystalline stationary phases. *Chromatographia*, 25(6):473–479.

[229] Wise, S. A., Benner, B. A., Byrd, G. D., Chesler, S. N., Rebbert, R. E., and Schantz, M. M. (1988b). Determination of polycyclic aromatic hydrocarbons in a coal tar reference material. *Analytical Chemistry*, 60:887–894.

[230] Wright, D. J., Birak, P. S., Pedit, J. A., and Miller, C. T. (2010a). Effectiveness of source-zone remediation of DNAPL–contaminated subsurface systems. *Journal of Environmental Engineering–ASCE*, 136(5):452–465.

[231] Wright, D. J., Pedit, J. A., Farthing, M. W., Murphy, L. L., Brubaker, G. R., Knight, S. R., and Miller, C. T. (2010b). Dense, viscous brine behavior in heterogeneous porous medium systems. *Journal of Contaminant Hydrology*, 115(1–4):46–63.

[232] Wu, J., Gong, Z., Zheng, L., Yi, Y., Jin, J., Li, X., and Li, P. (2010). Removal of high concentrations of polycyclic aromatic hydrocarbons from contaminated soil by biodiesel. *Frontiers of Environmental Science & Engineering in China*, 4(4):387–394.

[233] Xue, D. and Sethi, R. (2012). Viscoelastic gels of guar and xanthan gum mixtures provide long-term stabilization of iron micro-and nanoparticles. *Journal of Nanoparticle Research*, 14(11):1–14.

[234] Yalkowsky, S. H. (1981). Solubility and solubilization of nonelectrolytes; solubilization of drugs by cosolvents. In Yalkowsky, S. H., editor, *Techniques of Solubilization of Drugs*, pages 1–14;91–134. Marcel Dekker, Inc., New York.

[235] Yen, T. F. (1981). *Structural differences between asphaltenes isolated from petroleum and from coal liquid*, pages 39–51. Advances in Chemistry Series No. 195. American Chemical Society.

[236] Yeom, I. T., Ghosh, M. M., Cox, C. D., and Robinson, K. G. (1995). Micellar solubilization of polynuclear aromatic hydrocarbons in coal tar-contaminated soils. *Environmental Science & Technology*, 29(12):3015–3021.

[237] Zhang, L., Luo, L., Zhao, S., Xu, Z. C., An, J. Y., and Yu, J. Y. (2004). Effect of different acidic fractions in crude oil on dynamic interfacial tensions in surfactant/alkali/model oil systems. *Journal of Petroleum Science and Engineering*, 41(1-3):189–198.

[238] Zhang, M. J., Chen, B. J., Shen, S. D., and Chen, S. Y. (1997). Compositional studies of high-temperature coal tar by G.C.–FT-IR analysis of middle oil fractions. *Fuel*, 76(5):415–423.

[239] Zhang, M. J., Li, S. D., and Chen, B. J. (1992). Compositional studies of high-temperature coal-tar by GC/FTIR analysis of light oil fractions. *Chromatographia*, 33(3-4):138–146.

[240] Zheng, J. Z., Behrens, S. H., Borkovec, M., and Powers, S. E. (2001a). Predicting the wettability of quartz surfaces exposed to dense nonaqueous phase

liquids. *Environmental Science & Technology*, 35(11):2207–2213.

[241] Zheng, J. Z. and Powers, S. E. (1999). Organic bases in NAPLs and their impact on wettability. *Journal of Contaminant Hydrology*, 39(1–2):161–181.

[242] Zheng, J. Z. and Powers, S. E. (2003). Identifying the effect of polar constituents in coal-derived NAPLs on interfacial tension. *Environmental Science & Technology*, 37(14):3090–3094.

[243] Zheng, J. Z., Shao, J. H., and Powers, S. E. (2001b). Asphaltenes from coal tar and creosote: Their role in reversing the wettability of aquifer systems. *Journal of Colloid and Interface Science*, 244(2):365–371.

[244] Zhong, L., Oostrom, M., Wietsma, T. W., and Covert, M. A. (2008). Enhanced remedial amendment delivery through fluid viscosity modifications: Experiments and numerical simulations. *Journal of Contaminant Hydrology*, 101(1-4):29–41.